

DATING OF LAODIKEIA (DENIZLI) BUILDING CERAMICS USING
OPTICALLY STIMULATED LUMINESCENCE (OSL) TECHNIQUES

A THESIS SUBMITTED TO
THE GRADUATE SCHOOL OF NATURAL AND APPLIED SCIENCES
OF
MIDDLE EAST TECHNICAL UNIVERSITY

BY

TAYFUN DEMİRTÜRK

IN PARTIAL FULFILMENT OF THE REQUIREMENTS
FOR
THE DEGREE OF DOCTOR OF PHILOSOPHY
IN
PHYSICS

SEPTEMBER 2006

Approval of the Graduate School of Natural and Applied Sciences.

Prof. Dr. Canan Özgen
Director

I certify that this thesis satisfies all the requirements as a thesis for the degree of Doctor of Philosophy.

Prof. Dr. Sinan Bilikmen
Head of Department

This is to certify that we have read this thesis and that in our opinion it is full adequate, in scope and quality, as a thesis for the degree of Doctor of Philosophy.

Prof. Dr. Ay Melek Özer
Supervisor

Examining Committee Members

Prof. Dr. Şahinde Demirci	(METU, CHEM)	_____
Prof. Dr. Ay Melek Özer	(METU, PHYS)	_____
Prof. Dr. Selahattin Özdemir	(METU, PHYS)	_____
Assoc. Prof. Dr. Enver Bulur	(METU, PHYS)	_____
Asst. Prof. Dr. Esmâ B. Kırıkkaya	(KOU, SSME)	_____

“I hereby declare that all information in this document has been obtained and presented in accordance with academic rule and ethical conduct. I also declare that, as required by these rules and conduct, I have fully cited and referenced all material and results that are not original to this work.”

Name Surname: Tayfun Demirtürk

Signature:

ABSTRACT

DATING OF LAODIKEIA (DENIZLI) BUILDING CERAMICS USING OPTICALLY STIMULATED LUMINESCENCE (OSL) TECHNIQUES

Tayfun Demirtürk

Ph.D., Department of Physics

Supervisor: Prof. Dr. Ay Melek Özer

September 2006, 106 pages

The objective of this study is to perform Optically Stimulated Luminescence (OSL) dating on the ceramic samples from different parts of the Laodikeia by using Infra Red Stimulated Luminescence (IRSL) on polyminerals.

As a first step, a literature survey has been done about the dating system and the methodology of dating. The calibration of the system was done before carrying out the experiments. The six ceramic samples were collected from the site and dated.

The mineral compositions of the samples were examined by X-ray Diffraction Analysis, which showed that all samples contain quartz, feldspars, calcites and together with other minerals.

The equivalent dose was found by using Multiple Aliquot Additive Dose (MAAD) and Multiple Aliquot Regenerative Dose (MARD) techniques using Infra Red diode array of the system that gave the IRSL ages for samples. Alpha counter measured the

dose components of uranium and thorium contributions to the annual dose. The potassium concentration was determined by Atomic Emission Spectrometry. The cosmic ray component of annual dose was evaluated by the $\text{Al}_2\text{O}_3:\text{C}$ Thermoluminescence Dosimeter (TLD) discs which have been placed and kept for 8 and 11 months in the site.

From the data the IRSL ages were calculated for six ceramic samples LDKY-1, LDKY-2, LDKY-3, LDKY-4, LDKY-5 and LDKY-6 with the help of the OSL system software. The IRSL ages for these samples, in the given order, are 737 ± 60 , 1563 ± 120 , 1445 ± 110 , 1602 ± 120 , 1034 ± 80 and 1034 ± 80 years by using MAAD technique. The IRSL ages for the same samples are 870 ± 60 , 1550 ± 120 , 1440 ± 110 , 1600 ± 120 , 1030 ± 80 and 1030 ± 70 years by using MARD technique.

KEY WORDS: Dating, Optically Stimulated Luminescence (OSL), Infra Red Stimulated Luminescence (IRSL), Laodikeia, MAAD technique, MARD technique.

ÖZ

OPTİK UYARMALI LÜMİNESANS (OSL) TEKNİĞİ İLE LAODIKEIA (DENİZLİ) BİNA SERAMİKLERİNİN TARİHLENDİRİLMESİ

Tayfun Demirtürk

Doktora, Fizik Bölümü

Tez Danışmanı: Prof. Dr. Ay Melek Özer

Eylül 2006, 106 sayfa

Bu çalışmanın amacı Laodikeia kazısının farklı yerlerinden alınan seramik örneklerin optik uyarmalı lüminesans (OSL) tarihlerinin poliminerallere kızıl ötesi uyarmalı lüminesans (IRSL) uygulanarak tarihlendirilmesidir.

İlk adım olarak, tarihleme sistemi ve tarihleme metodu hakkında bir literatür taraması yapıldı. Deneylere başlamadan önce sistemin kalibrasyonu yapıldı. Altı seramik örnek kazı bölgesinden alındı ve tarihlendi.

Örneklerin mineral içerikleri X-ışını kırınım analizi yöntemiyle belirlendi, temelde kuvars, feldispat, kalsit ve diğer bazı minerallerin bulunduğu sonucuna varıldı.

Çalışmada eşdeğer doz ölçümü, sistemdeki kızıl ötesi diyotlar dizisi yardımıyla çok örnekli eklemeli doz (MAAD) ve çok örnekli rejenerasyon doz (MARD) teknikleriyle yapıldı. Yıllık doza uranyum ve toryum bileşenlerinin katkısı alfa

sayacı ile ölçüldü. Potasyum miktarı atomik emisyon spektrometresi ile bulundu. Yıllık dozun kozmik ışınlarla bağlı bileşeni kazı yerinde toprak altında 8 ve 12 ay süreyle tutulan $Al_2O_3:C$ ısı uyarmalı dozimetreleri (TLD) ile belirlendi.

Toplanan veriler ve OSL sisteminin yazılımı ile LDKY-1, LDKY-2, LDKY-3, LDKY-4, LDKY-5 ve LDKY-6 olarak simgelenen örneklerin MAAD yönteminden gidilerek IRSL yaşları sırasıyla 737 ± 60 , 1563 ± 120 , 1445 ± 110 , 1602 ± 120 , 1034 ± 80 ve 1034 ± 80 yıl olarak belirlendi. Aynı örneklerin yaşları MARD yönteminden gidilerek sırasıyla 870 ± 60 , 1550 ± 120 , 1440 ± 110 , 1600 ± 120 , 1030 ± 80 ve 1030 ± 80 yıl olarak bulundu.

Anahtar Sözcükler: Tarihleme, Optik Uyarmalı Luminesans (OSL), Kızılı Ötesi (Infra Red) Uyarmalı Lüminesans (IRSL), Laodikeia, MAAD tekniği, MARD tekniği..

TO MY FAMILY
and
TO MY TEACHERS

ACKNOWLEDGEMENTS

I am grateful to my supervisor Prof. Dr. Ay Melek Özer for her guidance and comprehension.

I would like to thank to Prof.Dr. Şahinde Demirci and Dr. Mustafa Özbakan, for their special guidance and support throughout my research.

It is a very big pleasure for me to thank to Assoc. Prof. Dr. Enver Bulur and Assoc. Prof. Dr. H. Yeter Göksu since they shared their endless experiences and knowledge during my work. If I had never met them, this work was not completed and meaningful.

I also thank to Prof. Dr. Selahattin Özdemir for his valuable criticisms during the committee meetings.

I am really thankful to Pamukkale University Excavation Team and especially to Assoc. Prof. Dr. Celal Şahin and Ali Ceylan who helped me during my visits to the site of Laodikeia for collecting the ceramic samples, placing and taking back TLDs.

I would like to thank all the people in the physics department for their endless help during this work.

I also would like to thank to my dear friend and also physics graduate student M. Altay Atlıhan with whom we spent hours in the dark rooms of OSL laboratories for preparing the samples and making luminescence measurements.

I am grateful to Prof. Dr. Veysel Kuzucu from Pamukkale University, Physics Department for guiding and encouraging me to study OSL.

It is also a pleasure for me to thank to Assoc. Prof. Dr. Birol Engin and Hayr nnisa Demirtař from Ankara N kleer Arařtırma ve Eđitim Merkezi for their help in TL measurements of the TLD dosimeters.

I would like to thank to the technician of METU Chemistry Department, Saliha Pirdođan for her help during the sample preparations for potassium analysis.

It is a great pleasure for me to thank to my parents, without their valuable support, all this work was not possible.

Special thanks go to my family who always shared my excitements and enthusiasms during my study.

TABLE OF CONTENTS

PLAGIARISM.....	iii
ABSTRACT.....	iv
ÖZ.....	vi
DEDICATION.....	viii
TABLE OF CONTENTS.....	xi
LIST OF TABLES.....	xiv
LIST OF FIGURES.....	xvi
CHAPTERS	
1 INTRODUCTION.....	1
2 FUNDAMENTALS OF LUMINESCENCE DATING.....	8
2.1 General principles of luminescence dating.....	12
2.2 Mechanism of luminescence.....	14
2.3 Signal growth and trap stability.....	18
2.4 Anomalous fading.....	22
2.5 Stimulation of the signal.....	23
2.6 Materials studied by OSL.....	25
3 MATERIALS and METHODS.....	27
3.1 Samples of Laodikeia Archaeological Site.....	27
3.2 Age Determination.....	30
3.3 Evaluation of Paleodose (Equivalent Dose, D_{eq}).....	32
3.3.1 MAAD (Multiple Aliquots Additive Dose) Technique.....	34
3.3.2 MARD (Multiple Aliquots Regenerated Dose) Technique.....	35
3.3.3 SAR (Single Aliquot Regeneration) Technique.....	36
3.4 Preheating.....	37
3.5 Normalization.....	37
3.6 Sample Preparation.....	38

3.7	Size distribution of the samples.....	39
3.8	Annual Dose Measurements.....	39
3.8.1	Water Saturation and Water Uptake Measurements.....	42
3.8.2	Determination of Potassium in Samples.....	43
3.9	Sources of α , β particles and γ rays.....	45
3.9.1	Contribution of Gamma and Cosmic Rays for Dose Rate... 46	
3.10	Supralinearity, Sensitization and Saturation.....	46
4	RESULTS and DISCUSSIONS	48
4.1	X-Ray Diffraction Analysis (XRD) and Sample Separation.....	59
4.1.1	Size distribution of the samples	62
4.2	Preheating.....	64
4.3	Normalization.....	68
4.4	MAAD (Multiple Aliquots Additive Dose) Technique.....	69
4.5	MARD (Multiple Aliquots Regenerated Dose) Technique.....	72
4.6	Annual Dose Measurements.....	76
4.6.1	Water Saturation and Water Uptake Measurements.....	76
4.6.2	Alpha Counting for LDKY Samples.....	77
4.6.3	Determination of Potassium in Samples.....	78
4.6.3.1	Preparation of the samples for potassium analysis (AES analysis).....	80
4.6.4	Contribution of Gamma and Cosmic Rays for Dose Rate..	81
4.7	Supralinearity, Sensitization and Saturation of the LDKY Samples..	83
5	CONCLUSION.....	85
APPENDICES		
A	88
A.1	The Parts of ELSEC 9010 Optical Dating System Comprises.....	88
A.2	Alpha Counting System.....	92
B	95
B.1	OSL Dating System.....	95
B.2	Calibration of Optical Dating System.....	95
B.3	Alpha Counting System.....	100

B.4	Calibration of Alpha Counter.....	100
B.5	Dose Rate Calculations of Sr-90 Beta Radiation Source.....	104
REFERENCES.....		

LIST OF TABLES

Table 2.1	Chart of some dating methods.....	13
Table 3.1	The samples examined in this study.....	30
Table 3.2	Components of annual dose from potassium, rubidium, thorium and uranium for given concentrations.....	39
Table 3.3	Radioactive properties of potassium-40.....	44
Table 3.4	The members of the U-238 and Th-232 decay series, their half-lives and their radiation types.....	45
Table 3.5	Half-lives and average abundances of natural radionuclides.....	46
Table 4.1	Age results of LDKY samples based on the OSL system and its associated software.....	50
Table 4.2	Annual dose and age calculation of LDKY-1 sample by MARD technique, based on the OSL system and its associated software.	53
Table 4.3	Annual dose and age calculation of LDKY-2 sample by MARD technique, based on the OSL system and its associated software.	54
Table 4.4	Annual dose and age calculation of LDKY-3 sample by MARD technique, based on the OSL system and its associated software.	55
Table 4.5	Annual dose and age calculation of LDKY-4 sample by MARD technique, based on the OSL system and its associated software.	56
Table 4.6	Annual dose and age calculation of LDKY-5 sample by MARD technique, based on the OSL system and its associated software.	57
Table 4.7	Annual dose and age calculation of LDKY-6 sample by MARD technique, based on the OSL system and its associated software.	58
Table 4.8	Luminescence and normalization constants of a group of LDKY-1 aliquots.....	68
Table 4.9	Equivalent doses of the LDKY samples with MAAD technique...	70
Table 4.10	Equivalent doses of the LDKY samples with MARD technique...	75

Table 4.11	Annual doses of LDKY samples.....	76
Table 4.12	Water saturation content and water uptake measurements for LDKY samples.....	77
Table 4.13	Unsealed and sealed alpha counts of LDKY samples.....	78
Table 4.14	Concentrations of potassium standards and their emission intensity readings by AES.....	79
Table 4.15	Atomic Emission Spectrometry results of LDKY samples for potassium content.....	80
Table 4.16	Thick Al ₂ O ₃ :C dose response table for gamma irradiation.....	82
Table 4.17	Dose rates of TLD dosimeters for annual γ and cosmic rays of LDKY samples.....	83
Table B.1	High Tension (HT) voltage calibration data of the PM tube of the OSL system.....	95
Table B.2	Threshold voltage calibration data of the PM tube of OSL system	96
Table B.3	High Tension (HT) voltage calibration data of the Alpha counter PM tube.....	99
Table B.4	Threshold voltage calibration data of the Alpha Counter PM tube	101
Table B.5	Sr-90 beta radiation source dose rates for feldspar and quartz components of the sample and its calculated activity values.....	106

LIST OF FIGURES

Figure 1.1	Satellite photo of Laodikeia site.....	4
Figure 1.2	Plan of Laodikeia.....	5
Figure 2.1	Simple types of defects in the lattice structure of an ionic crystal.....	10
Figure 2.2	Schematic representation of the event that is being used in the luminescence dating of pottery and sediments.....	14
Figure 2.3	Energy-level representation of the luminescence process.....	15
Figure 2.4	Anomalous fading of the trapped electrons.....	22
Figure 3.1	Ceramic Floor tiles of the room which is at the right side of North of the from church door entrance.....	28
Figure 3.2	The ceramic water pipes from the front of the north wall of the church.....	28
Figure 3.3	The ceramic ceiling tiles from the entrance of the church door...	29
Figure 3.4	Ceramic water pipes and a floor tile from Laodikeia site.....	29
Figure 3.5	The depletion of signal with time.....	31
Figure 3.6	Block diagram of OSL system and luminescence measurement..	33
Figure 3.7	Additive dose method of paleodose evaluation.....	34
Figure 3.8	Decay curve of luminescence signal from natural or already dosed sample.....	35
Figure 3.9	Additive regenerated dose method of paleodose evaluation.....	36
Figure 3.10	Luminescence growth characteristic showing supralinear and sublinear regions.	
Figure 4.1	XRD analysis of LDKY-1 ceramic sample.....	61
Figure 4.2	TL signal versus temperature curve for the feldspar component of LDKY-2 sample.....	65

Figure 4.3	(a) Luminescence versus temperature graph at constant heating time. (b) Luminescence versus time graph at 160 °C.....	66
Figure 4.4	Luminescence versus day graph for un-preheated polimineral aliquots.	67
Figure 4.5	Luminescence counts versus sample # graph.....	69
Figure 4.6	Grouping the samples on a tray and adding doses for (MAAD) luminescence measurements.....	71
Figure 4.7	Luminescence versus time graph for a polimineral LDKY sample.....	71
Figure 4.8	Luminescence versus added Dose graph for LDKY-1 sample.....	72
Figure 4.9	Arrangement of aliquots in the sample tray for natural luminescence measurements.....	73
Figure 4.10	Grouping the samples on a tray and adding doses for (MARD) luminescence measurements.....	74
Figure 4.11	Luminescence versus added dose graph.....	75
Figure 4.12	Potassium calibration curve.....	79
Figure 4.13	Thick Al ₂ O ₃ :C dose response curve for gamma irradiation.....	82
Figure 4.14	Luminescence versus dose graph for high dose response.....	84
Figure A.1	Sample Tray.....	88
Figure A.2	The graph of fractional transmission versus wavelength of Schott BG 39 filter.....	90
Figure A.3	Basic set-up for beta irradiation	92
Figure A.4	ELSEC 7286 Low Level Alpha Counter system.....	93
Figure A.5	Simplified block diagram of alpha counting system.....	94
Figure B.1	ELSEC 9010 Optical Dating System.....	95
Figure B.2	The apparent intensity versus HT voltage curve.....	97
Figure B.3	The calibration curve of the PM tube, apparent intensity versus threshold voltage graph.....	99
Figure B.4	HT voltage calibration curve of the Alpha counter PM tube.	102
Figure B.5	Threshold voltage calibration curve.....	104

CHAPTER 1

INTRODUCTION

Luminescence is the emission of light which is caused by the movement of electrons within a substance from more energetic states to less energetic states. Luminescence, general term applied to all forms of cool light, i.e., light emitted by sources other than a hot, incandescent body, such as a black body radiator.

Materials always contain some amount of radioactive impurities such as U, Th and K. These radioactive impurities radiate energy and this energy is accumulated and stored in the crystal lattice. In other words, the radiation energy is stored in the form of electrons that have been trapped at defects in the lattice.

When the material is heated or illuminated the trapped energy is released as light. This process is known as stimulated luminescence. The luminescence resulted from heat stimulation is called Thermoluminescence (TL) and the luminescence resulted from light is called Optically Stimulated Luminescence (OSL).

Over the past twenty years, the development of the OSL has made it a valuable tool for evaluating the equivalent dose (total dose, cumulative dose or burial dose) of quartz and feldspar. Over a long period of time, after the sample is buried, the natural ionizing radiation in the soil causes electrons and holes to become trapped in pre-existing defects in materials. If the material is heated to temperatures greater than 500 °C, nearly all the trapped electrons are released.

Also, exposure to sunlight will empty some or all of the traps. These are the two most common re-setting events. Infrared light has the frequency suitable for feldspar to stimulate electrons from their traps (Duller, 1991). These electrons recombine with the trapped holes and produce photons with frequencies higher than infrared. By measuring the number of emitted photons resulting from optical stimulation, the age of the sample can be determined. Huntley *et al.* (1985) were the first to demonstrate that optically stimulated luminescence could be used to find the equivalent dose of a sample to the same level of certainty as previously existing methods such as thermoluminescence and electron spin resonance.

The procedure for recording Optically Stimulated Luminescence (OSL) during dating and/or dosimeter applications is to record the luminescence as a function of illumination time at room temperature (McKeever *et al.* 1996). In the development in OSL instrumentation, two important studies can be mentioned. One of them is the single grain apparatus described by Duller *et al.* (1999) and the linear modulation technique described by Bulur (1996). Initial experiments with linearly modulated OSL (LM-OSL) were carried out using near-IR (approximately 880 nm) stimulation on feldspars (Bulur 1996); Bulur and Göksu (1999).

The first objective of this work is to explain and to apply luminescence mechanism on nonconductive which is well described in solid state physics. The second objective is to investigate the potential of applying optically stimulated luminescence (OSL) for dating studies. The application of OSL techniques to archaeological ceramics for the past assessment of natural radiation doses was first suggested by Huntley *et al.* (1985), and has been applied in natural dosimeter with great success (Aitken, 1985; Roberts, 1997; and Wagner, 1998), and the method became firmly established for testing the authenticity of art ceramics (Stoneham, 1991). These studies have all been carried out using heated materials. Fortunately, heated materials are frequently

available, especially in archeological environments, where heated building materials such as ceramics are more widely used. Ceramic materials are suitable in dating, since they mostly have been adequately zeroed in the last zeroing event (e.g., at the time of manufacture) and they usually have a sufficient luminescence sensitivity. In this work, experimental studies were carried out on two ceramic water pipes, two ceramic floor and two ceiling tiles samples from Laodikeia collected during the 2002 excavation. From now on the abbreviation LDKY will be used for Laodikeia.

In the Hellenistic era, LDKY was the name given to a number of cities, founded by the successors of Alexander the Great. Our site is marked by the river Lykos (Çürüksu), and thus was called LDKY ad Lycum (Roman name, following earlier Hellenistic practice). LDKY ad Lycum is 6 km north-east of Denizli, and modern villages incorporated within the Hellenistic city's borders are Eskihisar, Goncalı, and Bozburun villages (Figures 1.1 and 1.2). Once founded by the Seleucid King Antiochos II sometime before B.C. 253, and named for his wife Laodike, the new city soon became the largest and most important city in the Lycos Valley. LDKY was completely leveled in the devastating earthquake in A.D. 494 after which it has never quite recovered. The site continued to be inhabited, and Byzantine writers occasionally mentioned Laodikeia, (Şimşek, 2004). Pliny states that the Antiochian city of LDKY was formerly called Diospolis, "the city of Zeus," and then Rhoas (Pliny, AD 77).

For this site no dating study has been done before the LDKY excavation that has been conducted together with the Archaeology Department of Pamukkale University (P.U.) and Denizli Museum Directorate teams. However, even though we are the first sample takers from the site, a M.Sc. thesis has been done for the LDKY site at P.U. before this study was completed. In the study, building ceramic samples taken from Laodikeia archaeological site (Denizli) have been examined.



Figure 1.1 Satellite photo of Laodikeia site, (Şimşek, 2004).



Figure 1.2 Plan of Laodikeia, (Şimşek, 2004).

- | | |
|---|---|
| 1. Council Building (Bouleuterion) | 22. Aphrodisias Gate |
| 2. South Bath Complex | 23. West Market Place (Agora) |
| 3. I. Water Distributing Center | 24. Round Building nearby Ephesos Street |
| 4. Stadium | 25. Roman Bridge on Asopos River |
| 5. Bath- Basilica (where samples were taken) | 26. II. Water Distributing Center |
| 6. West Bath | 27. II. Monumental Entrance |
| 7. East Bath | 28. Central Market Place (Agora) |
| 8. North Theater | 29. Arched Passage |
| 9. West Theater | 30. I. Monumental Entrance |
| 10. Fountain of Emperor Caracalla | 31. Cemetery Areas (Necropolis) |
| 11. Syrian Street | 32. Early Byzantine City Walls |
| 12. Square of the Emperor Cult (Temple A) | 33. East Byzantine Gate |
| 13. Byzantine Building | 34. Fountain of Septimius Severus (A Nymphaeum) |
| 14. Octagonal East Byzantine Building | 35. Ephesos Street |
| 15. Temple and North Basilica | 36. South Market Place (Agora) |
| 16. Southwest Basilica | |
| 17. Northwest Basilica | |
| 18. Central Basilica | |
| 19. Ephesos Gate | |
| 20. Hierapolis Gate | |
| 21. Syrian Gate | |

In Chapter 2, the fundamental concepts of luminescence process are introduced including the mechanism based on the band model. The chapter discusses the band model, giving its use to describe the basic concepts of luminescence, Optically Stimulated Luminescence (OSL) and Thermoluminescence (TL). The natural materials of OSL, the development of OSL as dating method and the dosimeter applications are also introduced in this chapter.

Chapter 3 describes the important characteristic features of the OSL system in the Department of Physics, METU, (the ELSEC 9010 optical dating system). The samples of OSL are sensitive to light. Therefore, the 9010 system has been installed in a dark room. The system was established in 1995 and three theses have been completed in the laboratory already by Yurdatapan, (1997); Buluş-Kırıkkaya, (2002) and Akoğlu, (2003). The system is equipped with the parts and software utilized for the OSL studies in this work. There is also an alpha counter (the ELSEC 7286 low level alpha counter) in the laboratory. In addition, this chapter introduces the samples used and the experimental methods including the sample preparation techniques modified during the work. Two distinct measurements have been carried out in the Laboratory to determine the age of the LDKY samples. The first measurement is equivalent dose, the amount of radiation that samples were exposed during burial, which is measured in grays (Gy). A sample gives off luminescence when exposed to a light source (Aitken, 1998). Paleodose is determined from the intensity of the luminescence signal. The second measurement is dose rate, the annual radiation accumulation rate (Gy/year) of the sample, which is measured from the concentration of radioactive isotopes within the sample and from surrounding soil (Aitken, 1985). The dose rate is an approximation of the radiation a sample has received over time, based on the assumption that the concentration of radioactive isotopes has remained constant. Fluctuations in the radiation levels over time are difficult to account for, and result in much of the uncertainty in OSL ages (Taylor and Aitken, 1997).

Chapter 4 tabulates the data and discusses the results of OSL analysis. Age calculations of LDKY samples carried out with three different processes by using different radiation coefficients. In addition, this chapter deals with the results of two quantities which are the equivalent and the annual dose of six different LDKY ceramic samples. These quantities need to be experimentally determined to reach an OSL age. An overview is presented of the different measurement protocols and procedures for equivalent dose (D_{eq}) determination, with specific attention to those that have been developed for feldspar.

In chapter 5, the conclusions of the studies are given. LDKY has been destroyed as a result of an earthquake and all the water pipelines have been renewed as the archaeologists claimed so. The dates of the pipeline samples may give also the date of the earthquake. Archaeologists also claim that LDKY has been set into fire during the Seljuk invasion and the dates of the ceiling tiles may give the date of invasion and fire.

CHAPTER 2

FUNDAMENTALS OF LUMINESCENCE DATING

Luminescence is the cool emission of light from material which is caused by the electrons during their movements from high energy level through low energy level. It can also be caused by the stimulation of trapped electrons from metastable energy levels, which are related to their subsequent recombination under photon-emission.

Electrons trapped at meta-stable sites, become free under certain conditions such as heating and/or illumination. Some of the electrons reach to the luminescence centers resulting in emission of light. If the process is done by heating it is called Thermo Luminescence (TL), if it is done by illumination of light it is called Optically Stimulated Luminescence (OSL).

Luminescence dating exploits the fact that ionizing radiation from natural radioactivity and cosmic rays excite electrons, which are partly stored in the crystal lattice. Since these charges accumulate with time, their amount and thus the intensity of the luminescence signal can be used for dating (Lang *et al.*, 1996).

Luminescence dating utilizes sediments, ceramics and stones which contain quartz and feldspar as natural dosimeters. Quartz and feldspar minerals are complex solids and present in archaeological and geological samples.

TL or OSL is the luminescence emitted on heating or illumination, respectively, due to the release of stored energy which has been accumulated in

crystalline materials through the action of ionizing radiation from natural radioactivity. When the material (pottery, brick and so on) is heated, either in production or during use, and when sediment is exposed to sunlight prior to deposition, the TL/OSL acquired over geological time is removed. Therefore, the luminescence "clock" is set to zero. Then, the TL/OSL accumulates in response to the ionizing radiation received during the burial period of the material. The time elapsed since last heating or illumination of ancient materials depends on the total absorbed radiation dose. Knowing the dose received per year (during burial) the age of the ancient material can be calculated.

When ionizing radiation (α , β particles and γ rays) interacts with an insulating crystal lattice, a net redistribution of electronic charge takes place. Electrons are stripped from the outer shells of atoms and though most return immediately, a proportion escape and become trapped at 'meta-stable' states within the crystal lattice. The net charge redistribution continues for the duration of the exposure and the amount of trapped charge is therefore related to both the duration and intensity of radiation exposure.

The effect of radiation such as gamma rays, beta particles (electrons), and alpha particles on a sample can be expressed in terms of a quantity known as absorbed dose. This is a measure of the radiation dose (as energy per unit mass) absorbed by a specific sample. Its SI unit is the Gray (Gy). An older unit, the rad (from **r**adiation **a**bsorbed **d**ose) is still in common use. The two units are related as follow:

$$1 \text{ Gy} = 1 \text{ J/kg} = 100 \text{ rad}$$

Dating of archaeological materials by the OSL method depends on the fact that, when mineral grains are isolated from daylight by burial, they begin to accumulate electrons in their traps. These electrons result from exposure to the

ionizing radiation emitted by the decay of naturally occurring radioisotopes, K-40, Th-232 and U-238, within the material. If the flux of ionizing radiation is constant, then the burial time of the grains can simply be determined by dividing the total dose (also called as burial dose, equivalent dose or paleodose) which have been accumulated during burial time to the Dose-Rate i.e.,

$$\text{Burial Time (year)} = \frac{\text{Burial Dose (Gy)}}{\text{Dose - Rate (Gy/year)}} \quad (2.1)$$

The dose-rate is also called as annual dose and it is equal to the dose received per year.

The dose rate (annual dose) represents the yearly rate at which energy is absorbed from the flux of nuclear radiation provided by thorium, uranium and potassium-40 in the material, as well as by cosmic rays. The annual dose is assumed to be constant and evaluated by the assessment of the radioactivity of the material determined both in the laboratory and on-site by using dosimeters.

Although the process is much more complex the main features of the OSL dating can be studied in terms of a simple model, as shown in Figure 2.1, (Aitken, 1985). The figure represents an ionic crystal with some defects.

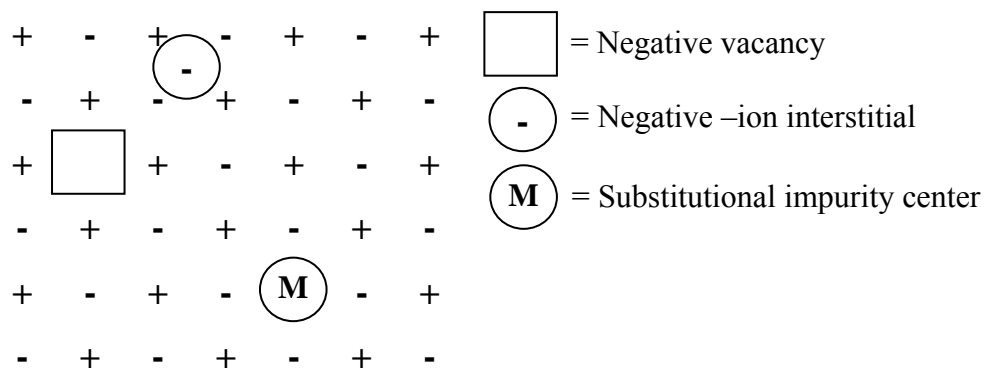


Figure 2.1 Simple types of defects in the lattice structure of an ionic crystal.

The defects in the mineral crystals i.e, negative ion vacancy, and negative ion interstitial, and substitutional impurity centers behave as the trap for electrons. The ionizing radiation from the decay of the naturally occurring radioisotopes (e.g. U, Th, K) interacts with a crystalline substance, freeing electrons from their normal atomic sites. Some of these electrons become trapped at the defect centers and, if the trap depth (E) is large enough, they will remain there indefinitely on a geological time scale. The number of these electrons is thus a measure of the total radiation dose since some event in which all the traps were emptied. It is assumed that electrons caught in traps stay in there indefinitely. In fact, the lifetime of an electron in a trap is not infinite but has a value that depends on the type of the trap (Aitken, 1989).

Luminescence dating is particularly appropriate when radiocarbon dating is not possible (either where no suitable material is available or for ages beyond the radiocarbon age limit). When the relationship between the organic materials and the archaeological context is uncertain, the particular advantage of luminescence dating is that the method provides a date for the archaeological artifact or deposit itself, rather than for organic material in assumed association. In the case of OSL dating, suitable material is usually available all throughout the site.

The age range for pottery and other ceramics covers the entire period in which these materials have been produced. The typical range for burnt flint, stone or sediment (burnt or un-burnt) is from about 50 to 300,000 years. The error limits on the dates obtained are typically in the range ± 3 to $\pm 8\%$, although recent technical developments now allow luminescence measurements to be made with a precision of in favorable circumstances.

Ceramics and burnt flint or stone must have been heated to at least up to 350°C in antiquity. The samples must be large enough to ensure that sufficient sample is available for dating after the removal of the outer 2 mm layer over the entire

surface. This removal will depend on the composition of the material. Typically a fragment whose volume is equivalent to at least 1 cm x 2cm x 2cm is required for measurement. In addition, as an absolute minimum, it is necessary to provide at least 100 gram soil or sediment sample in which the pottery, flint or other material was buried

It is preferred for the person that does luminescence dating should visit the site (during the excavation in archaeological contexts) either to collect samples or at least to advise for sample collection, and to measure the environmental contribution to the annual radiation dose using a portable gamma spectrometer or dosimeter. This can significantly improve the dating precision.

It is highly desirable that the deposits are as uniform as possible and that pottery or flint are not collected from near boundaries (edges of a trench or changes in soil type), or from a depth less than 30 cm from the present ground surface (Aitken, 1985).

2.1 General principles of luminescence dating

The luminescence dating is one of the radioactive dating techniques and it belongs to the subgroup which is based on the accumulation of radiation damage in a mineral. The radiation damage accumulation is the result of exposure to a low-level ionizing radiation in the soil. The longer the exposition of a mineral to the ionizing natural radiation the greater the intensity of the radiation accumulation is. The intensity of the radiation accumulation is consequently a measure for the total dose (the total amount of energy absorbed from the ionizing radiation) of the mineral that has received over a certain period of time.

In luminescence dating, the density of the radiation accumulation is detected as a small amount of light, which is called luminescence. The radiation

accumulation which is the hidden luminescence signal can be removed or set to zero by exposing to heat or light. For ancient pottery the ‘zeroing’ took place during manufacturing, when it was baked in a kiln. In the context of sediment dating, the zeroing event was the exposing to daylight during erosion, transport and deposition of the mineral grains (Figure 2.2) (Vandenberghe, 2003). This zeroing through exposure to sunlight is also called bleaching. Once the zeroing agent is no longer active, the luminescence signal can start to build up again. For instance, in the case of sedimentary mineral grains, the clock starts ticking when the samples were shielded from the sunlight by burial under other grains deposited on top of them. A comparison of the luminescence dating with the other dating methods is given in Table 2.1.

Table 2.1 Chart of some dating methods.

Method	Date Invented	Inventor	Materials	Dates B.P.
I. RADIOACTIVE				
1. Carbon 14	1949	Libby (Chicago)	Plant/animal life, charcoal, wood, burned bones	present- 70.000
2. Potassium-Argon	Late 1950	Korof (NYU) Many labs	Rocks, meteorites, feldspars, volcanic glasses	10.000-20.000.000
3. Thermoluminescence	1964	Johnson (Dartmouth)	Rocks, minerals, pottery	300-10.000
4. Optically Stimulated Luminescence	1985	Huntley et.al.	Rocks, minerals, pottery	50-500.000
5. Electron Spin Resonance	1945	M.Ikeya	Paramagnetic centers in minerals	present-billions
6. Fission Track	1965	Fleischer	Volcanic materials, glasses, apatites, micas, fossil bones	present-billions
II. GEOLOGICAL & BOTANICAL				
7. Varves	-	de Geer & Antevs (Sweden)	s Lake sediment from melting ice heets	present-10.000
8. Pollen Analysis	-	Van Post (Denmark)	pollen-trees, peat bogs	no accurate date
9. Dendrochronology	1901	Douglas (Arizona)	Tree-rings, sunspots, cross-dating	7.400
10. Archaeomagnetism Palaeomagnetism	1950s	-	Stone, baked clay, iron deposits	5.000-40.000
11. Shell	1960s	-	Shell refuse	-
12. Obsidian Hydration	1960s	U.S. Geological Survey	Obsidian	-
13. Parchment	1960s		Parchment, skins, leather	80 B.C.
14. Glass	1960s		Glass	Roman times - 1.st century

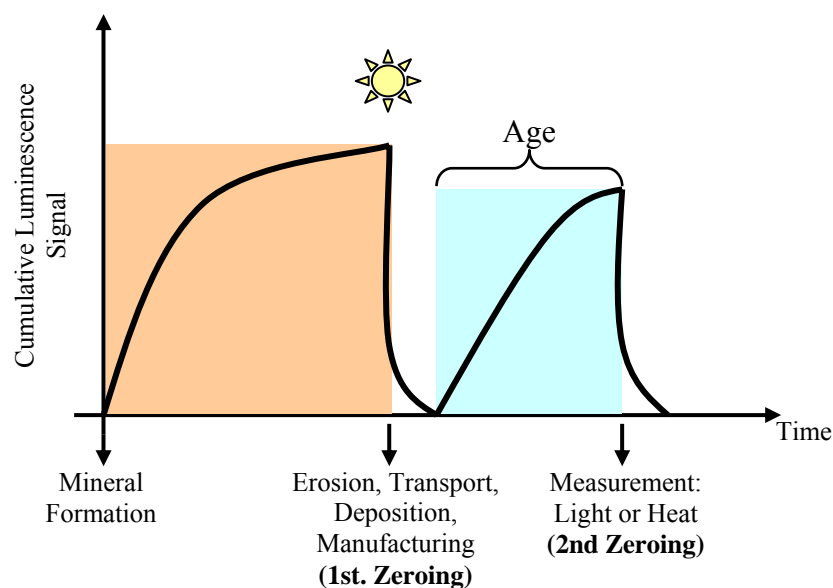


Figure 2.2 Schematic representation of the event that is being used in the luminescence dating of pottery and sediments. Minerals are continuously exposed to a low-level of natural radioactivity, through which they can acquire a latent luminescence signal. During erosion, transport and deposition, the minerals are exposed to sunlight and all the previously accumulated luminescence is removed (“bleaching”). Once shielded from the sunlight, the signal starts to build up again, until the moment of measurement in the laboratory. The age that is being determined is the time that has elapsed between these two zeroing events (Vandenberghe, 2003).

2.2 Mechanism of Stimulated Luminescence

The main processes causing luminescence can be described in terms of the energy level diagram for nonconducting ionic crystalline materials as shown in Figure 2.3; (Aitken, 1998 and Vandenberghe, 2003). In fact, other types of insulators such as covalent solids and glasses also exhibit TL or OSL; metals do not.

According to this model, electrons are associated with discrete ranges of energy, which are called bands. The lowest energy band is the valence band and the highest energy band is the conduction band. The gap between the two

bands is called ‘forbidden zone’. In a perfect crystal, no electron occupies a position in this zone.

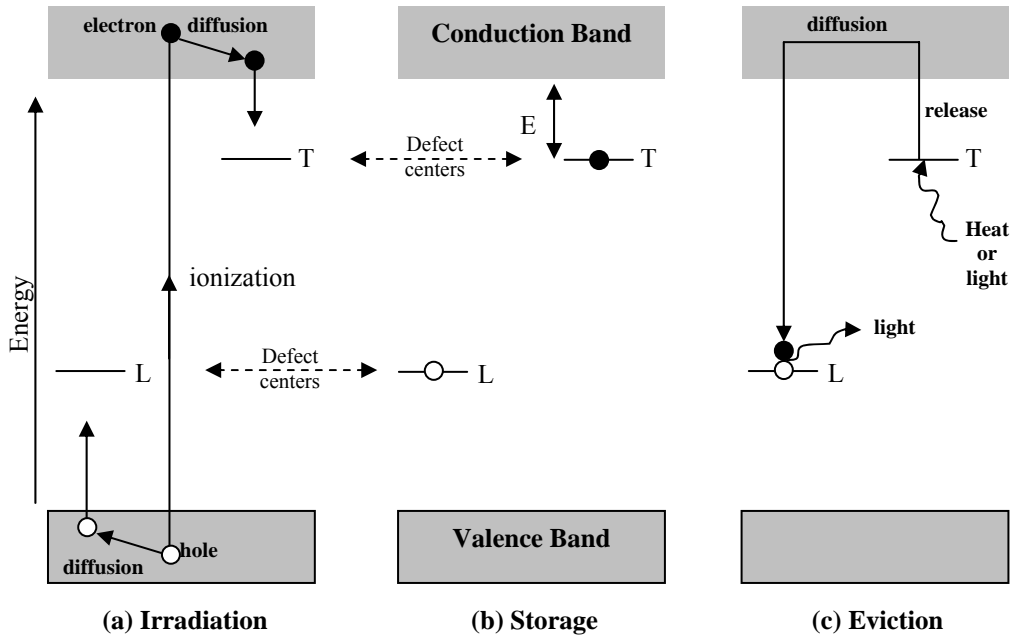


Figure 2.3 Energy-level representation of the luminescence process (Aitken, 1998 and Vandenberghe, 2003). ○: hole; ●: electron, L: luminescence center, T: trapped centre.

However, in any natural crystal, defects are present that disturb the perfectly ordered crystalline structure. Many types of defects are possible such as impurities and missing atoms. These defects give rise to the existence of energy levels within the forbidden zone. The defect states are associated with the defects themselves, and therefore they are called localized energy levels. These localized energy levels are the key to the luminescence phenomenon, as they carry the memory of exposure to nuclear radiation. In other words, luminescence requires the existence of lattice defects. In nature, a low level of nuclear radiation is universal. This radiation has ionizing effect and, upon interaction with the crystal, can promote an electron from the valence band into the conduction band, Figure 2.3(a). For every electron removed from the

valence band is an electron vacancy, termed a hole, is left behind and both the electron and hole are free to move throughout the crystal. In this way, energy of the nuclear radiation is taken up. The energy can be released again (usually as heat) by recombination. Although most of the charges recombine directly, another possibility is that the electron and the hole are trapped at the defect centers traps. In this case, the radiation energy is stored temporarily in the crystal lattice and the system is said to be in a metastable state, Figure 2.3(b). Energy is required to remove the electrons out of the traps and to return the system to a stable situation. The amount of energy that is necessary is determined by the depth (E) of the trap below the conduction band. This trap depth is one of the parameter to determine the life time of an electron in the trap. To empty deeper traps, more energy will be required and those traps are more stable over time. For dating, we are only concerned in those traps deep enough (i.e. ~ 1.6 eV or more) for the age of at least several million years. By heating or shining a light on the samples, electrons are removed from the electron traps and some of these reach luminescence centers (L) resulting in emission of light (Figure 2.3(c)). As mentioned before, if the process is done by heating it is called TL, if shining of light is used it is called OSL.

In summary, the steps were given in Figure 2.3 are as follows,

1. Ionization of electrons by nuclear radiation.
2. Immediate capture of some of these electrons at traps, where they remain stored as long as the temperature is not raised or not exposed to light.
3. Eviction from the traps due to heating or exposing to light during the measurement process centuries later.

4. Recombination almost instantaneously, some of these evicted electrons with luminescence centers, accompanied by emission of light. The amount of light is proportional to the number of trapped electrons, which in turn is proportional to the amount of nuclear radiation to which the crystal has been exposed and therefore to the time that has elapsed since the traps were last emptied.

The main difference between TL and OSL is the stimulating source. Although the mechanisms are the same for both techniques there are some advantages of OSL over TL. These can be summarized as follows:

- OSL can be measured near or at room temperature hence it is less destructive and more sensitive method than TL.
- Parts of OSL signal can be measured many times on same sample however in TL this is impossible since the measurement involves the total erasure of the signal. Therefore, for normalization of aliquots short shines of OSL can be used.
- After measurement of OSL a TL signal can be measured on the same sample however the reverse may not be possible.
- OSL measures the electrons held in traps, which are the most sensitive to light and is thus particularly important in dating geological sediment samples, which had been zeroed in the past by sun bleaching. Furthermore, in many cases, OSL has the same dose response as TL. (Bøtter -Jensen, 2000).

There are some studies for more complex and detailed accounts on the physical theory of the process (McKeever, 1985; Chen and McKeever, 1997; and Bøtter Jensen *et al.*, 2003a).

2.3 Signal growth and trap stability

From the previous section it is clear that the intensity of the luminescence signal is proportional to the number of electrons trapped: the longer the irradiation time, the more electrons will have become trapped and the higher the luminescence intensity. However, there are two limitations. First, the total number of traps that is available for storing the charge is limited. Consequently, under continuous irradiation, the available traps are filled step by step (Pauli exclusion principal) and sooner or later saturation will be reached. A second limitation is that electrons are also unexpectedly evicted from their traps, a process which is termed ‘thermal fading’.

Taking the effects of thermal fading and saturation into account, the growth of the luminescence intensity (I) as a function of time was described by the following Equation 2.3 (Wagner, 1995 and Vandenberghe, 2003):

$$I(t) = s \dot{D} \tau (1 - e^{-\frac{t}{\tau}}) \quad (2.3)$$

where:

s : the sensitivity; amount of luminescence per unit dose

\dot{D} : the dose rate; the dose received per unit time

τ : the apparent mean lifetime

t : the time span of signal accumulation

The term $(s \dot{D})$ refers to the increase in luminescence intensity due to the filling of the traps, while the term $\tau(1 - e^{-\frac{t}{\tau}})$ takes the saturation and thermal fading effects into account. Equation 2.3 can be simplified to:

$$I(t) = I_{max} (1 - e^{-\frac{t}{\tau}}) \quad (2.4)$$

where, “ $I_{max} = s \dot{D} \tau$ ”, i.e. the maximum intensity that can be built up and measured. The apparent mean lifetime, τ , can be written as follow (Wagner, 1995; Vancraeynest, 1998; Vandenberghe, 2003):

$$\tau = \frac{\tau_s \tau_T}{\tau_s + \tau_T} \quad (2.5)$$

where, τ_s is a decay constant (also saturation characteristic) taking into account that the number of traps is limited and τ_T is the mean lifetime. The mean lifetime is the average residence time of electrons in a given type of trap and at a certain given temperature T .

It is clear from the above Equation 2.5 that both the saturation characteristic (τ_s) and the long-term stability of the signal (τ_T) determine the highest intensity to which a luminescence signal can grow, and hence also the upper dating limit that can be attained.

Under these considerations the saturation dose of the mineral depends on the first approximation (saturation). For instance, quartz generally saturates at a much lower dose compared to feldspars. Prescott and Robertson (1997) proposed an age limit of 100-200 ka (1ka = 10^3 year) for quartz while age provides up to 1 Ma (1Ma = 10^6 year) for feldspar, if they do not suffer from anomalous fading (see section 2.4). However, if the quartz mineral is exposed to a very low-level of natural radioactivity, the traps are also less rapidly filled, which extends the age range over which this mineral can be used. When a low dose rate enabled, quartz-based luminescence ages was obtained as old as ~700-800 ka (Huntley *et al.*, 1993, 1994; Huntley and Prescott, 2001).

Besides the limitations imposed by signal saturation, the mean lifetime also restricts the age range over which a luminescence signal can be used for dating; the luminescence signal employed should be sufficiently stable. This means

that only those traps should be evicted during the measurement from which there has been a negligible loss of electrons over the time span that is being dated. It is usually assumed that unstable luminescence arises from shallow traps while stable luminescence arises from deep traps. The probability for electrons to escape from a deep trap is low, and the lifetime (τ_T) is correspondingly high. The possibility exists due to the random chance of an abnormally large energetic lattice vibration which causes the eviction.

At a constant temperature, the number of trapped electrons, n , decays exponentially with time according to Equation 2.6:

$$n(t_2) = n(t_1) e^{-\frac{t_2-t_1}{\tau_T}} \quad (2.6)$$

In the context of dating, the time interval t_2-t_1 of interest is the age of the sample. However, when calculating the fraction of electrons that spontaneously escape during this period of time, it must be taken into account that there are no electrons in their traps at time zero [i.e. at $t_1 = 0$, $n(t_1) = 0$] and that they become trapped at a uniform rate thereafter. For such a situation, it can be shown to a good approximation (Aitken, 1985) that the fractional loss of luminescence due to escape during the age span of the sample, t_s ($= t_2-t_1$), is given by $1/2(t_s/\tau_T)$ as long as t_s does not exceed one third of τ_T . This means that to avoid an age underestimation by e.g. 5%, the lifetime consequently needs to be at least 10 times the age.

The trapped electron mean lifetime, in the case of first order kinetics, is given by the following equation (Aitken, 1985; Vandenberghe, 2003)

$$\tau_T = s^{-1} e^{\frac{E}{k.T}} \quad (2.7)$$

where:

s : the frequency or pre-exponential factor (in s^{-1}); this may be thought of as the number of attempts to escape per second

- E : the depth of the trap (in eV)
 T : the absolute temperature (in K)
 k : Boltzmann's constant (8.6173×10^{-5} eV K⁻¹)

Predicting lifetimes (τ_T) is useful as it helps to establish the likely time-range over which a given signal from a given mineral will be used. It is also important because a measured OSL signal does not contain any intrinsic information with regard to its stability. Some further considerations regarding signal stability and lifetimes that are directly relevant to the present work are discussed in Chapter 4. The OSL signal arises from electrons that are evicted out of all traps that are sensitive to the light employed for stimulation, whether these traps are deep (stable) or shallow (unstable).

In nature, the filling rate of the traps is low. The luminescence signal measured from a natural sample will be primarily associated with deep traps since the shallow traps lose their electrons quickly due to thermal fading. However, it is necessary to irradiate the sample in the laboratory, and to compare the artificial luminescence signals so induced with the natural signal. In the laboratory, the doses are added to the samples at a much higher rate than those in nature. Now, the shallow traps will be filled and, owing to the short time scale over which the experiments are carried out, they may contribute significantly to the artificial signal. Therefore, it is necessary to remove this unstable "contaminating" luminescence by emptying the shallow traps before the signal is measured. This emptying is usually accomplished by heating the sample prior to measurement. This treatment is called preheating and it will be further discussed in Chapter 3 and 4, together with the additional reasons for why it is necessary.

2.4 Anomalous fading

Equation 2.7 describes the expected mean lifetime of an electron in a trap of depth E and escape frequency s at a storage temperature T . For deep traps and at low temperatures, the lifetime will consequently be quite large and leakage of electrons from these traps will be low. However, it has been observed for many materials that the electrons are released from their traps at a much faster rate than those predicted by Equation 2.7. This fading of the luminescence signal is therefore termed ‘anomalous’ (abnormal) fading, (Figure 2.4). For natural minerals relevant to dating, the result of anomalous fading is an age shortfall, regardless of whether TL or OSL signals are being used. The effect was first observed by Wintle *et al.* (1971) and Wintle (1973), when trying to date feldspars extracted from volcanic lava with TL. The ages obtained were significantly lower than the expected ages for the lava flows. The effect has been subsequently observed and investigated in a number of studies (Wintle, 1977; Clark and Templer, 1988; Spooner, 1992; 1994; Visocekas, 2000; Auclair *et al.*, 2003).

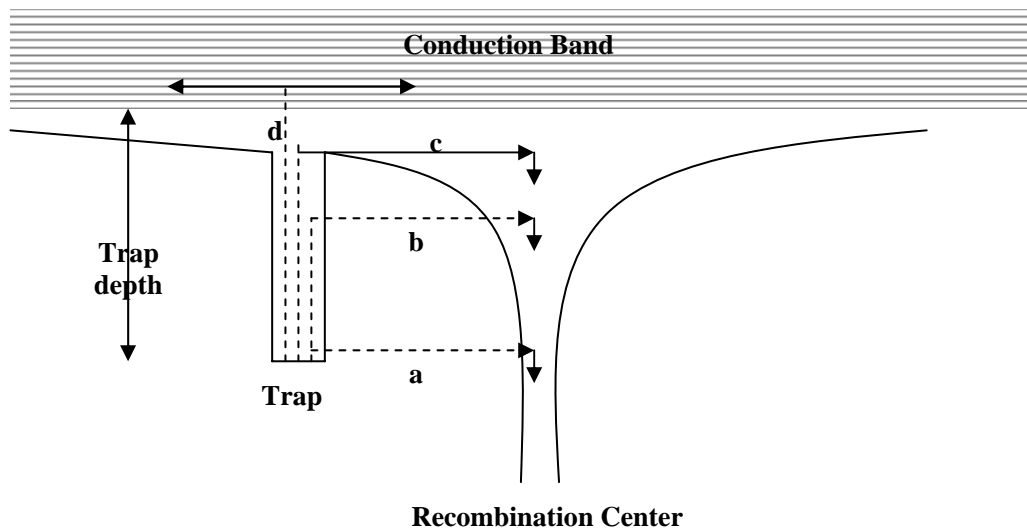


Figure 2.4 Anomalous fading of the trapped electrons. Escape roots from a trap: a) thermal tunneling, b) thermally or optically assisted tunneling, c) and d) thermal or optical eviction (Visocekas *et al.*, 1976 and Aitken, 1985).

A number of natural dosimeters, most notably zircon and several types of feldspars suffer from anomalous fading. It is generally accepted, however, that quartz is not affected by this phenomenon. Wintle (1973) reported no loss in TL after storage of the quartz for two years, while Roberts *et al.* (1994) did not detect any loss in the OSL from quartz after seventy days storage at room temperature. Readhead (1988) found anomalous fading of TL in quartz from Southeastern Australia, but Fragoulis and Stoebe (1990) and Fragoulis and Readhead (1991) subsequently found fading feldspar inclusions to be present in these quartz grains.

Among all of the mechanisms that have been proposed to explain anomalous fading, quantum mechanical tunneling of electrons to nearby recombination centers is probably the most accepted one. For more details on this, and other suggested explanations, reference is made to Aitken (1985), Aitken (1998), McKeever (1985), Chen and McKeever (1997) and Bøtter-Jensen *et al.* (2003a). These publications also provide a comprehensive overview on the reported observations of the effect, and address practical issues that are relevant in a dating context, such as ways to detect, overcome or correct for anomalous fading. Recent work on the correction for fading in feldspar minerals is that by Auclair *et al.* (2003) and Lamothe *et al.* (2003).

2.5 Stimulation of the signal

From sections 2.1 and 2.2, it is clear that the same production mechanism is responsible for the two luminescence phenomena, TL and OSL, and that the only difference between them lays in the way the electrons are stimulated out of their traps.

In OSL, the electron escapes from its trap as the result of the absorption of a photon of light with a sufficient energy. The rate of eviction depends on the intensity of the stimulating light, the wavelength of the light and the sensitivity

of the trap to light. There is also a dependency on the temperature of the material.

The intensity refers to the number of photons arriving at within a certain time. It can easily be understood that the more photons arrive at per unit of time, the more electrons will be stimulated out of their traps. The light-sensitivity of a trap is not well described by the trap depth E ; it depends on other characteristics of the trap, as well as on the wavelength of the stimulating light (Aitken, 1998). In general, shorter wavelengths (higher energy) are more effective in stimulating electrons from their traps. The trap depth is given as,

$$E(eV) = \frac{1240}{\lambda(nm)} \quad (2.8)$$

Hence, a first expectation would be that in order to evict an electron from a trap having sufficient depth, say 1.4 eV, to retain electrons without leakage on a long term time scale the wavelength of the stimulating light needs to be shorter than $\left(\frac{1240}{1.4} = 886 \text{ nm}\right)$. This means that eviction can be possible even with a wavelength as long as that of the near-infrared (700-800 nm). Consequently, stimulation and luminescence emission wavelength regions need to be well separated from each other. Furthermore, the wavelength of the luminescence signal that is used for dating should be shorter than the one used for stimulation. The type of mineral that is under investigation also plays a role in the selection of the most appropriate light source for stimulation. A given wavelength can be effective for stimulating a luminescence signal from some minerals, whereas for other minerals, it proves to be not suitable.

From the above considerations, it was found that for quartz, for instance, stimulation by visible light with a wavelength somewhere in the blue to green region of the spectrum is appropriate. For feldspathic minerals, on the other hand, it has been found that long wavelengths, in the infrared region (800-900

nm), can also be used (Hütt *et al.*, 1988). It can be mentioned here that longer wavelengths can also be effective, if the temperature of the sample is raised. This effect is called thermal assistance.

Depending on the wavelength used for stimulation, the resulting luminescence is termed **infrared stimulated luminescence** (IRSL), **blue-plus-green stimulated luminescence** (BGSL), **green light stimulated luminescence** (GLSL or GSL) or **blue light stimulated luminescence** (BLSL or BSL). OSL generally refers to any luminescence signal that is obtained via stimulation with light, regardless of the wavelength. In some literature, however, the term OSL should be read as encompassing visible stimulation wavelengths only. To avoid confusion, it is therefore more appropriate to specify the stimulation wavelength, for example as OSL (514.5 nm).

2.6 Materials Studied by OSL

Minerals such as feldspars and quartz are the most widely used minerals in the optical dating. The choice of the mineral that is being used usually depends on the availability of the mineral within the sample, the age of the samples and so on. Quartz saturates at lower doses than feldspars, and so the use of feldspar might prove to be advantageous for dating older deposits.

For coarse (sand-sized) grains (of ~0.1 mm in diameter), the different mineral fractions can be easily separated from each other, this is not the case for fine (silt-sized) grains (of ~0.01 mm in diameter). Usually, the measurements are then carried out on the polymineral fine fraction, which is a mixture of all kinds of minerals with a grain size within the range 4-11 μm .

Besides feldspar and quartz, ZrSiO_4 (Zircon) (Smith *et al.*, 1986; Smith, 1988) and $\text{Ca}_5(\text{PO}_4)_3(\text{F},\text{OH},\text{Cl})$ (Apatite) (Smith *et al.*, 1986) have been found to emit OSL as well.

Compared to feldspar and quartz, these minerals occur in materials in much smaller quantities, which limit their use in any case. Finally, it is perhaps worth mentioning that also glass extracted from volcanic ash deposits has been found to emit OSL (Berger and Huntley, 1994; Berger and Neil, 1999). Encouraging initial results were obtained, but further work is necessary to establish the full extent to which the glass might be suitable for optical dating.

CHAPTER 3

MATERIALS and METHODS

In this chapter, sampling, the OSL dating and Alpha counting systems, dose rate calculations of Sr-90 β radiation source, sample preparation techniques, measurement techniques of equivalent dose and annual dose of samples are described. In order to reduce noise level of the measurements, OSL dating and Alpha counting systems were explained and calibrated as given in Appendix A and B.

3.1 Samples of Laodikeia Archaeological Site

The ceramic samples of Laodikeia were taken under the red light during the night excavation. Before and while taking the samples, opinions and ideas of the archaeologists were considered and the six samples were selected. Figure 3.1(a, b), Figure 3.2(a, b) and Figure 3.3(a, b) show the places and the types of the samples, which were taken. Shapes of some samples are given in Figure 3.4.



Figure 3.1(a, b) Ceramic floor tiles of the room which is at the right side of North of the front church door entrance. (LDKY-1: ceramic floor tile which was exposed to the sunlight, LDKY-2: ceramic floor tile which was not exposed to the sunlight.)



Figure 3.2(a, b) Ceramic water pipes which were taken from the front of north wall of the church. (LDKY-3 and LDKY-4 are the ceramic water pipes which were not exposed to sunlight.)



Figure 3.3(a, b) Ceramic ceiling tiles which were taken from the entrance of the church door. (LDKY-5 and LDKY-6 are the ceramic ceiling tiles which were not exposed to sunlight but they were in a fire layer and hence were exposed to heat.)

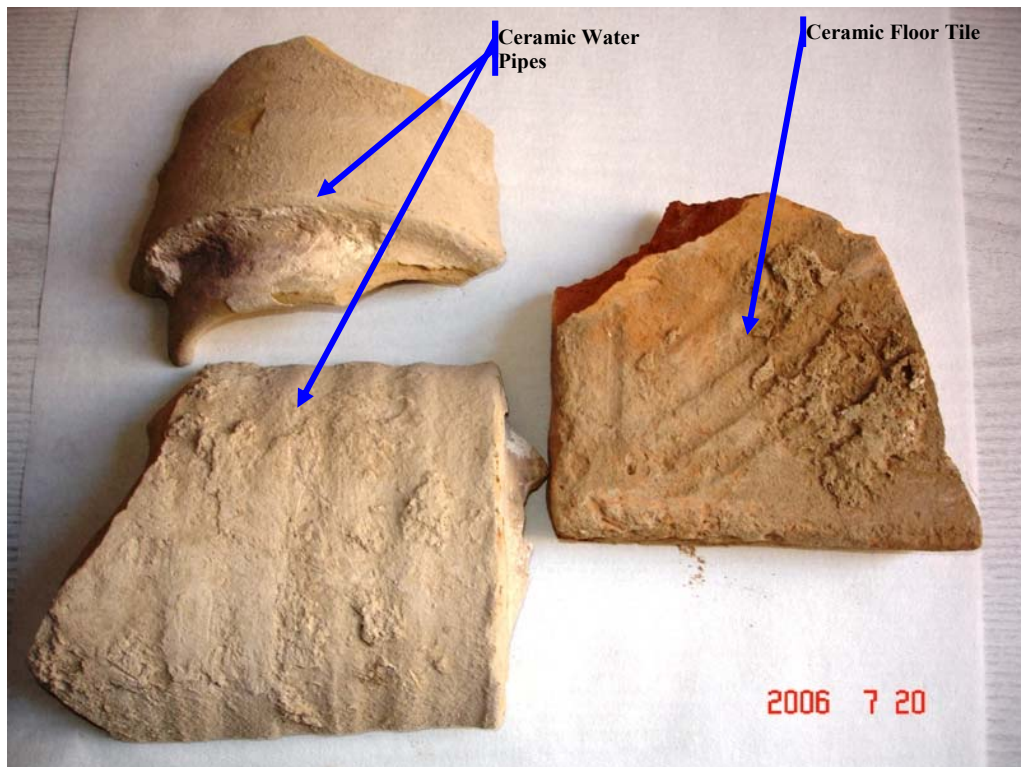


Figure 3.4 Ceramic water pipes and a floor tile taken from Laodikeia site.

The samples examined in this study are given in Table 3.1.

Table 3.1 The samples examined in this study.

Sample Name	Location	Sample Type	Remark
LDKY-1	Entrance of Bath-Basilica	floor tile	exposed to sunlight
LDKY-2	Entrance of Bath-Basilica	floor tile	not exposed to sunlight or fire
LDKY-3	Bath-Basilica Agora	water pipe	not exposed to sunlight or fire
LDKY-4	Bath-Basilica Agora	water pipe	not exposed to sunlight or fire
LDKY-5	Entrance of Bath-Basilica	ceiling tile	exposed to fire
LDKY-6	Entrance of Bath-Basilica	ceiling tile	exposed to fire

3.2 Age Determination

As mentioned in Chapter 2, age equation is,

$$Age (years) = \frac{Equivalent Dose (Gy)}{Annual Dose (Gy/year)} \quad (3.1)$$

Here, the equivalent dose (paleodose) is the dose accumulated during burial time of material and in general, denoted by D_{eq} . The annual dose is also known to be dose rate which represents the rate at which energies are absorbed from the flux of nuclear radiation; it is evaluated by assessment of the radioactivity of the sample, carried out both in the laboratory and on site (Aitken, 1998).

Procedures for evaluation of dose rate are the same for optical dating as for thermoluminescence. For evaluation of paleodose the basic principles are the same but there are substantial practical differences.

Figure 3.5 shows the dating signal as an example which obtained from a portion of the mineral (e.g. quartz) grains extracted from a sample deposited 12000 years ago. In this case a beam of green light from a laser was used to stimulate the signal but other stimulation sources and other wavelengths can also be used (Aitken, 1998).

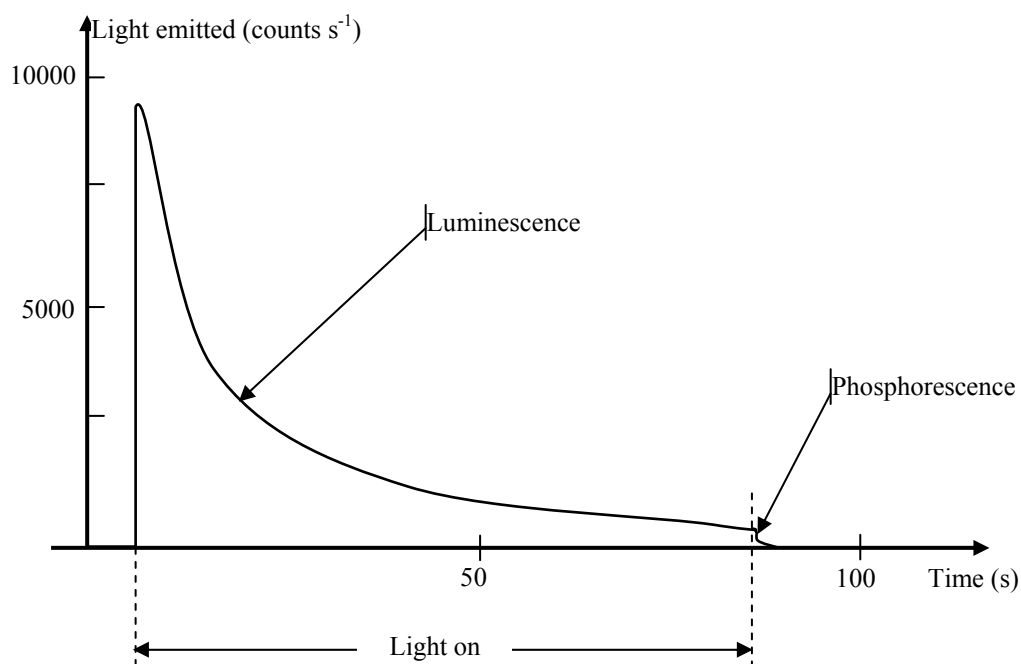


Figure 3.5 The depletion of signal with time (Aitken 1998).

The ‘shine-down’ curve (Figure 3.5) illustrates that bleaching is an inevitable accompaniment to signal stimulation. If the stimulation has not been continued long enough for the luminescence to reach zero, there is not an immediate fall to zero when the laser beam is shut off. This part is known as optically stimulated phosphorescence and there are some potential advantages, not yet fully explored, in using this part for dating, (Aitken, 1998).

3.3 Evaluation of Paleodose (Equivalent Dose, D_{eq})

One of the most important steps in determining the age of the sample is to measure the equivalent dose (paleodose). There are various methods for measuring the paleodose such as Multiple Aliquots Additive Dose (MAAD), Multiple Aliquots Regeneration Dose (MARD) and Single Aliquots Regeneration (SAR) techniques.

In order to measure luminescence intensities of aliquots of samples, Figure 3.6 shows the block diagram of OSL system. Figure 3.6a shows the trap mechanism for the nonconductive materials (luminescence mechanism was already given for nonconductive materials in Chapter 2). Figure 3.6b shows the stimulating light source and its wavelength specification for the eviction of the certain traps of the sample. IR diodes can be used as a stimulating light source. Other types of light sources such as laser or other type of diodes can also be used. In addition, stimulating light source and its wavelength is also depended on sample type. For example, while IR diodes or laser is suitable for feldspar and polymineral samples, green or blue light diodes or laser is suitable for quartz samples. Figure 3.6c shows the separation mechanism of the back-scattered and emitted photons from sample by using an optic filter. For example Schott BG-39 filter allows the transition of the photons which are in the range of 350 and 600 nm wavelengths. Figure 3.6d shows exponential decay of luminescence intensity in time when the current wave (CW) of the light source is continued. The CW-OSL measurement mode is most commonly employed technique, where intensity of the stimulated light is kept constant over time and luminescence decay is observed. However, one can also change the type of the current such as a pulse or a linear growth function (Bulur, 1996) but this time emitted luminescence curve is going to be different from the continues one, (CW-OSL).

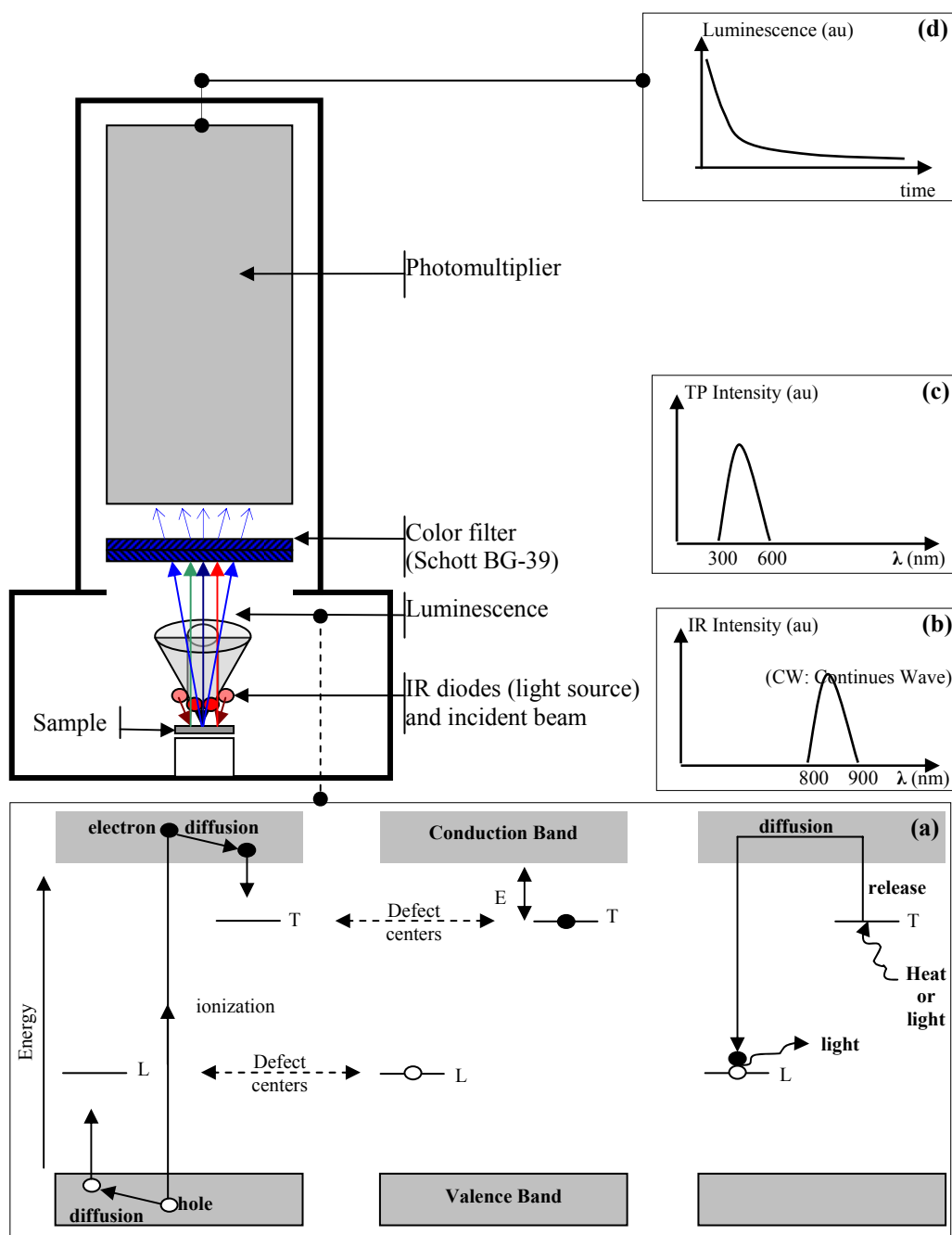


Figure 3.6 Block diagram of OSL system and luminescence measurement. (a) shows the mechanism of luminescence with band model, (b) shows the emitted photon spectrum range of the IR diodes, (c) shows the allowed transmitted photon (TP) spectrum range by the Schott BG-39 colour filter and (d) shows the decay of the luminescence signal (dating signal).

3.3.1 MAAD (Multiple Aliquots Additive Dose) Technique

The essential base of this method (alternatively, the additive-dose method, or, the extrapolation method (MAAD)) is illustrated in Figure 3.7. A number of equal portions-aliquots are prepared and divided into groups, with typically half-a-dozen or more in each group. One group is reserved for measurement of the natural OSL and the other groups are given various doses of laboratory radiation before measurement, the same dose for each member of a group.

The luminescence intensity versus added dose graph is a straight line with positive slope, as shown in Figure 3.7. The paleodose (or equivalent dose: D_{eq}) is determined from this graph by extrapolating the straight line to the horizontal added dose axis. The intercept is equal to the paleodose D_{eq} . The intensity of luminescence emitted by each aliquot is determined by integrating its luminescence decay curve (Figure 3.8).

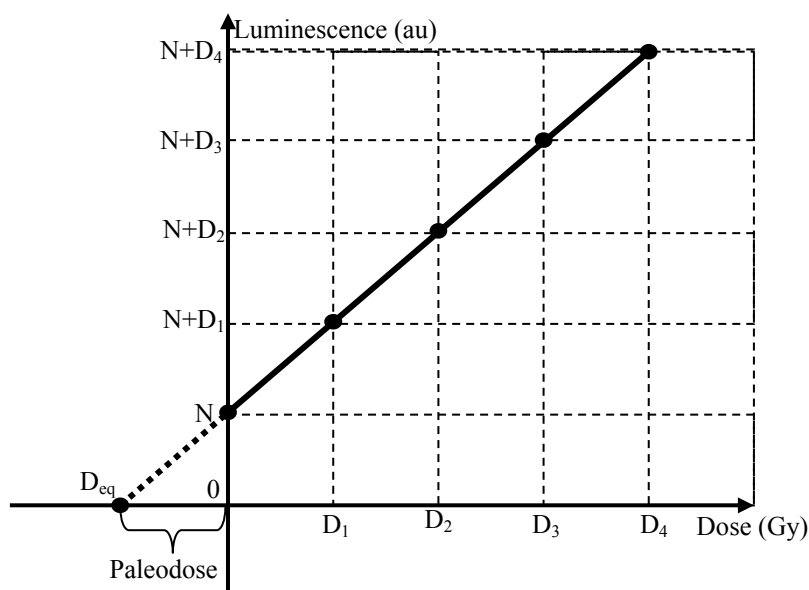


Figure 3.7 Additive dose method of paleodose evaluation. Each data point is the average OSL from a group of aliquots, all members of each group have been given the same laboratory dose (except for the lowest point, N, for which the laboratory dose is zero). In the case shown the growth is linear with dose, i.e. a straight line is a good fit to the data points; the paleodose, D_{eq} , is read off as the intercept on the dose axis.

Prior to measurement, all groups including those used for measurement of the natural radiation are normally subjected to preheating (Section 3.1.2); this is also the case with the regeneration method below.

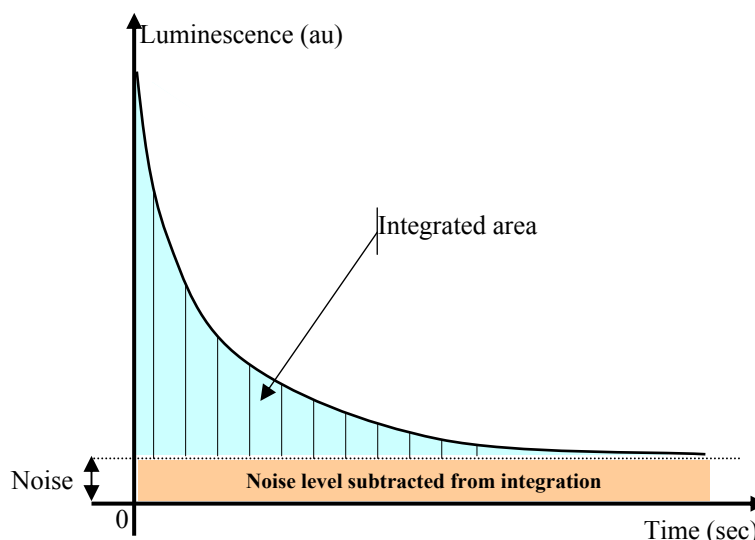


Figure 3.8 Decay curve of luminescence signal from natural or already dosed sample. The integration of this curve gives total luminescence during the illumination after subtracting the luminescence which comes from background noise of the device (PM tube).

3.3.2 **MARD (Multiple Aliquots Regenerated Dose) Technique**

In this method, all except the natural aliquots are bleached to near zero and then given laboratory doses as illustrated in Figure 3.9. The paleodose by regeneration is obtained by direct comparison of the natural OSL with the OSL resulting from laboratory irradiation as illustrated in Figure 3.9. The advantage of this method is that no extrapolation is induced, only interpolation, and so, uncertainties due to nonlinearity are reduced, if not eliminated. The critical disadvantage is that if there is a change in sensitivity (OSL per unit dose) between measurements of the natural OSL and measurements of the regenerated OSL the paleodose will be in error, unless correction for the change can be made.

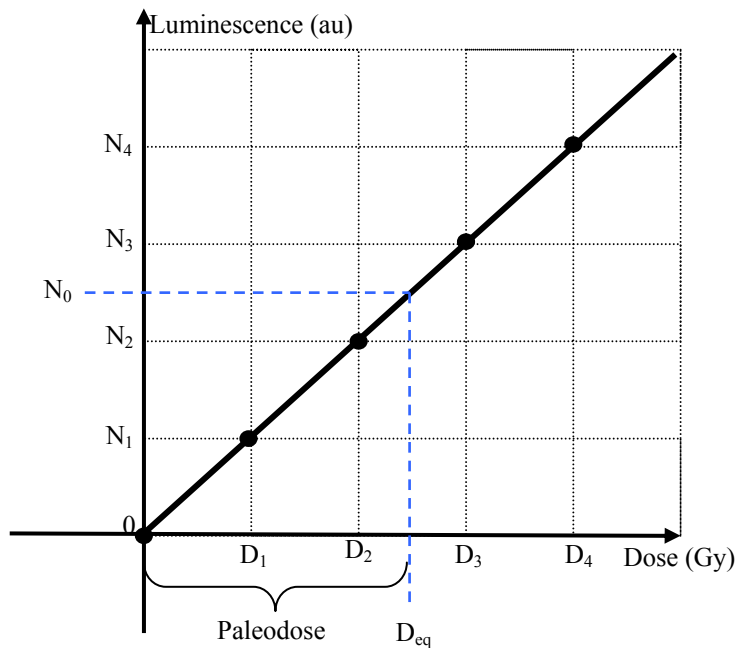


Figure 3.9 Additive regenerated dose method of paleodose evaluation. Each data point is the average OSL from a group of aliquots; all members of each group have been given the same laboratory dose (except for the 1st group, N_0 , for which the laboratory dose is zero). In the case shown the growth is linear with dose, i.e. a straight line is a good fit to the data points; the paleodose, D_{eq} , is read off as the interpolation of N_0 on the dose axis.

3.3.3 SAR (Single Aliquot Regeneration) Technique

SAR technique is similar to the MARD technique with the exception of the number of samples. In this method just one sample is enough for the measurements. The advantages of this method are that no normalisation and no more amount of sample are needed. One of the most important disadvantages of this technique is possibility of changing of sensitivity of the measurement since the sample will be dosed, illuminated and heated several times.

3.4 Preheating

In order to work with stable (deep) traps, unstable (shallow) traps must be emptied. Deep traps are more stable than the shallow ones. Working on stable traps is more convenient and better results can be obtained for dose measurements. Therefore, electrons from the shallow traps must be removed. The removal of the electrons from the shallow traps can be done by heating. This process is called preheating. The preheating temperature and heating time depend on the depths of the traps which will be emptied. Another correction factor is normalization as explained below.

In general, preheating temperature and duration time for quartz is 48 hours at 150 °C (Wolfe *et al.*, 1995), 16 hours at 160 °C (Stokes, 1992), 5 minutes at 220 °C (Rhodes, 1988 and 1990) and 1 minute at 240 °C (Franklin *et al.*, 1995). In addition, preheating temperature and duration time for feldspar is 2 hours at 160 °C (Aitken, 1998).

3.5 Normalisation

It is practically impossible to prepare identical aliquots of samples. Each aliquot may be different from the others with respect to the amount of the sample it contains. Furthermore, an aliquot may have grains of different size and type. By doing a normalisation process, these differences may be taken into account. For normalisation a relatively short shine (such as an IR shine for 0.1 s) is given to each aliquot before any additional dose (Aitken, 1985). After the short shine the luminescence is measured for each aliquot and the average luminescence \bar{L} is calculated as

$$\bar{L} = \frac{\sum_{i=1}^n L_i}{n} \quad (i = 1, 2, \dots, n) \quad (3.2)$$

Where n is the number of aliquots and L_i is the measured luminescence of the i^{th} aliquot. The normalisation constant C_i is defined as

$$C_i = \frac{\bar{L}}{L_i} \quad (3.3)$$

The normalised luminescence $(NL)_i$ for the i^{th} aliquot is calculated as

$$(NL)_i = C_i \cdot L_i \quad (3.4)$$

The normalisation process requires the same short shine for all aliquots.

Ideally there should be no scatter in the normalized OSL from a group of aliquots that have received the same dosing. In practice the scatter is often quite substantial and it is uncommon for the standard deviation to be much better than ± 5 per cent (Aitken, 1998).

3.6 Sample Preparation

Sample preparation is another important step in OSL measurements. The fine grain technique is used in order to include α -radiation contribution on natural dose measurements. Since the α -radiation has extremely short range of travel in pottery fabric (about 25 μm) grain size of the samples must be in the (1-9) μm range. For such grains there is full penetration of α particles and the attenuation of the α contribution is due to only its poor effectiveness (Aitken, 1998).

The mineralogical composition of each sample is generally determined using the X-ray diffraction analysis (XRD).

3.7 Size distribution of the samples

In order to obtain fine grains (1-9 μm) powdered samples should be subjected to the size distribution treatment and the size distribution is done in two ways;

1. by sieving the powdered dry sample with different sized screens,
2. by dispersing the powdered sample in a fluid and then by settling the grains at different time periods according to Stoke's law (Fleming, 1979).

3.8 Annual Dose Measurements

Naturally absorbed equivalent dose (paleodose) of the archaeological or geological sample is due to the radioactive isotopes present within the sample and in the surrounding soil. The internal radioactivity of the sample itself is related to its U, Th and K content. These elements emit α , β particles and γ rays (see Table 3.2). The same isotopes also exist in the soil around the sample and this external radioactivity also contributes to the equivalent dose. Another contribution is from the cosmic rays and their secondaries penetrating through the soil and sample.

Table 3.2 Components of annual dose from potassium, rubidium, thorium and uranium for given concentrations ^a (Aitken, 1985).

	Alpha	Effective alpha	Beta	Effective beta	Gamma	Effective gamma
Potassium	-	-	0.830	0.853	0.244	0.244
Rubidium	-	-	0.023		-	-
Thorium	0.738	0.308	0.029	0.0103	0.0514	0.0208
Uranium	2.779	1.260 ^b	0.146	0.0610	0.115	0.0056
Cosmic	-	-	-	-	0.30	0.15

^a Values are quoted in milligrays per year and they are for concentrations (by weight) as follows: 1% of natural K, 50 ppm of natural Rb, 1 ppm of natural Th, and 1 ppm of natural U.

^b The pre-radon components include radon-219 and its daughters.

The three types of radiation (α , β and γ) have different penetrating powers and this difference plays a very important role in luminescence dating. However, since the low energy α and β particles have low penetrating distance, external dose effects of these particles on the sample can be neglected by removing a few millimetres of outer layer of the sample (Aitken, 1998). For a correct age calculation, the annual dose absorption rate of the sample must be determined with almost no error in it.

There are four components of the annual dose accumulated in the sample. These components are indicated by kD_α , D_β , D_γ and D_{cosmic} (in short notation D_c). Here, kD_α is the effective alpha dose rate; D_β , D_γ and D_c are the effective beta, gamma and cosmic ray dose rates, respectively. α particles are less effective in inducing OSL than the lightly ionizing radiations. The relative measure of this poor effectiveness is the *k-value* and it is usually in the range 0.05-0.2; superseding approaches use *a-value* or *b-value*. The value of *k* has been assumed as 0.15 (Aitken, 1985).

Another important factor that must be taken into consideration is the water content of the sample. It is a well known fact that, the absorption coefficient of dry sample is higher than wet sample comparing with silicates which are the matrix components of the samples, (Zimmerman, 1971). These excesses of dry samples are about 50% for α radiation, 25% for β radiation and 14% for γ radiation. Thus, the attenuation factor for α is 1.5, for β 1.25 and for γ 1.14.

One can convert the dose rates determined for a “dry” sample to dose rates when the sample is “wet”. For such conversions, the components of annual dose are calculated. In this work, the values given in Table 3.1 can be used to calculate them. The equations to calculate these components are (Aitken, 1985):

$$D_{\alpha_{U,Th}} = \frac{1.280a\alpha_{U,Th}}{1 + 1.5WF} \quad (3.7)$$

$$D_{\beta_{U,Th}} = \frac{0.072\alpha_{U,Th}}{1+1.25WF} \quad (3.8)$$

$$D_{\beta_K} = \frac{0.830bm}{1+1.25WF} \quad (3.9)$$

$$D_{\beta} = D_{\beta_{U,Th}} + D_{\beta_K} \quad (3.10)$$

$$D_{\gamma_{U,Th}} = \frac{0.085\alpha_{U,Th}}{1+1.14WF} \quad (3.11)$$

$$D_{\gamma_K} = \frac{0.244bm}{1+1.14WF} \quad (3.12)$$

$$D_{\gamma} = D_{\gamma_{U,Th}} + D_{\gamma_K} \quad (3.13)$$

The annual dose rate for the fine grain technique is:

$$\text{Annual Dose} = kD_{\alpha} + D_{\beta} + D_{\gamma} + D_c \quad (3.14)$$

The parameters in the above equations are:

kD_{α} is effective alpha dose rate contribution and k can be taken as between 0.05 and 0.2.

D_{β} is total beta dose-rate,

$D_{\beta(U,Th)}$ is the effective beta dose rate due to the contributions of U and Th components of the sample,

D_{γ} is total gamma dose-rate,

$D_{\gamma(U, Th)}$ is the effective gamma dose rate due to contributions of U and Th components of the sample,

D_c is cosmic dose rate and has a value of 0.29 mGy/year at the ground surface of sea level. If the sample is 1-2 meter below the ground surface level it can be taken as 0.15 mGy/year (Aitken, 1985),

W is water saturation content (see Section 4.5.1) of LDKY ceramic samples,
 F is the fraction of saturation (see Section 4.5.1) to which the assumed average water content corresponds,

$\alpha_{U,Th}$ is the alpha counts which comes from uranium and thorium component of the sample

a is the attenuation constants of alpha radiations (in Equation 3.7) and a was taken as 0.15 in this study as proposed by Aitken (1985),

b is the attenuation constants of beta radiations (in Equation 3.9) and b was taken as 1 in this study as proposed by Aitken (1985),

m is the amount of potassium as weight percent.

3.8.1 Water Saturation and Water Uptake Measurements

The water saturation content can be calculated using the equation given below,

$$W = \frac{W_s - W_{dry}}{W_{dry}} \quad (3.15)$$

Where, W is the saturation water content, W_s is the saturated weight of the sample and W_{dry} is dry weight of the sample. For sediments, the water content W was reported as the values between 20% and 40% (Buluş-Kırıkkaya, 2002). For ceramics having high porosity water content is expected to be higher than this. It is also important to know how close to saturation the sample has been on the average during the entire burial time. The fraction F of saturation to the assumed average water content over the burial time is taken to be $F = 0.8 \pm 0.2$ (Aitken, 1985). This fraction F is also called as the water uptake. However, if W has a small value such as about 10% by weight, then F can take a value between the 0.1 and 0.3. Saturation water content and water uptake results of the LDKY samples were determined and they were given in Chapter 4.

3.8.2 Determination of Potassium in Samples

Potassium-40 is naturally occurring radioactive isotope of potassium element. Potassium is the seventh most abundant element in the earth's crust and the sixth most abundant element in the oceans. It is present in mineral waters, brines, and in various minerals such as carnallite ($\text{KMgCl}_3 \cdot 6\text{H}_2\text{O}$, Hydrated Potassium Magnesium Chloride), feldspar (KAlSi_3O_8 , Orthoclase or Microcline), saltpetre (KNO_3 , potassium nitrate), glauconite $\{\text{K}_2(\text{Mg,Fe})_2\text{Al}_6(\text{Si}_4\text{O}_{10})_3(\text{OH})_{12}\}$, and sylvite (KCl , Potassium Chloride).

Radioactive properties of potassium-40 are given in Table 3.3. K-40 emits β radiation and captures electron and this radiations can cause electron trapping in the crystal structure. Thus, K-40 gives two decay processes as shown in Equations 3.16 and 3.17.



Therefore, by the determination of the amount of potassium, it is possible to calculate the contribution of β radiation coming from K-40 in the sample irradiated.

Table 3.3 Radioactive properties of potassium-40. EC = electron capture, Ci = curie, g = gram, and MeV = million electron volts; a dash means that the entry is not applicable.

Radioactive Properties of Potassium-40							
Isotope	Half-Life (yr)	Natural Abundance (%)	Specific Activity (Ci/g)	Decay Mode	Radiation Energy (MeV)		
					Alpha (α)	Beta (β)	Gamma (γ)
K-40	1.3 billion	0.012	0.0000071	β , EC	-	0.52	0.16

The amount of potassium in a sample can be determined by using various methods including spectroscopic methods.

3.9 Sources of α , β particles and γ rays

The radioactive nuclei or radionuclides, found naturally on the earth and produce luminescence in minerals are given in Table 3.4 and Table 3.5.

Table 3.4 The members of the U-238 and Th-232 decay series, their half-lives and their radiation types. K-40 is the main source of β particles.

Uranium / radium series		Thorium Series		Potassium-40 (Natural abundance 0.0117 %)
Nuclide	Half-life	Nuclide	Half-life	
Uranium-238	4.47×10^9 year	Thorium-232	14.0×10^9 year	Potassium-40 (half-life: 1.25×10^9 years) ↓ 10.5 % γ (1.46 MeV) → Argon-40 (stable) ↓ 89.5 % β (1.36 MeV) → Calcium-40 (stable)
↓ $1\alpha, 2\beta$		↓ 1α		
Uranium-234	245×10^3 year	Radium-228	6.7 year	
↓ 1α		↓ $1\alpha, 2\beta$		
Thorium-230 (ionium)	75×10^3 year	Radium-224	3.6 day	
↓ 1α		↓ 1α		
Radium-226	1600 year	Radon-220 (thoron)	55 second	
↓ 1α		↓ $3\alpha, 2\beta$		
Radon-222	3.82 day	Polonium-216	0.16 second	
↓ 2β		↓ $2\alpha, 2\beta$		
Lead-210	22 year	Lead-208	stable	
↓ 1α				
Polonium-210	138 day			
↓ 1α				
Lead-206	stable			

Table 3.5 Half-lives and average abundances of natural radionuclides.

	⁴⁰ K	⁸⁷ Rb	²³² Th	²³⁸ U	²³⁵ U
Half-life (billion years)	1.277	47.5	14.05	4.468	0.7
Upper continental crust					
Elemental abundance (ppm)	28000	112	10.7	2.8	
Activity (Bq/kg)	870	102	43	35	

3.9.1 Contribution of Gamma and Cosmic rays for Dose Rate

To determine the external gamma (γ) and cosmic ray components of the annual dose, the thick $\text{Al}_2\text{O}_3:\text{C}$ Thermo-Luminescence Dosimeters (TLD) are used. These dosimeters are very sensitive to any kind of radiation, including the cosmic rays.

3.10 Supralinearity, Sensitization and Saturation

The growth of luminescence intensity with dose is not always linear, (Figure 3.10). Typically there can be an initial supralinear portion in which the sensitivity is increasing, followed by a linear portion of constant incremental sensitivity. Finally, the sensitivity falls off due to the onset of saturation. The saturation level is not necessarily constant, as with heavy doses there may be further increase or decrease. The initial portion of supralinearity occurs only for beta and gamma irradiation, not for alpha. It is the incremental sensitivity of the central portion that is used to define the luminescence sensitivity χ and to obtain the equivalent dose, (Aitken, 1985).

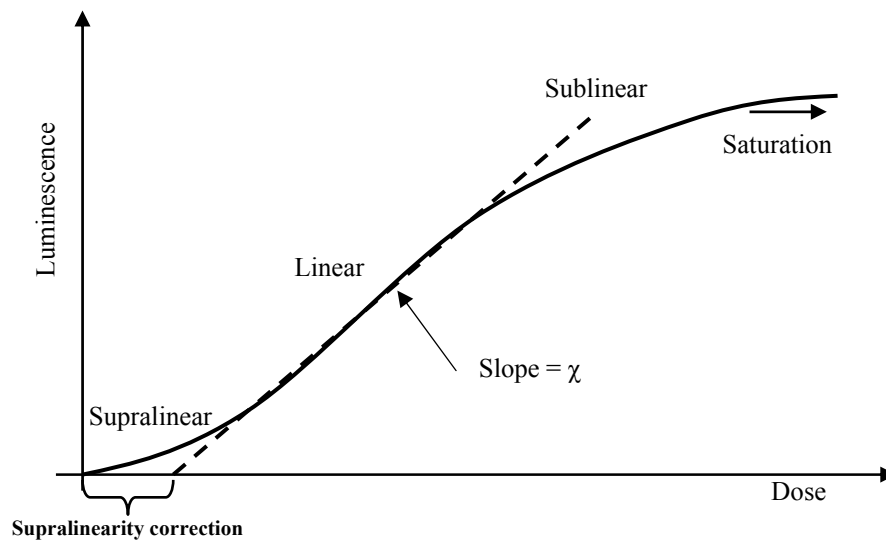


Figure 3.10 Luminescence growth characteristic showing supralinear and sublinear regions. Luminescence sensitivity, χ , refers to the luminescence per unit dose of the linear region.

CHAPTER 4

RESULTS and DISCUSSIONS

In order to reach the scope of the study and to increase the degree of sensitivity, accuracy and reliability of the results, first of all calibrations of OSL (including dose rate recalculation of Sr-90 β source) and Alpha counting systems have been done. These studies are given in detail in Appendix B. Here, in Chapter 4 a very brief summary of the work is given together with the discussion of the results.

The calibration of the ELSEC 9010 Optical Dating System has yielded the HT and threshold voltages of PM tube as 1250 ± 25 V and 3.30 ± 0.01 V, respectively (Tables B.1, B.2 and Figures B.2, B.3)

Dose rate calculations of Sr-90 β source have been carried out between the years of 2001 and 2006 and a decrease of the activity in accordance with the decay equation had been observed (Table B.6).

The HT and Threshold voltages of the Alpha Counter System were determined as 1150 ± 25 V and 1.15 ± 0.02 V, respectively (Tables B.3, B.4 and Figures B.5, B.6).

In order to determine radon escape, if there is, sealed and unsealed average alpha count rates of the LDKY samples have been measured and the results were given with their average U and Th contributions in Table 4.13.

In this study, samples of building materials (pieces of floor and ceiling tiles and water pipes) collected from Laodikeia archaeological site (Denizli) were

examined. Mineral structure of the samples have analysed from their XRD traces and results showed that the main minerals in the samples are quartz, feldspars (dominantly potassium feldspar), calcite and together with some other minerals (Figure 4.1).

Fine grained samples were prepared by the process given by Aitken (1985). For the grain size distribution wet sieving method was preferred since the openings of the sieves were filled by the particles in a short time in dry sieving. In the size distribution, the Stoke's law has been used and the fraction of (1-9) μm particles were settled on the aluminium discs for measurements.

For the calculation of the age of the samples their equivalent dose and annual dose have been determined. Before the calculation of equivalent dose, as a first step preheating and then normalisation process were applied to the samples. There after, two of the equivalent dose measurement techniques have been used.

Among the three methods mentioned in Chapter 3, MAAD and MARD techniques were used for the equivalent dose measurements. SAR technique was not used since the amount of samples is quite enough to use other two techniques. There was no big difference between the results obtained which is in the range of 2.21-6.30 Gy (Tables 4.3 and Table 4.10). This may be due to by two techniques for the same sample studied.

Contributions of α , β particles, γ and cosmic rays and saturation water content had been determined and from the annual dose equation the annual dose values of the samples were calculated. The results are in the range of 2.35 and 4.03 mGy per year, (Table 4.11).

The amount of water and humidity of material can affect the absorbed radiation amount because of the attenuation differences of the radiation inside the sample. Thus, water saturation content (W) should be determined and water uptake (F)

should be estimated according to the W value. W and F values of LDKY samples are given in Table 4.12

The amount of potassium in the sample has been measured by using AES and the results are given in Table 4.15.

By dividing the equivalent doses with annual dose the ages of six LDKY samples were calculated. The MAAD ages were in the range between 737 ± 60 years and 1602 ± 120 years and the MARD ages were in the range 870 ± 60 years and 1600 ± 120 years, (Table 4.1). In other words, their production years are between A.D. 404 ± 120 and A.D. 1269 ± 60 with an estimated uncertainty of 7%. The errors shown in Table 4.2 to Table 4.7 are given by the software of the system.

The percentage errors in the calculated ages are about 7% and they are comparable to similar OSL ages found in other laboratories (Liritzis and Vafiadau, 2005).

Table 4.1 Age results of LDKY samples based on the OSL system and its associated software.

Sample Name	LDKY-1 (floor tile)	LDKY-2 (floor tile)	LDKY-3 (water pipe)	LDKY-4 (water pipe)	LDKY-5 (ceiling tile)	LDKY-6 (ceiling tile)
Equivalent Dose with MAAD Technique (Gy)	2.21 ± 0.04	6.30 ± 0.13	4.45 ± 0.09	5.88 ± 0.12	2.47 ± 0.05	2.42 ± 0.05
Equivalent Dose with MARD Technique (Gy)	2.60 ± 0.05	6.25 ± 0.13	4.48 ± 0.09	5.85 ± 0.12	2.51 ± 0.05	2.38 ± 0.05
Annual Dose (mGy)	3.00 ± 0.06	4.03 ± 0.08	3.09 ± 0.06	3.68 ± 0.07	2.40 ± 0.05	2.35 ± 0.05
MAAD Age (year)	737 ± 60	1563 ± 120	1445 ± 110	1602 ± 120	1034 ± 80	1034 ± 80
MARD Age (year)	870 ± 60	1550 ± 120	1440 ± 110	1600 ± 120	1030 ± 80	1030 ± 80

The ages of the floor tiles “LDKY-1 and LDKY-2” have been found to be 870 ± 60 years (Table 4.2) and 1550 ± 120 years (Table 4.3) by MARD technique, respectively. These floor tiles had been collected from the same room but at different parts of it. The room is at the right side of the entrance door of the Laodikeia church (Figures 3.1a and 3.1b). However, before they were collected the roof had been already removed and the samples had been exposed to the sunlight. Two different floor tiles were collected from that room. First sample (LDKY-1) had been illuminated by the sun light for a couple of weeks but second sample (LDKY-2) was not, because that tile was found underground in front of the wall of the room (Figures 3.1a and 3.1b). Archaeologists were interested in the construction date of the room. The age of LDKY-1 was found to be younger than LDKY-2. This is an expected result since some of the traps were emptied by sunlight.

The age of the second sample (LDKY-2) gives us the construction date of the room, since it was not exposed to the sun light until it was collected. This is an expected age by the archaeologists of Laodikeia excavation (Şimşek, 2004).

The ages of the water pipe samples, LDKY-3 and LDKY-4, have been found to be 1440 ± 110 years (Table 4.4) and 1600 ± 120 years (Table 4.5) by MARD technique, respectively. These samples had been collected at the side of the north wall of the Laodikeia church (Figures 3.2a and 3.2b).

The archaeologists claimed that the earthquake, which happened in A.D. 494 according to the archaeological written records, destroyed Laodikeia completely and the city was reconstructed. So, LDKY-3 and LDKY-4 samples are expected to give a date indicating this earthquake.

Consequently, the dates determined in this work for LDKY-3 and LDKY-4 samples are completely consistent with the earthquake date. This may indicate that water pipes were made just after the devastating earthquake in A.D. 494.

The ages of the ceiling tile samples, LDKY-5 and LDKY-6, were found to be 1030 ± 80 years (Tables 4.6) and 1030 ± 80 years (Tables 4.7) by MARD technique, respectively. These samples had been collected from the entrance door of the Laodikeia church, one above the burnt layer and the other below this layer (Figures 3.3a and 3.3b). According to the archaeologists, probably the ceiling of the church was wooden and the top of it had been covered with the ceramic ceiling tiles. In the fire this wooden ceiling were burnt and collapsed with the ceramic tiles on it. According to the archaeologists, this fire had been set up during the invasion of Seljuks, in A.D. 1176. So, the date of LDKY-5 and LDKY-6 samples could be comparable with this invasion date, and the fire has been acted as a zeroing event.

The glow curve of the LDKY samples has not shown any supralinearity, (Figure 4.14). The sensitivities were constant, for all LDKY samples. For LDKY ceramic samples studied, sublinearity started after 500 Gy, (Figure 4.14). This shows that ceramic is a good natural dosimeter and age estimation can be done up to 100-150 kyear without making any supralinearity correction.

In this work preheating temperature for LDKY samples was determined to be 160 degrees of Celsius with 20 minutes duration time (Figure 4.3). In addition, removal dose rate of the shallow traps was 30-35% of the total dose before preheating applied on the LDKY aliquots. This result may show that the future OSL analysis of other LDKY samples can be done by directly subtracting 30-35 % of the total luminescence for the shallow traps without preheating.

Table 4.2 Annual dose and age calculation of LDKY-1 sample by MARD technique, based on the OSL system and its associated software.

Constants	mGy/yr
α Dose Rate for $a=1$, $\alpha=1$ from U and Th	1.2800
β Dose Rate for $\alpha=1$ from U and Th	0.0720
β Dose Rate for $\alpha=1$ from U	0.0866
β Dose Rate for $\alpha=1$ from Th	0.0573
β Dose Rate for $m=1$ from K	0.6970
γ Dose Rate for $\alpha=1$ from U and Th	0.0850
γ Dose Rate for $\alpha=1$ from U	0.0670
γ Dose Rate for $\alpha=1$ from Th	0.1047
γ Dose Rate for $m=1$ from K	0.2020

Constants and ratios without any unit	
Dry/Wet concentration ratio	1.14
Threshold fraction	0.85
Water Coefficients of α	1.50
Water Coefficients of β	1.25
Water Coefficients of γ	1.14

Measurements	
Unsealed α count rate (counts/ksec)	9.23
Unsealed α count rate due to Thorium	3.54
Unsealed α count rate due to Uranium	5.69
Sealed α count rate (counts/ksec)	9.13
K ₂ O%	1.79
K percentage by weight (m) = K ₂ O%/1.2	1.49
Saturation water content (W)	0.67
Water uptake during burial (F)	0.80
a value	0.15
Cosmic dose rate (mGy/a)	0.15
Equivalent dose (Gy) =	2.60

Calculation		
	DR (mGy/yr)	% OF TOTAL
α from U and Th	0.980	32.71
β from U	0.183	6.11
β from Th	0.195	6.51
β from K	0.747	24.93
Total β	1.125	37.55
γ from U	0.147	4.91
γ from Th	0.369	12.32
γ from K	0.224	7.48
Total γ	0.741	24.73
Cosmic Ray	0.150	5.01
Total Annual Dose	2.996	100.00

Age (year)	870	± 60
-------------------	------------	-------------

Table 4.3 Annual dose and age calculations of LDKY-2 sample by MARD technique, based on the OSL system and its associated software.

Constants	mGy/yr
α Dose Rate for $a=1$, $\alpha=1$ from U and Th	1.2800
β Dose Rate for $\alpha=1$ from U and Th	0.0720
β Dose Rate for $\alpha=1$ from U	0.0866
β Dose Rate for $\alpha=1$ from Th	0.0573
β Dose Rate for $m=1$ from K	0.6970
γ Dose Rate for $\alpha=1$ from U and Th	0.0850
γ Dose Rate for $\alpha=1$ from U	0.0670
γ Dose Rate for $\alpha=1$ from Th	0.1047
γ Dose Rate for $m=1$ from K	0.2020

Constants and ratios without any unit	
Dry/Wet concentration ratio	1.14
Threshold fraction	0.85
Water Coefficients of α	1.50
Water Coefficients of β	1.25
Water Coefficients of γ	1.14

Measurements	
Unsealed α count rate (counts/ksec)	11.05
Unsealed α count rate due to Thorium	7.72
Unsealed α count rate due to Uranium	3.33
Sealed α count rate (counts/ksec)	11.31
K ₂ O%	1.38
K percentage by weight (m) = K ₂ O%/1.2	1.15
Saturation water content (W)	0.60
Water uptake during burial (F)	0.40
a value	0.15
Cosmic dose rate (mGy/a)	0.15
Equivalent dose (Gy) =	6.30

Calculation		
	DR (mGy/yr)	% OF TOTAL
α from U and Th	1.568	38.99
β from U	0.517	12.85
β from Th	0.147	3.65
β from K	0.740	18.40
Total β	1.404	34.91
γ from U	0.406	10.09
γ from Th	0.275	6.84
γ from K	0.219	5.45
Total γ	0.900	22.38
Cosmic Ray	0.150	3.73
Total Annual Dose	4.022	100.00

Age (year)	1550	± 120
------------	------	-------

Table 4.4 Annual dose and age calculations of LDKY-3 sample by MARD technique, based on the OSL system and its associated software.

Constants	mGy/yr
α Dose Rate for $a=1$, $\alpha=1$ from U and Th	1.2800
β Dose Rate for $\alpha=1$ from U and Th	0.0720
β Dose Rate for $\alpha=1$ from U	0.0866
β Dose Rate for $\alpha=1$ from Th	0.0573
β Dose Rate for $m=1$ from K	0.6970
γ Dose Rate for $\alpha=1$ from U and Th	0.0850
γ Dose Rate for $\alpha=1$ from U	0.0670
γ Dose Rate for $\alpha=1$ from Th	0.1047
γ Dose Rate for $m=1$ from K	0.2020

Constants and ratios without any unit	
Dry/Wet concentration ratio	1.14
Threshold fraction	0.85
Water Coefficients of α	1.50
Water Coefficients of β	1.25
Water Coefficients of γ	1.14

Measurements	
Unsealed α count rate (counts/ksec)	10.85
Unsealed α count rate due to Thorium	4.52
Unsealed α count rate due to Uranium	6.33
Sealed α count rate (counts/ksec)	11.02
K ₂ O%	0.85
K percentage by weight (m) = K ₂ O%/1.2	0.71
Saturation water content (W)	0.70
Water uptake during burial (F)	0.60
a value	0.15
Cosmic dose rate (mGy/a)	0.15
Equivalent dose (Gy) =	4.45

Calculation		
	DR (mGy/yr)	% OF TOTAL
α from U and Th	1.282	41.52
β from U	0.258	8.35
β from Th	0.239	7.74
β from K	0.388	12.56
Total β	0.885	28.66
γ from U	0.205	6.64
γ from Th	0.450	14.57
γ from K	0.116	3.76
Total γ	0.771	24.97
Cosmic Ray	0.150	4.86
Total Annual Dose	3.088	100.00

Age (year)	1440	± 110
------------	------	-------

Table 4.5 Annual dose and age calculations of LDKY-4 sample by MARD technique, based on the OSL system and its associated software.

Constants	mGy/yr
α Dose Rate for $a=1$, $\alpha=1$ from U and Th	1.2800
β Dose Rate for $\alpha=1$ from U and Th	0.0720
β Dose Rate for $\alpha=1$ from U	0.0866
β Dose Rate for $\alpha=1$ from Th	0.0573
β Dose Rate for $m=1$ from K	0.6970
γ Dose Rate for $\alpha=1$ from U and Th	0.0850
γ Dose Rate for $\alpha=1$ from U	0.0670
γ Dose Rate for $\alpha=1$ from Th	0.1047
γ Dose Rate for $m=1$ from K	0.2020

Constants and ratios without any unit	
Dry/Wet concentration ratio	1.14
Threshold fraction	0.85
Water Coefficients of α	1.50
Water Coefficients of β	1.25
Water Coefficients of γ	1.14

Measurements	
Unsealed α count rate (counts/ksec)	8.53
Unsealed α count rate due to Thorium	3.64
Unsealed α count rate due to Uranium	4.89
Sealed α count rate (counts/ksec)	8.77
K ₂ O%	0.69
K percentage by weight (m) = K ₂ O%/1.2	0.57
Saturation water content (W)	0.10
Water uptake during burial (F)	0.20
a value	0.15
Cosmic dose rate (mGy/a)	0.15
Equivalent dose (Gy) =	5.88

Calculation		
	DR (mGy/yr)	% OF TOTAL
α from U and Th	1.600	43.45
β from U	0.309	8.40
β from Th	0.275	7.46
β from K	0.469	12.75
Total β	1.053	28.61
γ from U	0.239	6.48
γ from Th	0.503	13.67
γ from K	0.136	3.70
Total γ	0.878	23.86
Cosmic Ray	0.150	4.07
Total Annual Dose	3.681	100.00

Age (year)	1600	± 120
------------	------	-------

Table 4.6 Annual dose and age calculations of LDKY-5 sample by MARD technique, based on the OSL system and its associated software.

Constants	mGy/yr
α Dose Rate for $a=1$, $\alpha=1$ from U and Th	1.2800
β Dose Rate for $\alpha=1$ from U and Th	0.0720
β Dose Rate for $\alpha=1$ from U	0.0866
β Dose Rate for $\alpha=1$ from Th	0.0573
β Dose Rate for $m=1$ from K	0.6970
γ Dose Rate for $\alpha=1$ from U and Th	0.0850
γ Dose Rate for $\alpha=1$ from U	0.0670
γ Dose Rate for $\alpha=1$ from Th	0.1047
γ Dose Rate for $m=1$ from K	0.2020

Constants and ratios without any unit	
Dry/Wet concentration ratio	1.14
Threshold fraction	0.85
Water Coefficients of α	1.50
Water Coefficients of β	1.25
Water Coefficients of γ	1.14

Measurements	
Unsealed α count rate (counts/ksec)	8.77
Unsealed α count rate due to Thorium	3.60
Unsealed α count rate due to Uranium	5.17
Sealed α count rate (counts/ksec)	9.80
K ₂ O%	0.85
K percentage by weight (m) = K ₂ O%/1.2	0.71
Saturation water content (W)	0.69
Water uptake during burial (F)	0.80
a value	0.15
Cosmic dose rate (mGy/a)	0.15
Equivalent dose (Gy) =	2.47

Calculation		
	DR (mGy/yr)	% OF TOTAL
α from U and Th	0.944	39.22
β from U	0.189	7.85
β from Th	0.179	7.44
β from K	0.351	14.58
Total β	0.719	29.87
γ from U	0.148	6.15
γ from Th	0.340	14.13
γ from K	0.105	4.36
Total γ	0.594	24.68
Cosmic Ray	0.150	6.23
Total Annual Dose	2.407	100.00

Age (year)	1030	± 80
------------	------	------

Table 4.7 Annual dose and age calculations of LDKY-6 sample by MARD technique, based on the OSL system and its associated software.

Constants	mGy/yr
α Dose Rate for $a=1$, $\alpha=1$ from U and Th	1.2800
β Dose Rate for $\alpha=1$ from U and Th	0.0720
β Dose Rate for $\alpha=1$ from U	0.0866
β Dose Rate for $\alpha=1$ from Th	0.0573
β Dose Rate for $m=1$ from K	0.6970
γ Dose Rate for $\alpha=1$ from U and Th	0.0850
γ Dose Rate for $\alpha=1$ from U	0.0670
γ Dose Rate for $\alpha=1$ from Th	0.1047
γ Dose Rate for $m=1$ from K	0.2020

Constants and ratios without any unit	
Dry/Wet concentration ratio	1.14
Threshold fraction	0.85
Water Coefficients of α	1.50
Water Coefficients of β	1.25
Water Coefficients of γ	1.14

Measurements	
Unsealed α count rate (counts/ksec)	6.54
Unsealed α count rate due to Thorium	2.56
Unsealed α count rate due to Uranium	3.98
Sealed α count rate (counts/ksec)	7.14
$K_2O\%$	1.31
K percentage by weight (m) = $K_2O\%/2.4$	1.10
Saturation water content (W)	0.70
Water uptake during burial (F)	0.65
a value	0.15
Cosmic dose rate (mGy/a)	0.15
Equivalent dose (Gy) =	2.42

Calculation		
	DR (mGy/yr)	% OF TOTAL
α from U and Th	0.761	32.36
β from U	0.144	6.12
β from Th	0.148	6.29
β from K	0.582	24.74
Total β	0.874	37.16
γ from U	0.113	4.80
γ from Th	0.279	11.86
γ from K	0.174	7.40
Total γ	0.567	24.11
Cosmic Ray	0.150	6.38
Total Annual Dose	2.352	100.00

Age (year)	1030	± 80
------------	------	----------

4.1 X-Ray Diffraction Analysis (XRD) and Sample Preparation

In order to determine the mineral compositions of LDKY ceramic samples (Table 3.1) their outer surfaces were removed up to few mm depths by using an adze or a file. After powdering the sample in an agate mortar, XRD traces were obtained.

In the study a “Rigaku MiniFlex” X-ray diffractometer, adjusted to 30 kV and 15 mA, was used. The analysis was performed by using Cu K_{α} with a K_{β} filter. In the measurement 2θ values were changed from 5° to 80° . The main minerals identified were quartz, feldspars (K-feldspar dominantly) and calcite together with some other minerals. In Figure 4.1, XRD trace of LDKY-1 sample is given as an example. The differences between ceramics regarding mineral composition were negligible.

In this study, the feldspar component of ceramic samples was studied because of instrumental suitability. For this reason, the feldspar component of the samples was separated by the following procedures (Aitken, 1985).

The outer surfaces of samples were removed up to few mm depths and then they were powdered. The powdered sample was divided into two equal parts. One part was kept as it is without any chemical treatment. The second part was treated with excess amount of 10% hydrochloric acid, HCl, and kept in acid until the evolved gas ceases. In this treatment, the carbonates in the sample react with HCl, according to the reaction,



The carbon dioxide gas (CO_2) is given off as bubbles and the all carbonates dissolves in water. Any acid can produce these results, but dilute hydrochloric acid or acetic acid is the two recommended acids for this treatment.

At the end of this process, the suspension is kept aside to settle down all the undissolved components. Then, the supernatant solution was decanted. The remaining residue was rinsed with distilled water for several times to be sure the residue became clean. Then, the sample was treated with excess amount of 38% H_2O_2 to remove any organic matter and keep waiting until the evolved gas ceases, and the suspension is kept aside to settle down all the undissolved components. Then, the supernatant solution was decanted. The remaining residue was rinsed with distilled water for several times. Rinsing process was repeated by adding acetone last time for the final process to remove all chemical impurities. So the samples became ready for size distribution analysis after drying for all dose measurements.

The XRD trace of treated sample was taken which is shown in Figure 4.1b.

As it is seen in Figure 4.1b, some of the calcite peaks observed clearly in untreated sample, Figure 4.1a, were decreased after the treatment of the sample with HCl and H_2O_2 .

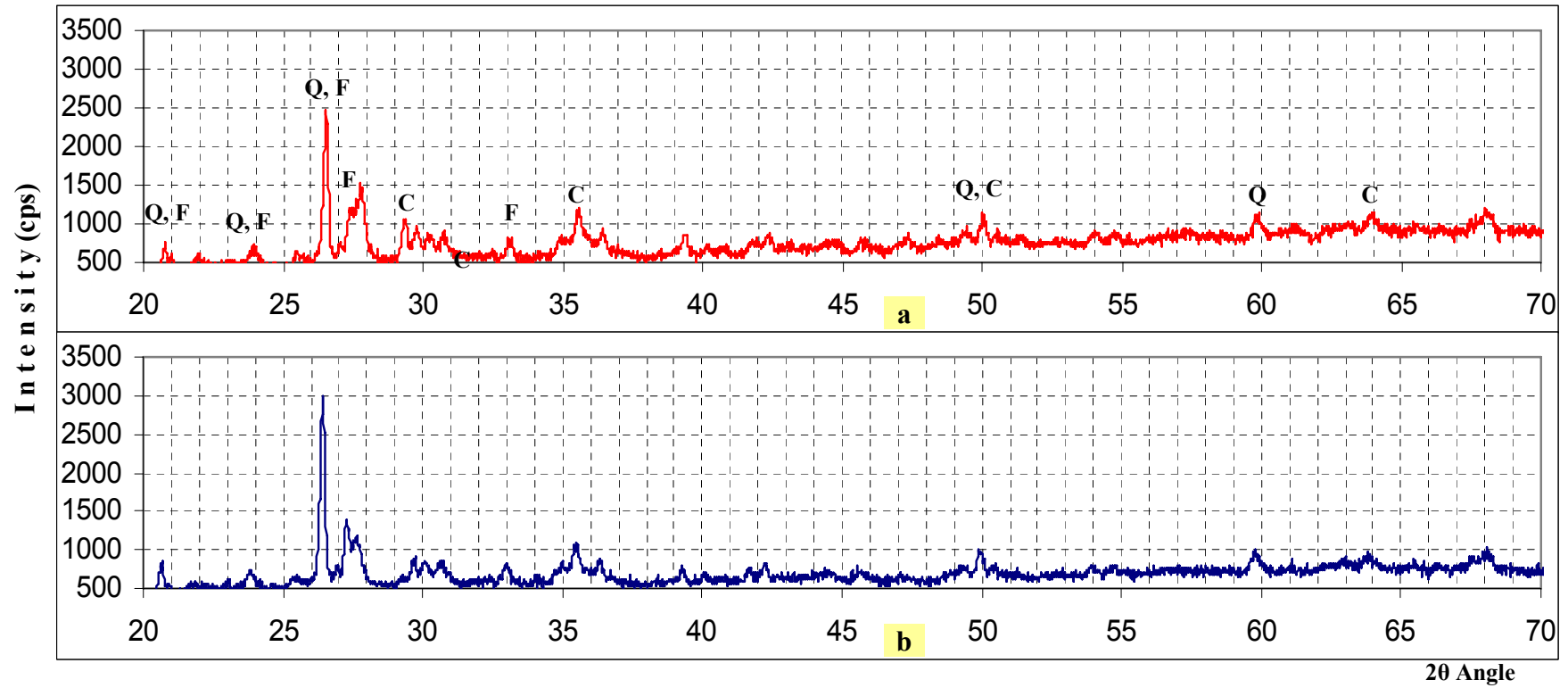


Figure 4.1 XRD analysis of LDKY1 ceramic sample.
a) Untreated (red line),
b) Treated sample (blue line) with HCl and H₂O₂.
Where, Q: quartz, F: feldspar, C: calcite.

4.1.1 Size distribution of the samples

In order to obtain fine grains (1-9 μm) powdered samples should be subjected to the size distribution treatment and the size distribution is done in two ways;

1. by sieving the powdered dry sample with different sized screens,
2. by dispersing the powdered sample in a fluid and then by settling the grains at different time periods according to Stoke's law (Fleming 1979).

Dry sieving method is not found sufficient since the openings of the sieve will be filled by the particles in a short time and the fine grains tended to conglomerate.

In the second method, the sample is dispersed in a solvent like acetone and a uniform suspension is obtained. The suspension is kept aside until the particles in it settle down under the action of gravity. Stoke's law gives the settling speed of a particle dropped into a fluid as

$$v = \frac{1}{18} \left[\frac{(\rho_s - \rho_F)gd^2}{\mu} \right] \quad (4.2)$$

where,

v : settling speed (cm/s)

g : gravitational acceleration ($g = 980 \text{ cm/s}^2$)

ρ_s : density of dropped object (if feldspar is used density of feldspar :
2.55-2.76 gr/cm^3 , Cornelius and Hurlbut, 1971)

d : diameter of particle (assumed to be $(2-9) \times 10^{-4} \text{ cm}$)

ρ_F : density of fluid (density of acetone = 0.79 gr/cm^3)

μ : viscosity of fluid (viscosity of acetone = $0.0032 \text{ gr.cm}^{-1}.\text{s}^{-1}$).

The time t it takes a particle to go down a vertical distance h in the suspension is given by

$$t = \frac{h}{v} \quad (4.3)$$

After size distribution treatment, samples are placed on the aluminium discs in equal amount of about 1 mgr/cm². Then, paleodose measurements can be carried out.

If the values given above are substituted in Equation 4.2 and Equation 4.3, t is found as 120 seconds for the particles to settle down in a 6-cm suspension height formed in a 3.5-cm diameter graduated cylinder.

In the method used, 5-10 gr of powdered sample was dispersed in 100 ml of acetone and a stock suspension was prepared. From this stock suspension, about 30 ml suspension is poured into a graduated cylinder and a 6-cm suspension height is obtained. The suspension is settled for 2 minutes to settle out the grains with diameters larger than 9 μm (as obtained from Stoke's law). The supernatant solution is decanted to another graduated cylinder and allowed for 20 minutes to settle down the grains with diameters larger than 2.5 μm .

After decantation of supernatant solution, the grains with diameters between 2.5 μm and 9 μm are taken out and are put into sufficient amount of acetone to produce homogeneous suspension and this is a new stock suspension is prepared

This homogenous suspension is poured, in equal amounts, to 30 small, flat-bottomed tubes, each with a thin aluminium disc located at the bottom. Then these tubes are inserted in an oven at 50 °C to evaporate acetone. By this way a series of individual aluminium discs, each with a layer of sample grains is obtained. Each aluminium disc with sample on it is called aliquot. It was estimated that each aluminium disc had about 1 mg/cm² of grains on it.

4.2 Preheating

As mentioned in Section 2.2, Mechanism of Luminescence, ionized electrons can be trapped between the valence and conduction bands because of the impurities of the crystals. If a trap level is close to the conduction band, this is called shallow trap and if a trap is far from the conduction band, this is called deep trap. Deep traps are more stable than the shallow ones. Shallow traps can be emptied even at room temperature. To work on stable traps is more convenient and better results can be obtained for dose measurements. Therefore, electrons from the shallow traps must be removed. The removal of the electrons from the shallow traps can be done by heating. This process is called preheating. The preheating temperature and heating time depend on the characteristics of the sample and the depths of the traps which will be emptied.

The feldspar component of a sample, LDKY-2, was irradiated with Sr-90 beta source and a total dose of 30 Gy was given to it. The irradiated sample was analyzed in “Ankara Nükleer Araştırma ve Eğitim Merkezi TL Laboratuvarı”, by using a “Harshaw Model 2000” TL system. The TL signal versus temperature curve of the sample was obtained by varying the temperature from the room temperature to 350 °C, with a few degrees of Celsius increments. The curve is shown in Figure 4.2. The graph indicates that the feldspar has several well known traps; one of them is very distinct corresponding to the temperature value of 150 °C. The other traps are between 210 °C and 350 °C. If the higher doses at the order of kGys were given to the sample, there would be sharp and distinct peaks instead of the wide peak seen in Figure 4.2. As this TL analysis indicates, the deep OSL traps correspond to temperatures between 200 °C and 350 °C. Thus, the preheating temperature is expected to be between 100 °C and 200 °C. The exact preheating temperature was determined by doing a preheating experiment.

The experiment has started by giving equal dose to all aliquots, using Sr-90 beta source. Then, the aliquots have been divided into several groups and each group has been kept in the furnace at different temperatures between 100 °C and about

300 °C, with 20 °C increments, and in equal time intervals, (5 minutes). After that, the remaining luminescence has been measured and the average value for each group has been calculated. These average values of luminescence have been plotted as a function of temperature, as shown in Figure 4.3a. The midpoint of the plateau was estimated as 160 °C, and this temperature has been chosen as the preheating temperature.

To find the duration time of preheating, a procedure similar to the procedure explained above was followed. The furnace temperature was kept at 160 °C, but each aliquots group was heated in different time intervals. The luminescence versus time graph is shown in Figure 4.3b. As the graph indicates, a preheating time of about 20 minutes is sufficient to empty the shallow traps of the samples.

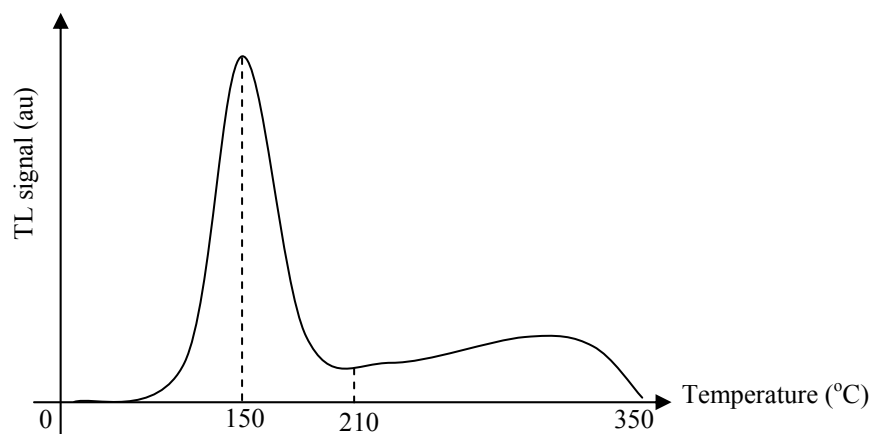


Figure 4.2 TL signal versus temperature curve for the LDKY-2 sample. There is a distinct peak at 150 °C.

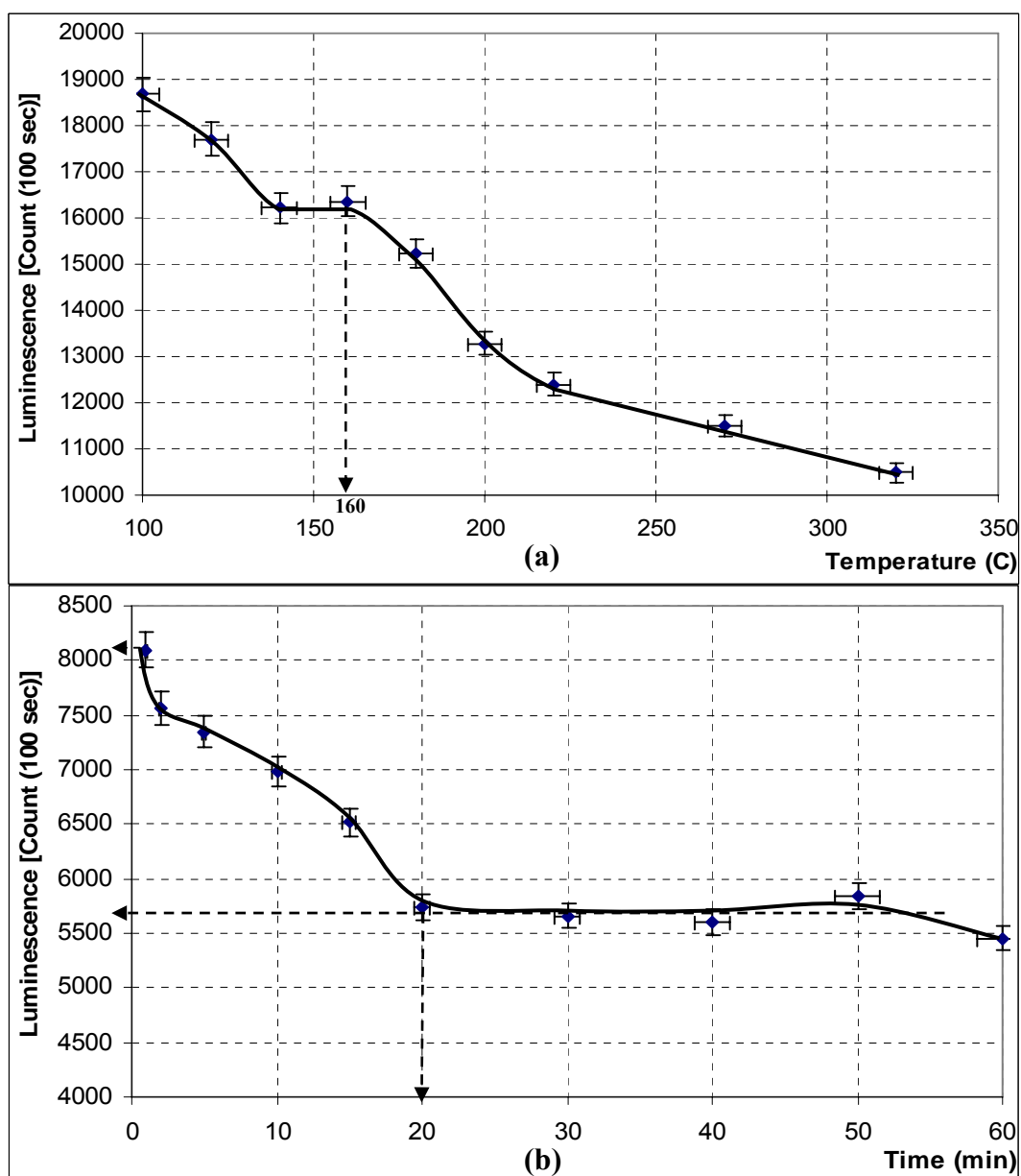


Figure 4.3 (a) Luminescence versus temperature graph at constant heating time. At 150 °C there are shallow traps and after 220 °C there could be more than one deep trap. (b) Luminescence versus time graph at 160 °C. All shallow traps disappear after 20 minutes at 160 °C.

In addition, dose measurements of the aliquots were done without preheating. In this process aliquots were kept at room temperature and in a dark place at least 30-40 days. At the end of this period all of the unstable shallow traps were emptied as seen in Figure 4.4 and the luminescence signal of the sample became stable. In

this study, groups of aliquots were prepared from un-irradiated ceramic samples. The 120 Gy dose was given to each aliquot and the aliquots were kept in a dark place. The luminescences of each group of aliquots were measured and their doses or dose rates were recorded.

In Figure 4.3b, the OSL intensity ratio of 5700 to 8200 is approximately 0.7. Similarly, in Figure 4.4, the OSL intensity ratio of the 17000 to 25000 is again approximately 0.7 as found in Figure 4.3b. This means, dose rate of the shallow traps is approximately 30-35% of the total dose before preheating applied on the polimineral sample aliquots.

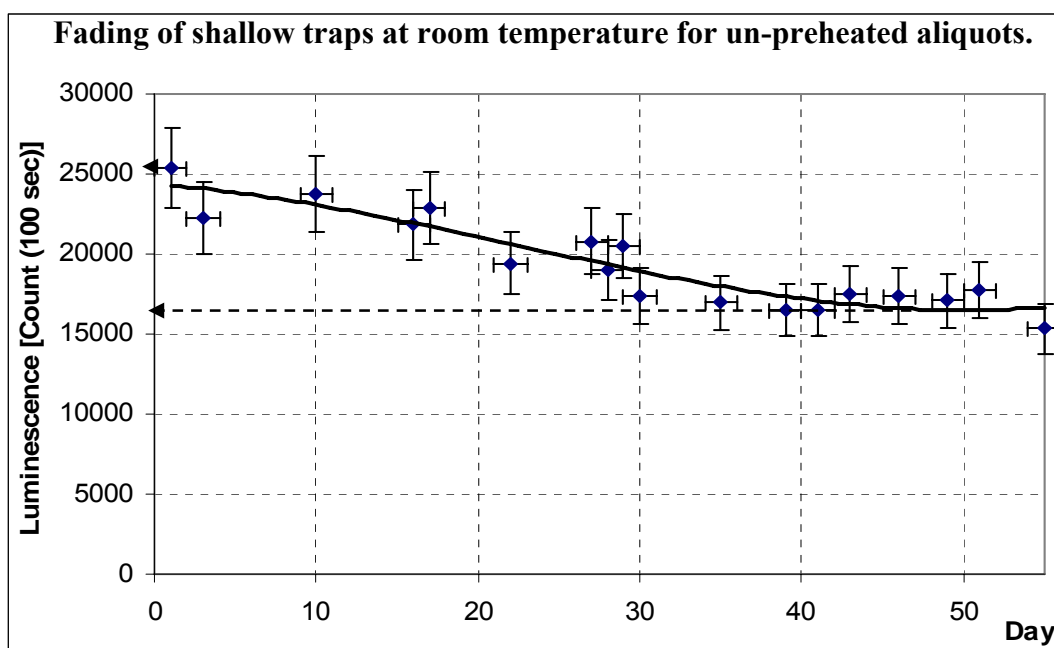


Figure 4.4 Luminescence versus day graph for un-preheated polimineral aliquots. The fading of shallow traps ceases approximately after 40 days after irradiation.

4.3 Normalisation

It is practically impossible to prepare identical aliquots. Each aliquot may be different from the others with respect to the amount of the sample it contains. Furthermore, an aliquot may have grains of different size and type. By doing a normalisation process, these differences may be taken into account. For normalisation a relatively short shine (such as an IR shine for 0.1 s) is given to each aliquot before any added dose (Aitken, 1985). After the short shine, the luminescence is measured for each sample and the average luminescence \bar{L} is calculated by using Equation 3.2. The normalisation constant C_i is calculated by using Equation 3.3. The normalised luminescence $(NL)_i$ for the i^{th} sample is calculated by using Equation 3.4. The normalisation process requires the same short shine for all samples.

The normalisation values for 24 aliquots of LDKY-1 sample are given in Table 4.8 and Figure 4.5, as an example. Aliquot-6 and Aliquot-17 are quite out of $\pm 5\%$ range, and therefore they are excluded from the calculation.

Table 4.8 Luminescence and normalisation constants of a group of LDKY-1 aliquots. Yellow rows are out of $\pm 5\%$ range.

Aliquot#	Luminescence (count-100 s)	Normalization Constant	Aliquot#	Luminescence (count-100 s)	Normalization Constant
1	3683	0.95	13	3365	1.04
2	3601	0.97	14	3507	1.00
3	3717	0.94	15	3329	1.05
4	3830	0.92	16	3690	0.95
5	3536	0.99	17	4210	0.83
6	3939	0.89	18	3543	0.99
7	3334	1.05	19	3477	1.01
8	3290	1.07	20	3402	1.03
9	3527	1.00	21	3382	1.04
10	3430	1.02	22	3662	0.96
11	3554	0.99	23	3560	0.99
12	3436	1.02	24	3409	1.03
Average = 3512					

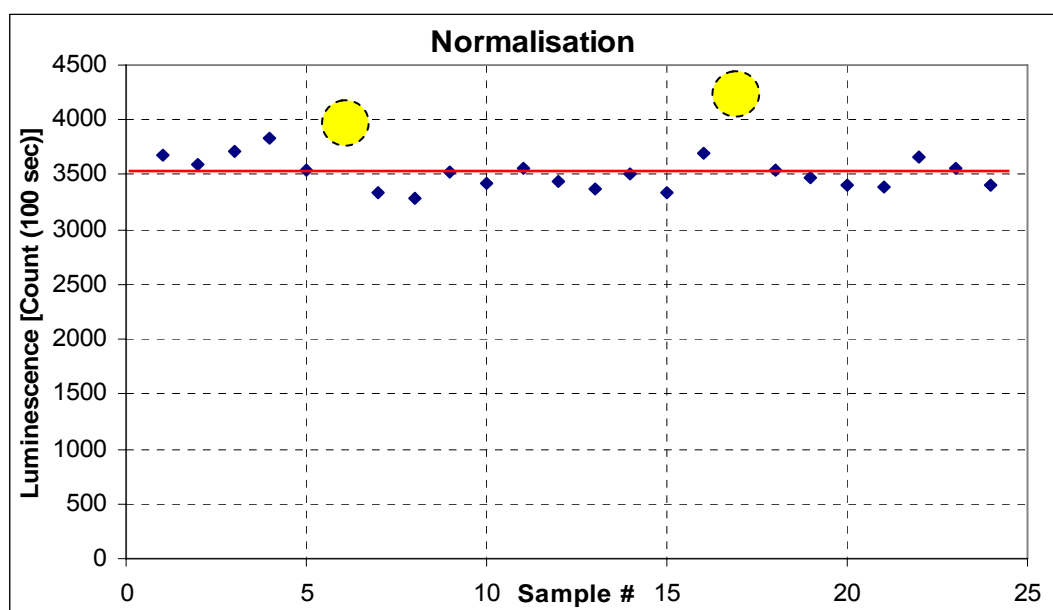


Figure 4.5 Luminescence counts versus sample # graph. Red line shows the average luminescence intensity of a group of LDKY-1 aliquots. Yellow circles show that these two aliquots are out of $\pm 5\%$ limits of the average value.

4.4 MAAD (Multiple Aliquots Additive Dose) Technique

All of the aliquots have been normalized following the procedure given in the previous section. Their normalisation constants have been determined. The illumination (shine) time of normalisation process is relatively short, between 0.1 s or 0.5 s depending on the sample decay characteristics. The time was chosen such that the decrease in luminescence during illumination is to be very small and could be neglected.

After the normalisation process, the aliquots were divided into three groups:

1. Group: Unexposed aliquot group: these aliquots have never been exposed to any light, even during the excavation. They were used for the natural dose (N) measurement.

2. Group: Dose added aliquot group: these aliquots were given different radiation doses D_i added to their natural dose N . They were denoted as $(N+D_i)$, where N is the natural dose present in the aliquots and D_i is the dose added to the i^{th} subgroup (mentioned as Sample 1, Sample 2 etc. in Figure 4.6).
3. Dead aliquot group: these aliquots have been exposed sufficiently to the daylight and their traps were assumed to be completely empty.

After completing the irradiation of the aliquots in 2. group, all the aliquots in 1. and 2. groups were subjected to preheating process. Then, the aliquots of all three groups were arranged as shown in Figure 4.6 on the sample tray (see Appendix-A, Figure A.1). The intensity of luminescence emitted by each aliquot was determined by integrating its luminescence decay curve (Figure 4.7). The luminescence intensity versus added dose graph is a straight line with positive slope, as shown in Figure 4.8. The paleodose (or equivalent dose: D_{eq}) is determined from this graph by extrapolating the straight line to the horizontal added dose axis. The intercept is equal to the paleodose D_{eq} . The paleodose for LDKY-1 sample was estimated as (2.21 ± 0.04) Gy from the graph. The paleodose values of all LDKY samples estimated by using the MAAD technique are tabulated in Table 4.9.

Table 4.9 Equivalent doses of the LDKY samples with MAAD technique.

Sample Name	LDKY-1	LDKY-2	LDKY-3	LDKY-4	LDKY-5	LDKY-6
$D_{eq}(\text{MAAD})$ (Gy)	2.21 ± 0.04	6.30 ± 0.13	4.45 ± 0.09	5.88 ± 0.12	2.47 ± 0.05	2.42 ± 0.05

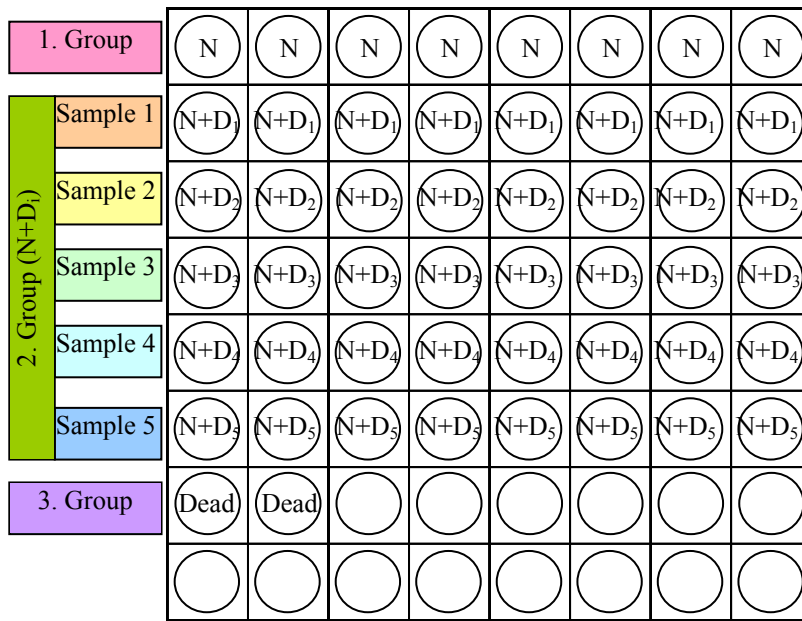


Figure 4.6 Grouping the samples on a tray and adding doses for luminescence measurements. Tray contains 64 holes for discs.

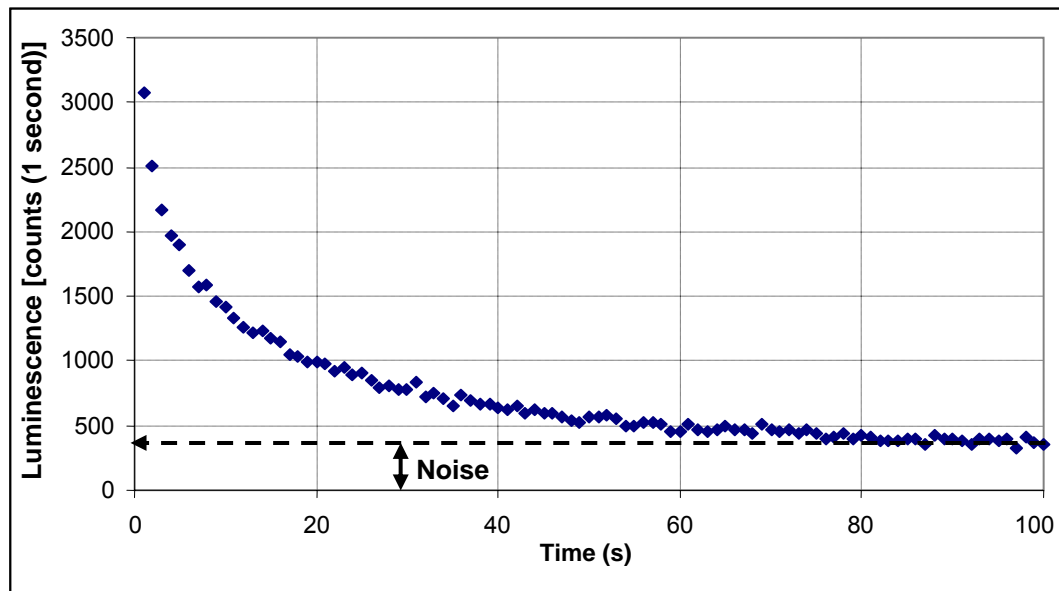


Figure 4.7 Luminescence versus time graph for a polymineral LDKY sample. The total luminescence was calculated by integrating the curve from 0 and 100 seconds.

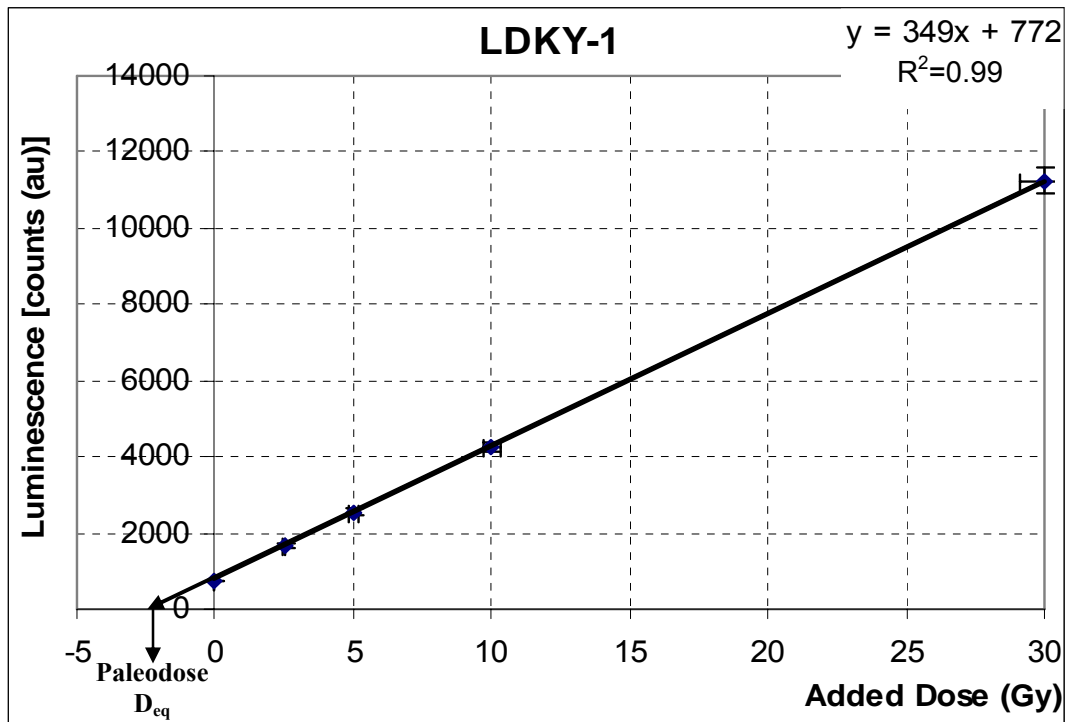


Figure 4.8 Luminescence versus added dose graph for LDKY-1 sample. The intercept of the extrapolated line on the horizontal axis gives the paleodose D_{eq} (Aitken 1998). For LDKY-1 sample, it is 2.21 Gy.

4.5 MARD (Multiple Aliquots Regenerated Dose) Technique

This technique is an alternative to the MAAD technique and it is especially advised for the samples that have low equivalent dose. Such samples may lose a considerable amount of their equivalent dose during the normalisation process, even during the application of a short time illumination (e.g. during the 0.1 second illumination suggested in the manual of the OSL system). Certainly, such a loss in the equivalent dose will lead to a wrong OSL age. In order not to have such a problem, one must prefer the MARD technique that is explained below, instead of the MAAD technique.

The aliquots were prepared for this technique in the same way as they were prepared in the MAAD technique. All the aliquots were preheated at 160 °C for 20 minutes to empty the shallow traps. They were arranged in the sample tray as

shown in Figure 4.9. Then, all the aliquots were measured by illuminating them for an extended time interval of 100 seconds, so that all the light sensitive traps were emptied. The data of this measurement was used to determine the normalisation constants and also used to find the natural average luminescence (\bar{N}), from the equation

$$\bar{N} = \frac{\sum_{i=1}^n N_i}{n} \quad (4.4)$$

where n is the number of aliquots and N_i is the measured natural luminescence of the i^{th} aliquot.

In order to be sure that all traps were emptied, all aliquots were heated at 350 °C for a few minutes. They were relaxed for few hours until they have cooled down to the room temperature. The aliquots were arranged in the sample tray, as shown in Figure 4.10, for adding the same dose to the aliquots of the same group, but a different dose to each group, up to 60 Gy.

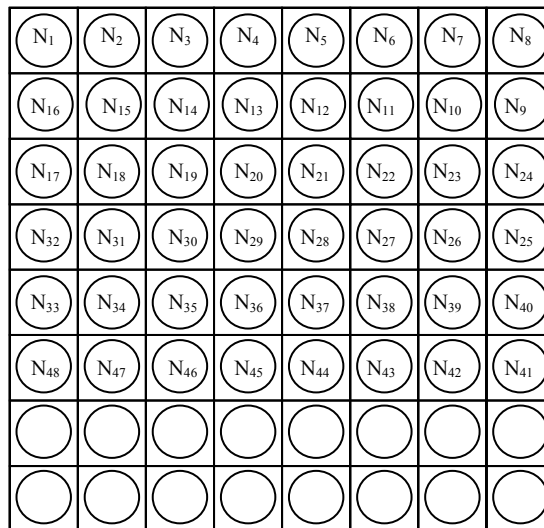


Figure 4.9 Arrangement of aliquots in the sample tray for natural luminescence measurement.

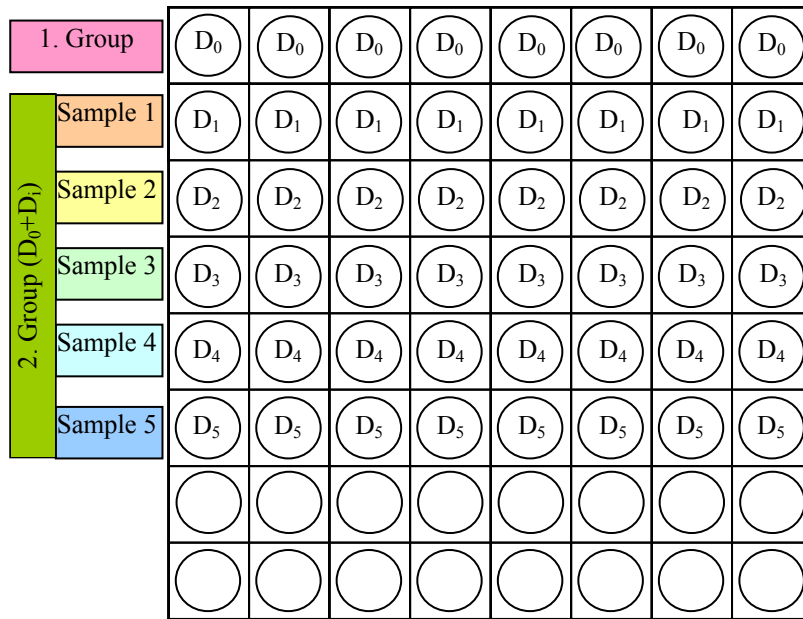


Figure 4.10 Grouping the samples on the tray and adding doses for luminescence measurements. (D_0 is the remaining dose after zeroing processes and D_i is the added dose on the aliquots of the i^{th} group).

Those aliquots denoted by D_0 were not given any dose and they were used to check whether the zeroing at 350 °C was complete or some natural dose was still remained. After giving dose to each group, the aliquots were kept waiting for several hours to relax. After their relaxation, they were preheated to empty the shallow traps and waited until they cool down to the room temperature.

Finally, the luminescences of aliquots were measured using IR illumination (shine) and the luminescence versus added dose graph for each sample was plotted. The plot for LDKY-1 sample is given in Figure 4.11 as an example. The equivalent dose (paleodose) of this sample has determined as $D_{eq} = (2.60 \pm 0.05)$ Gy from the graph as indicated. Knowing the natural average luminescence \bar{N} on the vertical axis, one can get the corresponding value D_{eq} on the horizontal axis through a simple projection process.

The equivalent dose (paleodose) values that have been determined using the MARD technique for the LDKY samples were tabulated with their estimated percentage errors ($\pm 2\%$), in Table 4.10.

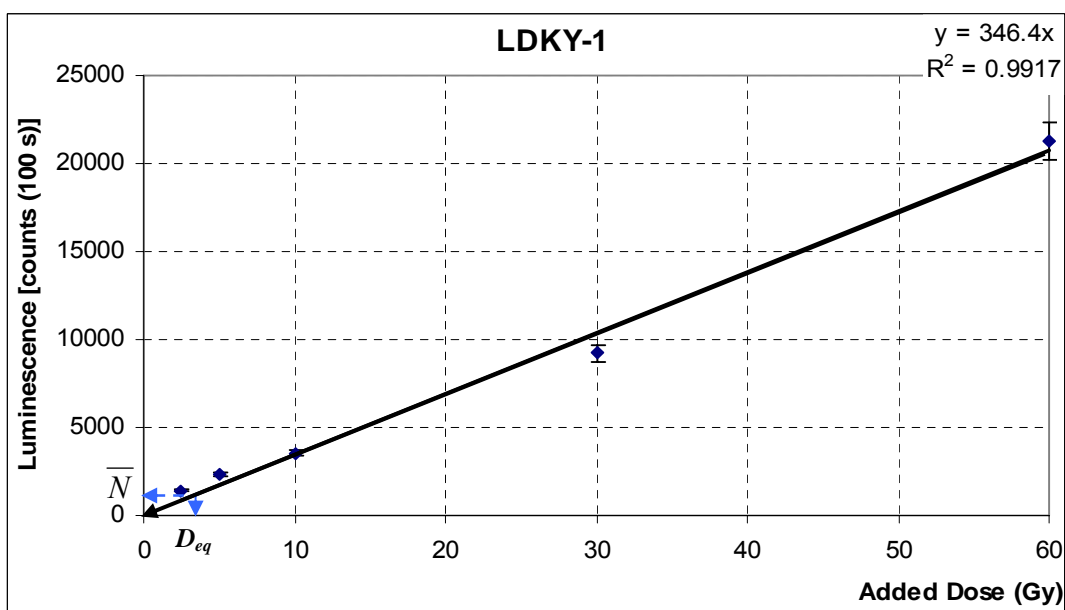


Figure 4.11 Luminescence versus added dose graph. The projection of \bar{N} on the curve gives Paleodose D_{eq} (equivalent dose).

Table 4.10 Equivalent doses of the LDKY samples with MARD technique.

Sample Name	LDKY-1	LDKY-2	LDKY-3	LDKY-4	LDKY-5	LDKY-6
$D_{eq}(\text{MARD})$ (Gy)	2.60 ± 0.05	6.25 ± 0.13	4.48 ± 0.09	5.85 ± 0.12	2.51 ± 0.05	2.38 ± 0.05

4.6 Annual Dose Measurements

In this study, the annual dose has been determined for the contribution of α , β particles, γ and cosmic rays. The annual dose components were measured as follows:

- The α dose rate was measured by the ELSEC 7286 low level alpha counter.
- The β dose rate was measured by the same alpha counting system. The potassium content has been determined using AES.
- γ and cosmic ray dose rates were measured by alpha counting system and gamma dosimeters ($\text{Al}_2\text{O}_3:\text{C}$).

Using Equations 3.7-3.14 annual doses for LDKY samples were calculated. The results were given in Table 4.11.

Table 4.11 Annual doses of LDKY samples.

Sample Name	LDKY-1	LDKY-2	LDKY-3	LDKY-4	LDKY-5	LDKY-6
Annual Dose (mGy/year)	3.00 ± 0.09	4.03 ± 0.12	3.08 ± 0.09	3.67 ± 0.10	2.39 ± 0.05	2.34 ± 0.05

4.6.1 Water Saturation and Water Uptake Measurements

The water saturation and water uptake determination have been done according to the following procedure (Buluş-Kırıkkaya, 2002)

1. Five medium sized porcelain crucibles were heated at 200 °C for 30 minutes in an oven and cooled in a desiccator. Then the crucibles were weighed. Heating process was repeated until each crucible reaches the constant weight.
2. Small amount of the powdered samples were put inside the crucibles and weighed to get the weight of the sample.
3. The samples were wetted with distilled water and heated at low temperature until they are completely wetted to get a hard mud.

4. The wet samples with crucibles were weighed again to get water saturated weight (W_s).
5. The samples inside the crucibles were heated at 200 °C until dryness and after cooling the crucibles in desiccator they were weighed again to get dry weight (W_{dry}).

Saturation water content and water uptake results of the LDKY samples were determined and they are given in Table 4.12.

Table 4.12 Water saturation content and water uptake measurements for LDKY samples.

Sample	Crucible Average Weight (g)	Crucible and Dry Sample Weight (g)	Crucible and Wet Sample Weight (g)	Saturation Water Content % (W)	Water Uptake During Burial (F)
LDKY-1	24.04	24.84	25.37	67	0.8
LDKY-2	25.28	25.93	26.34	60	0.4
LDKY-3	24.69	25.29	25.72	70	0.6
LDKY-4	23.24	24.25	24.36	10	0.2
LDKY-5	25.20	25.71	26.06	69	0.8
LDKY-6	25.45	25.95	26.31	70	0.7

4.6.2 Alpha Counting for LDKY Samples

In order to determine the alpha contributions from U and Th to the annual dose, alpha counting has been done by using ELSEC 7286 Low Level Alpha Counter. Sealed and unsealed alpha counts have been measured to determine the radon escape “if there is” for each sample for 24 hours with a period of 5000 seconds. The results are tabulated in Table 4.13. The measurement results and their errors were tabulated by the system itself using the computer program associated with the system.

Table 4.13 Unsealed and sealed alpha counts of LDKY samples.

SAMPLE NAME	UNSEALED α COUNTS / 5ksec			SEALED α COUNTS / 5ksec		
	Mean counts	Mean Th counts	Mean U counts	Mean counts	Mean Th counts	Mean U counts
LDKY1	46.14 \pm 6.79	17.69 \pm 6,08	28.46 \pm 6.34	45.66 \pm 6.71	21.10 \pm 6.69	23.90 \pm 6.95
LDKY2	55.25 \pm 7.43	38.62 \pm 7,99	16.63 \pm 8.20	56.58 \pm 7.52	37.80 \pm 3.43	18.78 \pm 3.53
LDKY3	54.24 \pm 7.36	22.59 \pm 6,30	31.65 \pm 6.55	55.09 \pm 7.42	33.50 \pm 9.11	21.59 \pm 9.38
LDKY4	42.64 \pm 6.53	18.18 \pm 6,79	24.45 \pm 7.07	43.85 \pm 6.62	22.89 \pm 6.87	20.96 \pm 7.11
LDKY5	43.86 \pm 6.62	18.02 \pm 8,54	25.84 \pm 8.90	49.00 \pm 7.00	20.26 \pm 9.18	28.74 \pm 9.55
LDKY6	32.69 \pm 5.72	12.79 \pm 4,62	19.89 \pm 4.84	35.70 \pm 5.97	17.14 \pm 3.68	18.56 \pm 3.83

As seen in Table 4.13 there is no significant difference between sealed and unsealed alpha counts of LDKY samples except LDKY-5 and 6. This shows effect of radon escape is not important except those twosamples. The reason for this is not known yet.

4.6.3 Determination of Potassium in Samples

The amount of potassium in a sample can be determined by using various methods including spectroscopic methods. In this study atomic emission spectrometer (Ati Unicam 923) (AES) in the Chemistry Department of METU was used. In the analysis, standard potassium solutions have been prepared using KCl (Merck) and emission intensities were measured. The results were given in Table 4.14. The calibration curve has been drawn (Figure 4.12).

Table 4.14 Concentrations of potassium standards and their emission intensity readings by AES. A and B shows two different measurements for the same potassium standard.

Concentration (ppm)	Intensity A	Intensity B
0,2	30,7	28,9
0,4	46,0	43,3
0,6	65,9	62,9
0,8	86,8	83,1
1,0	101,0	96,9

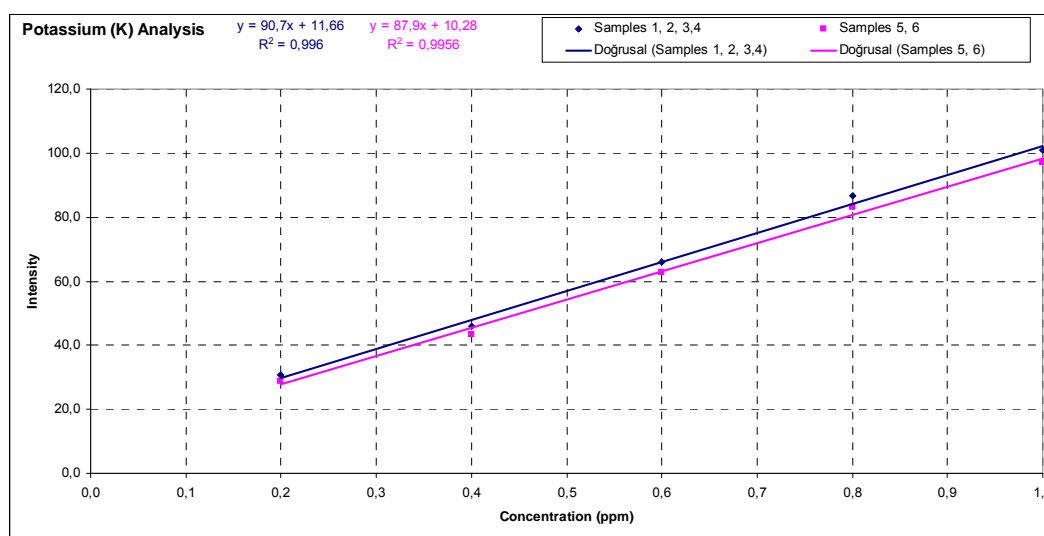


Figure 4.12 Potassium calibration curve. y and x are emission intensity and concentration (in ppm), respectively. Red and blue lines are showing two different measurements for the standard preparations. In this case, average of two lines was taken.

Potassium amounts of the LDKY samples have been determined by using the calibration curve and the results were given in Table 4.15.

Table 4.15 Atomic Emission Spectrometry results of LDKY samples for potassium content. [$K(g) = \text{Concentration} \times 50 \times 100 \times 0.000001$, where 50 is the volume of dissolved material solution in balon joje, 100 is the repeated dissolve factor and 0.000001 is the multiplication factor of ppm to g]

Sample	Average Intensity (au)	Standard Deviation	Concentration (ppm)	Sample (g)	K (g)	K (%)	K ₂ O (g)	K ₂ O (%)
LDKY-1	51.2	0.19	0.44	0.1460	0.0022	1.4945	0.026	1.7934
LDKY-2	59.3	1.34	0.53	0.2286	0.0026	1.1488	0.0032	1.3786
LDKY-3	29.7	0.44	0.20	0.1404	0.0010	0.7083	0.0012	0.8500
LDKY-4	28.4	0.26	0.18	0.1611	0.0009	0.5715	0.0011	0.6857
LDKY-5	33.7	0.30	0.27	0.1873	0.0013	0.7100	0.0016	0.8521
LDKY-6	33.4	0.30	0.26	0.1203	0.0013	1.0951	0.0016	1.3141

4.6.3.1 Preparation of the samples for potassium analysis (AES analysis)

The samples were prepared according to the following procedure (Black, 1965):

1. Ceramic samples were finely powdered in an agate mortar and approximately 0.1 gram was accurately weighed and placed in a platinum crucible. Three samples were studied at the same time. The procedure followed for each sample is given below.
2. Sample was wetted with a few drop of distilled water. Then, 5 ml 48% HF and 0.5 ml 70% HClO₄ were added to the crucible. The crucible was placed on a heated sand pool and heating was continued until white smokes were seen over the crucible.
3. Now 5 ml 48% HF was added and the crucible was placed on the sand pool buried in the sand almost completely. Crucible was heated up to 200 °C and heating was continued until all the solutions evaporate and sample get dry.

4. After the crucible was cool down, 2 ml distilled water and a few drop of HClO_4 were added. The crucible was placed inside the sand pool and heating was continued until all the liquid evaporates.
5. After cooling the crucible, 5ml of 6M HCl and 5 ml distilled water were added. This time crucible was heated with Bunsen burner until the solution was boiled and the sample was dried. Here, sample was expected to be fused completely.
6. If considerable amount of sample remained, fusion process (step 1 to 5) should be repeated.
7. The fused sample was treated with dilute HCl. Then, filtered using blue band filter paper. The filtrate was put in 50 ml or 100 ml graduated flask and diluted to the mark with distilled water.

4.6.4 Contribution of Gamma and Cosmic rays for Dose Rate

To determine the gamma (γ) and cosmic ray components of the annual dose, the thick $\text{Al}_2\text{O}_3:\text{C}$ Thermo-Luminescence Dosimeters (TLD) were used. These dosimeters are very sensitive to any kind of radiation, including the cosmic rays.

In this work eight commercial thick TLD were used. They were heated at 400 °C (Buluş-Kırıkkaya, 2002) to empty all the traps completely. In order to determine the gamma dose response characteristics of the dosimeters, they were exposed to γ radiation in “Ankara Nükleer Araştırma ve Eğitim Merkezi” and their TL were measured with the “Harshaw TL system” in the same laboratory. The measurement results are tabulated in Table 4.16 and the gamma dose response curve is given in Figure 4.13. The system used has recorded the amount of TL accumulated as TL voltage and therefore a TL voltage versus dose graph was plotted.

Following the gamma dose response measurements, the dosimeters were heated again at 400 °C until the TL accumulated during the γ radiation exposure was completely removed. Then, they were covered with aluminum folio and placed inside a plastic box, to prevent the penetrations of alpha and beta particles into the TLD's due to the radioactive isotopes in the soil. The covered TLD's were placed at a depth of 30 cm near the original places from which the LDKY samples were collected. They were kept in place approximately 8 to 11 months in Laodikeia site.

The dosimeters were collected from the site and brought to the laboratory immediately to determine the amount of gamma dose accumulated in them during their burial period. The results of measurements are tabulated in Table 4.17.

Table 4.16 Thick $\text{Al}_2\text{O}_3:\text{C}$ dose response table for gamma irradiation.

<u>Dose (mGy)</u>	<u>Voltage (Volt)</u>
0.000	0.00
0.530±0.011	6.65±0.13
1.325±0.027	17.25±0.35
2.650±0.053	33.60±0.67

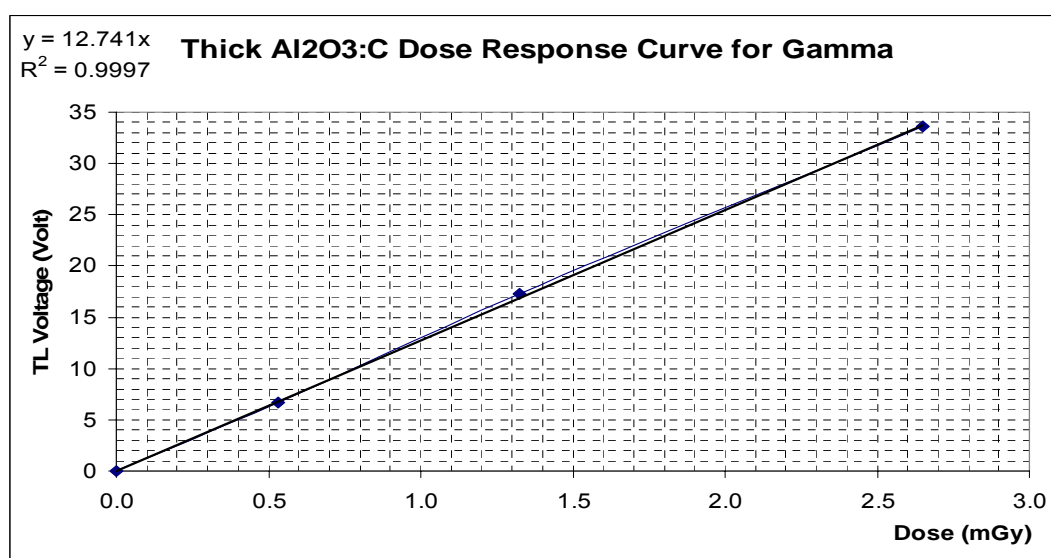


Figure 4.13 Thick $\text{Al}_2\text{O}_3:\text{C}$ dose response curve for gamma irradiation. y and x axes are representing the TL voltage (Volt) and dose (mGy), respectively.

Table 4.17 Dose rates of TLD dosimeters for annual γ and cosmic rays of LDKY samples.

Dosimeter # (Al ₂ O ₃ :C)	Dosimeter was kept on the site (day)	Measured γ and cosmic dose (mGy)	Annual γ and cosmic dose rate (mGy/year)
D1 and D2	267	0.77 ± 0.01	1.05 ± 0.02
D3 and D4	322	1.00 ± 0.02	1.13 ± 0.02
D5 and D6	322	1.37 ± 0.03	1.56 ± 0.03
D7 and D8	322	1.44 ± 0.03	1.64 ± 0.03

From Table 4.17, the average gamma dose was determined as 1.15±0.02 mGy/year and cosmic ray dose contribution was assumed as 0.15±0.01 mGy/year (Aitken, 1985) corresponding to a burial depth of one or two meters at low altitude. Actual value of the cosmic dose contribution at the sea level is 0.29 mGy/year (Aitken, 1985).

4.7 Supralinearity, Sensitization and Saturation of the LDKY Samples

In low dose rates, supralinearity was not observed for the LDKY samples until 500 Gy dose. Sublinearity was beginning after 500 Gy dose and the luminescence growth curve was linear until 1000 Gy, as seen in Figure 4.14. Since there is no supralinearity observed for LDKY ceramic samples, there is no need to make any correction for supralinearity. If the annual dose of samples were about 4 mGy, it would be possible to obtain OSL ages up to 125 kyear

$$\left(\frac{500000 \text{ mGy}}{4 \text{ mGy / year}} = 125000 \text{ years} = 125 \text{ kyear} \right).$$

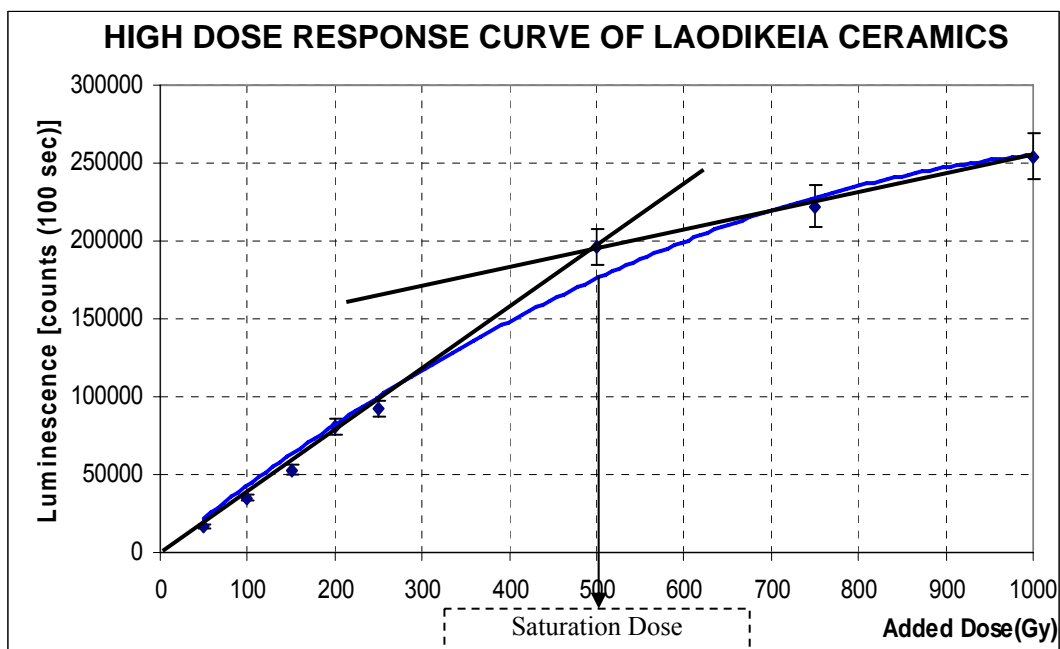


Figure 4.14 luminescence versus dose graph for high dose response.

CHAPTER 5

CONCLUSIONS

In this work, the optically stimulated luminescence of the ceramic samples collected from Laodikeia archaeological site was measured with ELSEC 9010 optical dating system. An array of IR diode was used to stimulate only the feldspar component of the samples. The data obtained was normalized using the normalization technique (Aitken, 1985). Equivalent dose (D_{eq}) was determined by the additive dose technique, in which the laboratory doses were added to the aliquots of the natural sample and the growth curve is extrapolated to zero luminescence signal to obtain the equivalent dose values. Samples were irradiated by a Sr-90 β source which has 0.0269 Gy/s dose rate for feldspar.

All the shallow electron traps that were filled during the laboratory irradiation were emptied by applying preheating process at 160 °C for 20 minutes. Then, they were illuminated by the IR light to measure the luminescence.

The uranium and thorium contribution to annual dose rate were determined by low level alpha counting (Elsec low level alpha counter 7286) system. Contribution of potassium content have been determined by using the atomic emission spectrometry (AES) and the cosmic ray component of annual dose rate was determined by placing TLD discs ($Al_2O_3:C$) at the site where samples were collected.

The ages calculated for the LDKY samples were found to be consistent with the values expected by the archaeologists.

The results of the study are promising and need further study, especially for the annual dose measurements. In this work, the age calculations were based on actual measurement results, but also some assumptions were made. In the annual dose calculation, suggested values of a , b and k parameters (Aitken, 1985) were used. These parameters for the LDKY site can also be determined experimentally in the future works.

There was no chronology done for LDKY site, based on laboratory techniques as far as archaeologists stated. Therefore, to establish a chronology for the site based on OSL technique has considerable importance.

In determining the annual dose of the samples, following assumptions were made;

- The LDKY samples had constant annual dose rate during their burial time.
- In the measurements, humidity of the sample was assumed to be zero, although samples may contain some amount of humidity.

In determining the annual dose and equivalent dose of the samples, the following precautions were taken;

- The samples were taken from the same level and they were close to each other.
- The samples were kept open after grinding for radon escape.
- The samples always were stored up in a dark place.
- The samples were handled all the times in red light.

Annual dose has been calculated from internal radioactive impurities of the sample itself such as U, Th and K. These elements emit α , β particles and γ radiation. The dose rate contributions of α , β particles and γ radiation have been determined with different methods. The α contribution has been determined by using alpha counter which measures the total amount of alpha particles coming from radioactive impurities (U and Th). The β and γ contributions have been determined by using alpha counter and potassium amount using AES.

Radon escape has been observed by measuring the alpha particles with sealed and unsealed fine grained samples. However, there was no appreciable difference between sealed and unsealed α measurements. Therefore, it can be assumed that radon escape has no effect in annual dose measurements.

Instead of applying preheating process to the radiated aliquots in order to remove the electrons from shallow traps, a correction factor can be used as a constant for polimineral fine grain aliquots. In this study, this correction factor has been found as 0.7. Because, the 30% of the total Luminescence (counts) were disappeared during the 20 minutes preheating at 160 °C. In addition, the fading of the unpreheated aliquots occurs during the 30-40 days period at room temperature. However, this work has been done three times for one ceramic sample (LDKY-3). Therefore, it is difficult to say that the founded correction factor is exactly suitable and same for all other types of the samples.

For the further studies, annual and equivalent doses of the samples must be determined with some other techniques and methods by using alternative devices. As a suggestion, for the annual dose determination U, Th and K amounts can be determined altogether by using a method such as Inductively Coupled Plasma – Optical Emission Spectroscopy (ICP-OES) or an X-Ray Fluorescence (XRF).

For the LDKY samples one can also use quartz component of the samples in the OSL measurement.

As mentioned before, LDKY samples have not shown any supralinearity and sensitivities were constant for all LDKY samples. Saturation started after 500 Gy for LDKY ceramic samples and this shows that ceramic is a good natural dosimeter and age estimation can be done up to 100-150 kyear without making any supralinearity correction.

APPENDIX-A

A.1 The Parts of ELSEC 9010 Optical Dating System comprises

- 1. Control Computer:** IBM-PC compatible with 80386 micro processor, 40 MB hard disc and a monitor.
- 2. Computer Interface Cards:** 2 cards are required that plug into the computer which are Stepper and Counter Driver cards.
- 3. Interface module:** This contains high and low voltage power supplies, control circuits for the IR LEDs, displays for LED current, sample temperature and IR intensity.
- 4. Sample tray:** A black anodised aluminium tray (Figure A.1) with 64 machined positions for standard (9.7 mm diameter) sample discs. A light-tight, screw-down lid fitted with a viton rubber o-ring provided for safe sample transport.

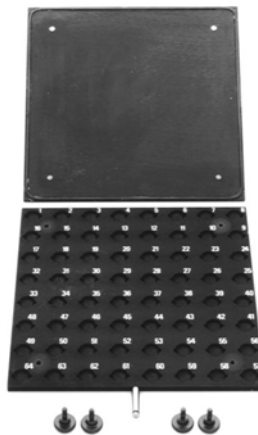


Figure A.1 Sample Tray.

5. Sample handling module: An X-Y stepper-motor positioning unit takes the sample tray and positions samples under the photomultiplier on command from the control computer. It is mounted in a heavy-duty light tight box. The sample is held on a heavy copper plate that is temperature controlled by Peltier devices at 22.0 ± 0.5 °C. This generates waste heat that needs to be removed with water cooling. The water is connected to the back of the sample positioning unit.

6. Sample Illumination Assembly: There are several optional modules that can be used for sample illumination. However, only one module which is IR LED Module has been used in this research.

7. IR LED Module: 24 IR LEDs are mounted in machined aluminium block for accurate alignment and temperature stability. A photodiode is fitted for closed loop IR intensity control or LEDs can be operated in a constant current mode. Even illumination of the sample is ensured with a plastic diffuser. The module also has a fused silica light guide to transmit the emitted luminescence to the photomultiplier.

8. Photomultiplier assembly: This assembly is consisting of low-noise photomultiplier mounted in a light tight housing. There is a build in preamplifier with user adjustable discriminator. In order to reject stimulating light, optical filters are presented. An optical filter in front of the photomultiplier tube is used to eliminate the stimulating wavelengths. To access this filter (44 mm diameter) the bottom of the photomultiplier assembly is removed. The filter for IR diodes is a Schott BG 39. The fractional transmission versus wavelength curve of the filter is given in Figure A.2.

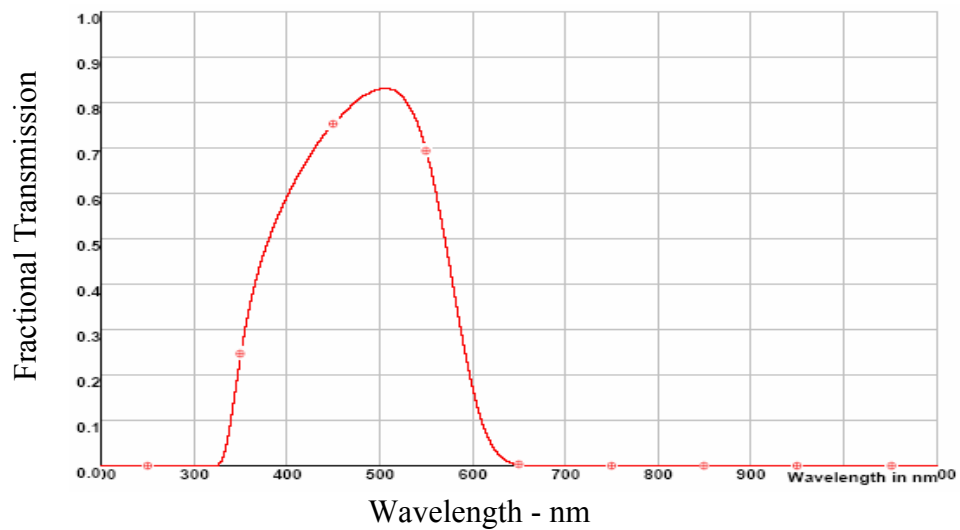


Figure A.2 The graph of fractional transmission versus wavelength of Schott BG 39 filter. <http://www.galvoptics.fsnet.co.uk/bg39.htm>

9. Printer: It is an 80 column 24 pin dot matrix printer. It is used to print out the data collected by the computer.

10. Software: The standard program supplied with OSL unit. “OSL” software allows the user to manually control the unit, sample position under the photomultiplier and record data on a sample by sample basis. Alternatively, the system can be set up to automatically record the results for all 64 (or fewer) samples on the tray. Results can be viewed and edited in tabular form. All shine curves (i.e. the luminescence signal observed) can be viewed on screen either singly, overlain as a group for a given dose point or the full data set can be shown with color coding of each dose group. These graphs can be dumped to a dot matrix printer, plotted on a pen plotter or laser printer or converted to PCX format (PCX files are used for graphic data storage) for incorporation in to word processed documents. Data are stored in binary format and full information on file structure is provided to enable the user to write software to access the results. Utilities are provided to convert results to ASCII (American Standard Code for Information Interchange is a character encoding based on the English alphabet) text can be read into spreadsheets.

11. “PLATO” software: This is the main data analysis program. “PLATO” and the “OSL” programs are designed to be flexible and to permit different methods of paleodose estimation. The period over which luminescence is measured can be subdivided into a maximum 16383 channels with variable duration (10 ms to 43x10⁶ seconds with 10 ms resolution). This permits user selection of the integration periods of interest, such as greater time resolution of the shine curves in the early stages of the luminescence decay. Normalization factors can be either read in from a pre-measured “short exposure” file or inserted by the user. The background subtracted from each shine curve can be chosen from the mean count rate of the final part of that shine curve, a value obtained from a “dead” sample or a user inserted number. A separate growth curve fitting for each integral period is currently performed both by linear fitting and exponential fitting using an algorithm developed by B.W. Smith (9010 Optical Dating System user Manual, 1993). Additional curve fitting algorithms can be incorporated.

12. “AGE” software: This program takes the paleodose from the “PLATO” program and other user input dosimetric data (such as radioisotope concentrations or fractional dose rates, cosmic ray dose rate, water content, burial depth etc.) and calculates an age for the sample and an error estimate for that age.

13. Beta Irradiator unit: Sr-90 source was installed the system shown in Figure A.3. The radioisotope compound is incorporated into the front surface of the silver disc in a very thin layer about 2mm for a 1.5 GBq source. There is a 0.1 mm screen of silver on which is a protective coating of gold or palladium.

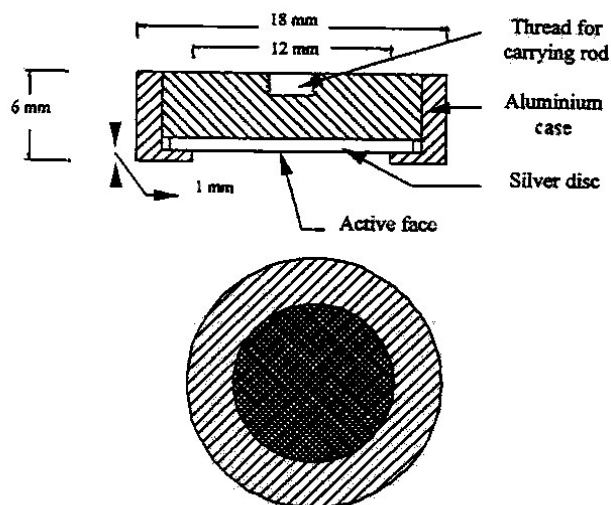


Figure A.3 Basic set-up for beta irradiation (Aitken 1998, Akoğlu 2005)

A.2 Alpha Counting System

The alpha counting system used in the study is 7286 Low Level Alpha Counting System has been developed mainly for dating studies where the counting rate is small and background noise is very low. Up to four scintillation-photomultiplier assemblies can be controlled from the one printer and one control unit. There is an adjustable high voltage supply and discriminator unit for each photomultiplier tube (PM). The output pulses from the discriminator circuit are fed into an internal microprocessor which keeps track of the total number of fast pairs which occur within 4 msec. and slow pairs which occur between 20 and 400 msec. apart. These pair counts allow the user to estimate the uranium and thorium contents. ELSEC 7286 Low Level Alpha Counter is shown in Figure A.4.

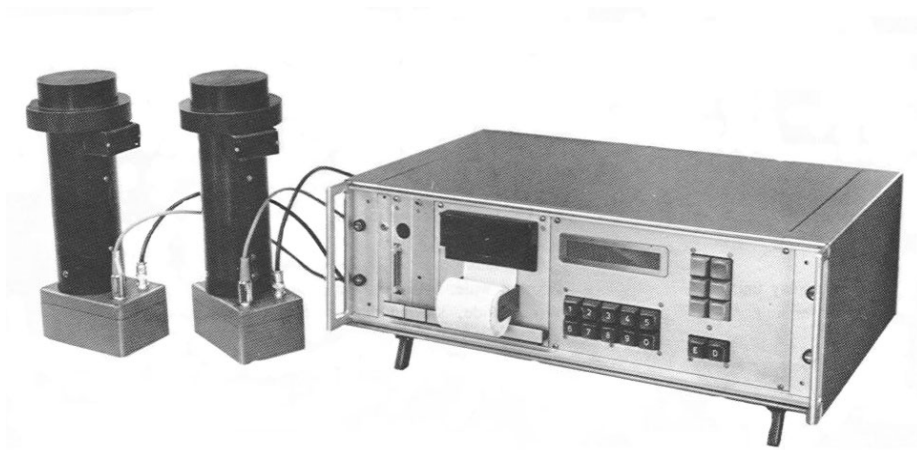


Figure A.4 ELSEC 7286 Low Level Alpha Counter system.

In this system, a powdered layer of sample is placed on top of a scintillation screen. The scintillation screen is ZnS coated mylar film which produces a scintillation. Electronic scheme of alpha counting system is shown in Figure A.5. The range of the most energetic alpha particles from thorium and uranium are around 50 μm . When these particles hit ZnS coated Mylar surface which produces light and this light produce photoelectrons from the photocathode of the photomultiplier tube (PM). After amplification these photoelectrons become an electrical pulse at the anode of the photomultiplier. Then this pulse is registered on a counting device.

The scintillation screen is made by sprinkling zinc sulphide onto cello tape or Mylar. The advantage of zinc sulphide is that the pulses corresponding to the scintillation produced by alpha particles are much larger than those produced by beta particles and gamma radiation. This enables easy rejection of the latter in the electronics. In addition, the powdered sample is placed in direct contact with a suitable detergent or methanol to avoid errors coming from the previous usage. The sample plus photomultiplier must be enclosed in a dark box because of the light sensitivity of photomultiplier.

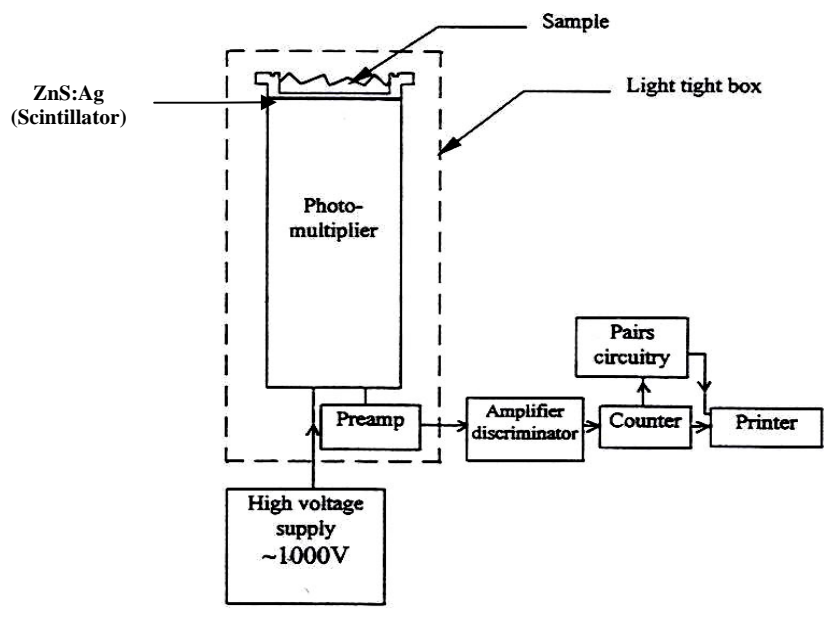


Figure A.5 Simplified block diagram of alpha counting system.

APPENDIX-B

B.1 OSL Dating System

In this study ELSEC 9010 Optical Dating System present in the Department of Physics, METU was used (Figure B.1). The parts and the working procedures of the system have been given in Appendix-A. The calibration of the system is given in the following sections.



Figure B.1 ELSEC 9010 Optical Dating System.

B.2 Calibration of Optical Dating System

Calibration of the system consists of setting High Tension (HT) and Threshold voltages of photomultiplier (PM) tube and recalculation of dose rates of Sr-90 beta (β) source. As it is written in the manual of the system, the random error

in each measurement is at most 5%, but about 2% has been estimated in the previous measurements with the system (Akoğlu 2004 and Buluş-Kırıkkaya 2002). In this work the estimated instrumental random error is also 2%.

Setting High Tension Voltage

The sensitivity of the PM tube depends on the voltage applied to it; in general, the larger the voltage the greater the sensitivity is. If the voltage is too high, however, the background noise level will be increased. So, for the measurements the most suitable operating HT voltage must be determined through a calibration process. For the process a calibration light source (a C-14 doped phosphorus) is provided as a part of the system. The threshold control potentiometer at the top of the PM tube housing was set to a value between 3 and 4 volts during this measurement as recommended in the manual of the OSL system. The calibration light source has been placed into a sample tray and positioned under the PM tube in manual mode. Then, in the LEDs off condition a series of measurements has been done.

A series of measurements of the apparent intensity of the light source was taken in equal time periods for various HT voltages, with 25 volt increments from 850 V to 1400 V. The measurement results are tabulated in Table B.1 and the calibration curve is given in Figure B.2.

The calibration curve has a plateau region between 1200 V and 1300 V, as seen in Figure B.2. The operating HT voltage is taken at the midpoint of the plateau region to have minimum variation in the luminescence intensity measurements relative to the variations of HT voltage.

Table B.1 High Tension (HT) voltage calibration data of the PM tube of the OSL system. Yellow rows show the plateau region between 1200V and 1300V.

HT Voltage (V)	Apparent Intensity (counts / s)	HT Voltage (V)	Apparent Intensity (counts / s)
850	0	1125	1296
875	1	1150	1630
900	1	1175	1847
925	3	1200	1911
950	6	1225	2033
975	17	1250	2062
1000	41	1275	2083
1025	99	1300	2165
1050	217	1375	4049
1075	498	1400	5996
1100	915		

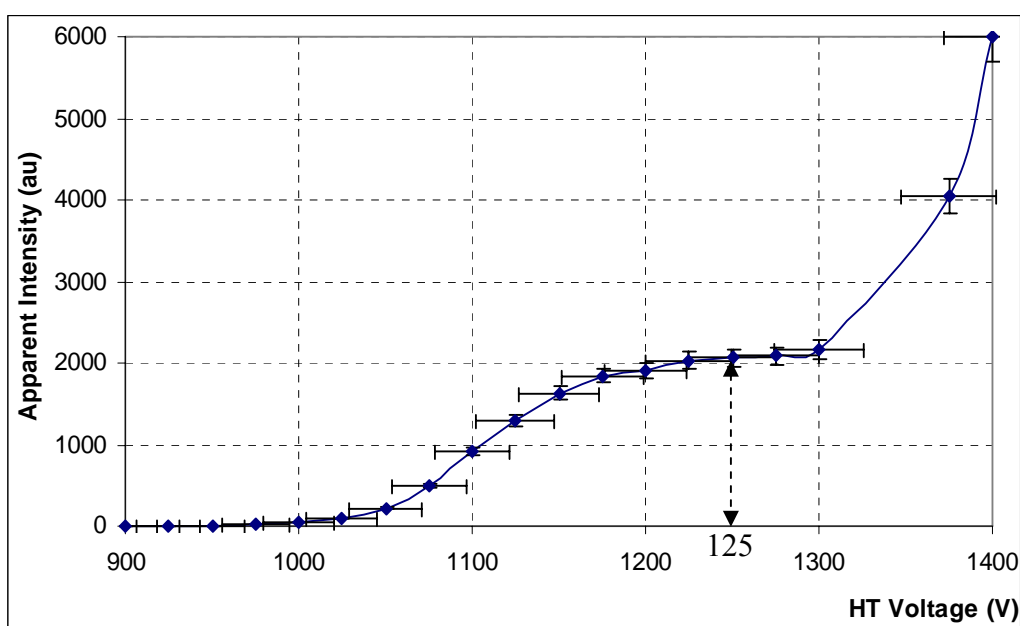


Figure B.2 The apparent intensity versus HT voltage curve. The plato region is between 1200 V and 1300 V.

The calibration curve has yielded the operating HT voltage of 1250 ± 25 V. Here, ± 25 V corresponds to the instrumental error. This voltage has been used to operate the PM tube during the sample intensity measurements.

Setting Threshold Voltage

The threshold value should be set to a level that eliminates as much noise as possible, without losing the smaller true pulses. The calibration light source should be inserted in the same way as described above for setting HT voltage. The determined HT voltage 1250 V was set during the threshold voltage measurements.

A series of readings was taken for various threshold settings between 2.0 and 10.0 volts with 0.25 V increments using the LEDs off condition as described above for setting HT voltage. The measurement results are tabulated in Table B.2 and the calibration curve based on these results is given in Figure B.3.

The threshold voltage is determined from the calibration curve (Figure B.3) using the 85% rule, (Aitken, 1985).

Table B.2 Threshold voltage calibration data of the PM tube of the OSL system.

Threshold Voltage (V)	Apparent Intensity (counts / s)	Threshold Voltage (V)	Apparent Intensity (counts / s)
2.00	1912	6.25	1649
2.25	1913	6.50	1616
2.50	1900	6.75	1571
2.75	1880	7.00	1556
3.00	1859	7.25	1528
3.25	1852	7.50	1502
3.50	1845	7.75	1494
3.75	1814	8.00	1436
4.00	1819	8.25	1382
4.25	1793	8.50	1356
4.50	1803	8.75	1316
4.75	1756	9.00	1262
5.00	1736	9.25	1231
5.25	1730	9.50	1186
5.50	1709	9.75	1129
5.75	1679	10.00	1058
6.00	1663	HT Voltage: 1250 V kept constant	

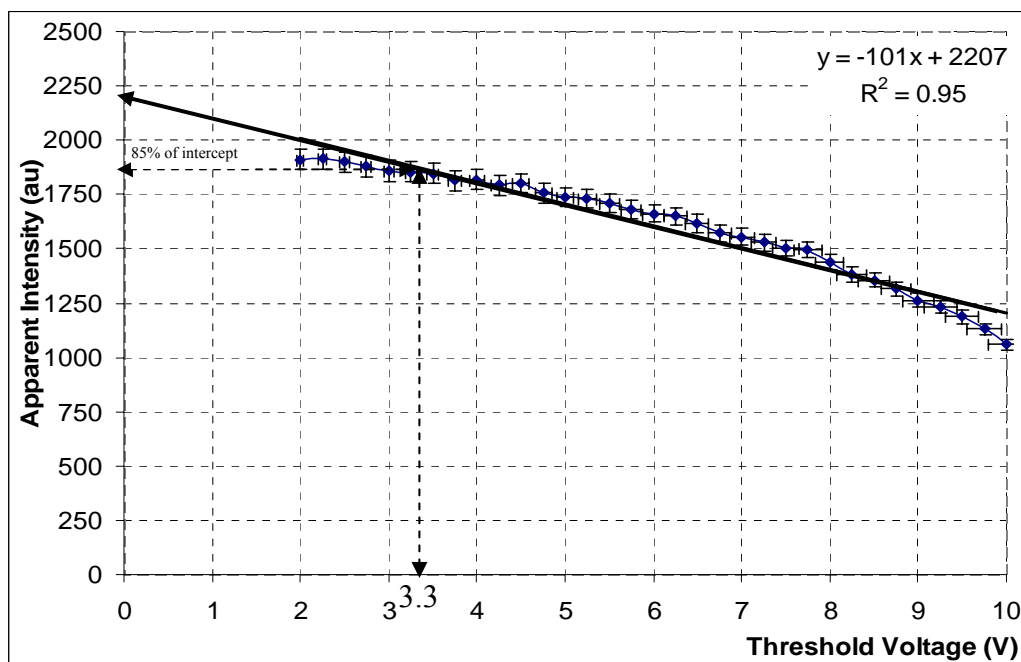


Figure B.3 The calibration curve of the PM tube, apparent intensity versus threshold voltage graph. Threshold voltage was calculated as 3.30 V from the graph. The straight line fitted has a negative slope and a relatively high R^2 -factor.

The rule is based on the alpha counter calibration (see, Appendix B.2.1) for the threshold voltage setting to eliminate the background noises of PM tube (Aitken, 1985).

The threshold voltage is determined from the graph (Figure B.3) as 3.30 ± 0.08 V. Here ± 0.08 V corresponds to instrumental error. This threshold voltage has been used to operate the PM tube throughout the intensity measurements of the samples.

B.3 Alpha Counting System

In this study the ELSEC 7286 Low Level Alpha Counting System (Figure A.4) has been used. The system designed and developed specifically for dating studies where the counting rate is small and the background noise level is very low. See Appendix-A for its operating procedure and parts.

B.4 Calibration of Alpha Counter

Every photomultiplier tube has different characteristics, thus, the ELSEC 7286 Low Level Alpha Counter has to be calibrated before the sample measurements. The calibration procedure is similar to that of the optical and alpha counting systems.

Setting High Tension (HT) Voltage

As recommended in the manual, the threshold control on the back panel is set to 1.0 V. For calibration, an alpha source which is strong enough to provide about 10 counts per second, such as Monazite sand is needed. Monazite (Ce, La, Y, Th)PO₄ sand is the main source of thorium oxide, which contains in amounts varying between 1 and 20 per cent thorium oxide by weight. Commercial monazite usually contains between 3 and 9 percent thorium oxide by weight, (Cornelius and Hurlbut, 1971). Thorium oxide is used in the manufacture of mantles for incandescent gas lights. Monazite sand used in this study was obtained from the burned propane lamp mantle. In addition, Sand 109 provided with the system, containing Thorium and Uranium could also be used for the calibration. Since the Sand 109 (specified as Thorium content of 104 ppm plus Uranium content of 3.7 ppm) gives approximately 60 counts per ksec (Aitken, 1979), the calibration process would take too much time, and therefore it has not been preferred.

It is recommended that the HT voltage must start at about 1250 V and then decrease down to 800 V in steps of 25 V. The time interval for each measurement was 100 seconds, and the results are listed in Table B.3. After each step to allow the PM tube to recover, a time interval of about 5 minutes was needed. The calibration curve based on values in Table B.3 is shown in Figure B.4. The curve has a plateau region between 1125 V and 1275 V, as indicated in Table B.3. From the plateau, the midpoint voltage is determined with its instrumental error as 1150 ± 25 V. This voltage has been used in this study for α counting measurement.

Table B.3 High Tension (HT) voltage calibration data of the Alpha counter PM tube. Yellow rows show the plateau region.

HT Potential (Volt)	Count (100 sec)	HT Potential (Volt)	Count (100 sec)
800	221	1125	595
825	317	1150	604
850	368	1175	610
875	423	1200	600
900	467	1225	595
925	521	1250	600
950	542	1275	598
975	556	1300	609
1000	568	1325	618
1025	579	1350	658
1050	584	1375	685
1075	589	1400	742
1100	589		

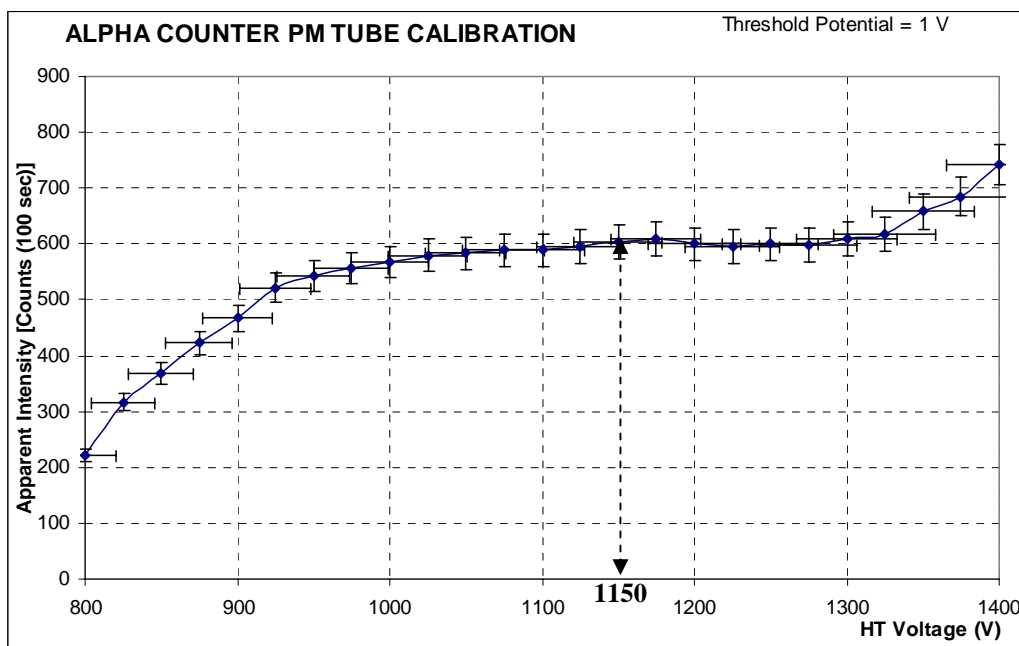


Figure B.4 HT voltage calibration curve of the Alpha counter PM tube. The threshold potential is kept constant at 1 Volt. The plateau region is between 1125 V and 1275 V.

Setting Threshold Voltage

The same alpha source, monazite sand, has been used in the calibration measurements. The operating voltage of the alpha counter PM tube has been set at 1150 V and a series of results has been obtained for threshold voltages between 0.25 V and 2.5 V. The measurement results are tabulated in Table B.4 and the calibration curve based on these results is given in Figure B.5.

For a perfect counting system with no electrical noise and other imperfections, no threshold is needed and one can set the threshold voltage to zero. For a real system, as mentioned before, a threshold voltage should be set to a level to eliminate the noise inherent in the system, but it must be a minimum not to lose the actual pulses of the measurement.

The threshold calibration curve (Figure B.5) is linear with negative slope and, when extended, it cuts the vertical axis at about 608 counts per 100 seconds.

This is the count rate at the zero thresholds. It is the rule (Aitken 1985) that a certain percentage (85% for the thorium series and 82% for the uranium series) of this value will be used to determine the threshold voltage. In other words, about 15% of this count is assumed to be due to the beta particles and the PM noise, and it must be eliminated.

The value 517(=85% of 608) is substituted in the linear equation and the operating threshold voltage is determined as 1.15 ± 0.02 V. This value has been used in the measurements.

Table B.4 Threshold voltage calibration data of the Alpha Counter PM tube.

Threshold Voltage (x0.25V)	Apparent Intensity Counts (100 s)	Threshold Voltage (x0.25V)	Apparent Intensity Counts (100 s)
1.0	565	6.0	517
1.5	573	6.5	470
2.0	527	7.0	465
2.5	581	7.5	454
3.0	537	8.0	450
3.5	589	8.5	423
4.0	555	9.0	429
4.5	515	9.5	436
5.0	484	10.0	381
5.5	515		

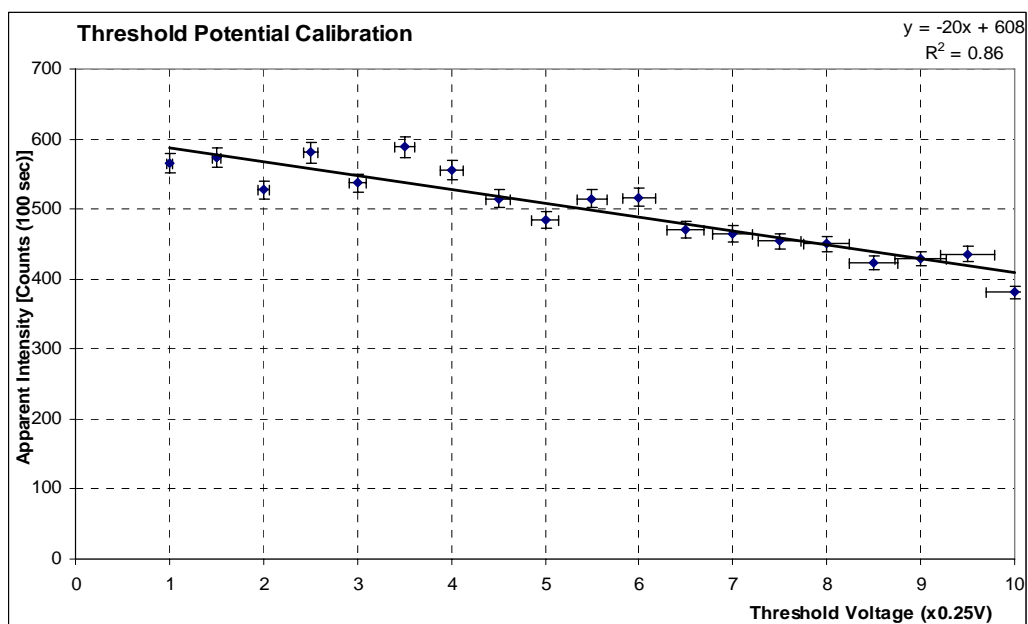


Figure B.5 Threshold voltage calibration curve. The horizontal values are the readings from the potentiometer and each increment corresponds to 0.25 V.

The alpha counter was set at 1150 V with a threshold voltage of 1.15 V and then Sand-109 source has been measured to check the calibration values. The counter yielded a result in between 56-59 counts in 1000 seconds, which is in accordance with the manual.

After calibration has been finished, the measurements of the samples have been carried out as given below.

B.5 Dose Rate Calculations of Sr-90 Beta Radiation Source

A radiation source is needed in dose determinations of the samples. The source in the OSL laboratory is Sr-90 beta radiation source which has arrived to the laboratory in 1994. It has characteristic properties given in Table B.6. The dose rates of the source for feldspar and quartz have been determined in years after 1993, and the values are given in Table B.6.

The dose rates of the source depend on time and therefore the present value of the dose rate must be determined prior to each measurement. In this work the values of the year 2004 are used, and they are based on the 2001 values (Buluş-Kırıkkaya, 2002).

A radioactive nuclide, like Sr-90, decays with time t according to the law of radioactive decay.

$$N(t) = N_0 e^{-\lambda t} \quad (\text{B.1})$$

where, N_0 is the number of radioactive nuclei in the sample at $t=0$ and $N(t)$ is the number remaining at any later time t . The decay constant (or disintegration constant) λ has a characteristic value for every radionuclide. It is related to the half-life $t_{1/2}$ as

$$\lambda = \frac{\ln 2}{t_{1/2}} \quad (\text{B.2})$$

where, $t_{1/2} = 28$ years for Sr-90.

The decay rate $R(= -dN/dt)$ is more often used than $N(t)$. Differentiating Equation 3-1, we find

$$R(t) = -\frac{dN(t)}{dt} = \lambda N_0 e^{-\lambda t}$$

or

$$R(t) = R_0 e^{-\lambda t} \quad (\text{B.3})$$

as an alternative form of the law of radioactive decay. Here, R_0 is the decay rate at time $t=0$ and $R(t)$ is the rate at any subsequent time t .

The decay rate R of a sample is called the activity of that sample. The SI unit for activity is becquerel:

$$1 \text{ becquerel} = 1 \text{ Bq} = 1 \text{ decay per second.}$$

Another unit in common use is the curie:

$$1 \text{ curie} = 1 \text{ Ci} = 3.7 \times 10^{10} \text{ Bq.}$$

In the OSL laboratory the activity of the Sr-90 beta radiation source has been determined for six months periods between 25.01.2004 and 11.05.2006 and the values are given in Table B.6. Equation B.2 is used to find the decay constant λ and then its value is substituted in Equation B.3 to obtain the dose rate.

Table B.5 Sr-90 beta radiation source dose rates for feldspar and quartz components of the sample and its calculated activity values. The yellow row shows the activity for year 1993 and the green row shows the activity in 2001 (Buluş-Kırıkkaya, 2002). The estimated percentage error in each result is $\pm 2\%$.

Date	Dose Rate for Feldspar (Gy/sec)	Dose Rate for Quartz (Gy/sec)	Calculated Activity (GBq)
04.11.1993	0.0438	0.0550	3.700
11.05.2001	0.0308	0.0386	2.600
25.01.2004	0.0286	0.0357	2.414
11.05.2004	0.0282	0.0353	2.384
11.11.2004	0.0279	0.0349	2.355
11.05.2005	0.0276	0.0344	2.326
11.11.2005	0.0272	0.0340	2.297
11.05.2006	0.0269	0.0336	2.269

REFERENCES

Aitken M.J., (1979). Values observed at Research Lab for Archaeology and the History of art, Oxford University (7286 Low Level Alpha Counter User Manual).

Aitken M.J. (1985). Thermoluminescence Dating. Academic Press, London, 359p. ISBN: 0-12-046380-6.

Aitken, M.J., (1989). Luminescence dating: a guide for non-specialists. *Archaeometry* 31, 2, 147-159.

Aitken M.J. (1998). An introduction to optical dating .The Dating of Quaternary Sediments by the Use of Photon-Stimulated Luminescence. Oxford University Press, Oxford, 267p., ISBN: 0-19-854092-2.

Akoğlu K.G., (2003). M.Sc. Thesis: Optically Stimulated Luminescence (OSL) Dating of Çatalhöyük Samples. *METU Graduate School of Natural and Applied Sciences*.

Auclair M., Lamothe M. and Huot S. (2003). Measurement of anomalous fading for feldspar IRSL using SAR. *Radiation Measurements* 37, 487-492.

Berger G.W. and Huntley D.J. (1994). Tests for optically stimulated luminescence from tephra glass. *Quaternary Geochronology (Quaternary Science Reviews)* 13, 509-511.

Berger G.W. and Neil P.A. (1999). Photon-stimulated-luminescence (PSL) dating tests of glass-rich volcanic ash. Book of Abstract LED99: 138.

Black C.A., (1965). Method of Soil Analysis (part 2) Chemical and Microbiological Properties. American Society of Agromony.

Bøtter-Jensen L., (2000). Development of Optically Stimulated Luminescence Techniques using Natural Minerals and Ceramics, and their Application to Retrospective Dosimetry. *Risø National Laboratory, Roskilde*. ISBN 87-550-2755-5

Bøtter-Jensen L., Solongo S., Murray A. S., Banerjee D. and Jungner H. (2000). Using the OSL single-aliquot regenerative-dose protocol with quartz extracted from building materials in retrospective dosimetry. *Radiation Measurements* **32**, 841-845

Bøtter-Jensen L., McKeever S.W.S. and Wintle A.G. (2003a). Optically Stimulated Luminescence Dosimetry. Elsevier Science, The Netherlands, 355p., ISBN: 0-444-50684-5.

Bøtter-Jensen L., Andersen C.E., Duller G.A.T. and Murray A.S. (2003b). Developments in radiation, stimulation and observation facilities in luminescence measurements. *Radiation Measurements* **37**, 535-541.

Bulur E., (1996). An alternative technique for optically stimulated luminescence (OSL) experiment. *Radiation Measurements* **26**, 701-709.

Bulur E. and Göksu H. Y., (1997). Pulsed optically stimulated luminescence from α -Al₂O₃:C using green light emitting diodes. *Radiation Measurements*, **27**, 479-488.

Bulur E. and Göksu H. Y., (1999). Infrared (IR) stimulated luminescence from feldspars with linearly increasing excitation light intensity. *Radiation Measurement* **30**, 505-512.

Buluş-Kırıkkaya E., (2002). Ph.D. Thesis: Kocaeli (Kullar-Yaylacık) Fayından Alınan Kuvars Örneklerinin Optik Uyarmalı Lüminesans (OSL) ve Termolüminesans (TL) Yöntemleri ile İncelenmesi. *Kocaeli Üniversitesi Fizik Bölümü*.

Chen R. and McKeever S.W.S. (1997). Theory of thermoluminescence and related phenomena. World Scientific Publishing, Singapore, 559p., ISBN: 9810222955.

Clark P.A. and Templer R.H. (1988). Thermoluminescence dating of materials which exhibit anomalous fading. *Archaeometry* **30**, 19-36.

Cornelius S. Hurlbut, JR. (1971). Dana's Manual of Mineralogy. Wiley International Edition, Newyork, 579p., ISBN: 0-471-42225-8.

Duller G.A.T. (1991). Equivalent dose determination using single aliquots. *Nuclear Tracks and Radiation Measurements* **18**, 371-378.

Duller G.A.T., Botter-Jensen L. and Markey B.G., (1997). A Luminescence Imaging System Based on a CCD Camera. *Radiation Measurements* **27**, 91-99.

Duller G. A. T., Bøtter-Jensen L., Murray A. S. and Truscott A. J., (1999). Single grain laser luminescence (SGLL) measurements using a novel automated reader *Nuclear Instruments and Methods in Physics Research Section B: Beam Interactions with Materials and Atoms*, **155**, 506-514

Fleming S., (1979). Thermoluminescence techniques in archaeology. Oxford University Pres, London, 212p., ISBN: 0-19-859929-3.

Fragoulis D. and Stoebe T.G. (1990). Relationship of anomalous fading to feldspar inclusions in quartz. *Radiation Protection Dosimetry* **34**, 65-68.

Fragoulis D.V. and Readhead M.L. (1991). Feldspar inclusions and the anomalous fading and enhancement of thermoluminescence in quartz grains. *Nuclear Tracks and Radiation Measurements* **18**, 291-296.

Franklin A.D., Prescott J.R. and Scholefield R.B. (1995). The mechanism of thermoluminescence in an Australian sedimentary quartz. *Journal of Luminescence* **63**, 317-326.

Forman, S. L., and Pierson, J., (2003). Formation of linear and parabolic dunes on the eastern Snake River Plain, Idaho in the nineteenth century: *Geomorphology*, v. 1354, 1-12.

Huntley D.J., Godfrey-Smith D.I. and Thewalt M.L.W. (1985). Optical dating of sediments. *Nature*, **313**, 105-107.

Huntley D.J., Hutton J.T. and Prescott J.R. (1993). The stranded beach-dune sequence of south-east South Australia: A test of thermoluminescence dating, 0-800 ka. *Quaternary Science Reviews* **12**, 1-20.

Huntley D.J., Hutton J.T. and Prescott J.R. (1994). Further thermoluminescence dates from the dune sequence in the southeast of South Australia. *Quaternary Science Reviews* **13**, 201-207.

Huntley D.J. and Prescott J.R. (2001). Improved methodology and new thermoluminescence ages for the dune sequence in south-east South Australia. *Quaternary Science Reviews* **20**, 687-699.

Hütt G., Jaek I. and Tchonka J., (1988). Optical Dating: K-Feldspars Optical Response Stimulation Spectra. *Quaternary Science Reviews* **7**, 381-385.

Lamothe M., Auclair M., Hamzaoui C. and Huot S. (2003). Towards a prediction of long-term anomalous fading of feldspar IRSL. *Radiation Measurements* **37**, 493-498.

Lang A., Lindauer S., Kuhn R. and Wagner G.A. (1996). Procedures used for Optically and Infrared Stimulated Luminescence Dating of Sediments in Heidelberg. *Ancient TL* **14**, 7-11.

Liritzis I. and Vafiadou A., (2005). Dating by Luminescence of Ancient Megalithic Masonry. *Mediterranean Archaeology and Archaeometry* **5**, No 1, 25-38

McKeever S.W.S., (1985). Thermoluminescence of solids. Cambridge University Press, London, 376p. ISBN: 0-521-36811-1.

McKeever S. W. S., Alselrod M. S. and Markey B. G., (1996). Pulsed optically stimulated luminescence dosimetry using α -Al₂O₃:C. *Radiation Protection Dosimetry*, **65**, 267-72.

McKeever S.W.S., Botter-Jensen L., Larsen N.A. and Duller G.A.T., (1997). Temperature Dependence of OSL Decay Curves: Experimental and Theoretical Aspects. *Radiation Measurements* **27**. 161-170.

Pliny (AD77). Pliny online: complete translation, by John Bostock and H. T Riley (1855). <http://www.perseus.tufts.edu/cgi-bin/ptext?lookup=Plin.+Nat.+toc>

Poolton N.R.J., Botter-Jensen L. and Johnson O., (1995). Thermo-Optical Properties of Optically Stimulated Luminescence in Feldspars. *Radiation Measurements* **24**, 531-534.

Prescott J.R. and Robertson G.B. (1997). Sediment dating by luminescence: a review. *Radiation Measurements* **27**, 893-922.

Readhead M.L. (1988). Thermoluminescence dating study of quartz in aeolian sediments from southeastern Australia. *Quaternary Science Reviews* **7**, 257-264.

Rhodes E.J. (1988). Methodological considerations in the optical dating of quartz. *Quaternary Science Reviews* **7**, 395-400.

Rhodes E.J. (1990). Optical dating of quartz from sediments. Unpublished D.Phil. Thesis, Oxford University.

Roberts R.G., Jones R., Spooner N.A., Head M.J., Murray A.S. and Smith M.A. (1994). The human colonisation of Australia: optical dates of 53,000 and 60,000 years bracket human arrival at Deaf Adder George, Northern Territory. *Quaternary Geochronology (Quaternary Science Reviews)* **13**, 575-583.

Roberts R.G. (1997). Luminescence dating in archaeology: from origins to optical. *Radiation Measurements* **27**, 819-892.

Smith B.W., Aitken M.J., Rhodes E.J., Robinson P.D. and Geldard D.M. (1986). Optical dating: methodological aspects. *Radiation Protection Dosimetry* **17**, 229-233.

Smith B.W. (1988). Zircon from sediments: a combined OSL and TL auto regenerative dating technique. *Quaternary Science Reviews* **7**, 401-406.

Spooner N.A. (1992). Optical dating: preliminary results on the anomalous fading of luminescence from feldspars. *Quaternary Science Reviews* **11**, 139-145.

Spooner N.A. (1994). The anomalous fading of infra-red stimulated luminescence from feldspars. *Radiation Measurements* **23**, 625-632.

Stokes S. (1992). Optically dating of young (modern) sediments using quartz: Result from a selection of depositional environments. *Quaternary Science Reviews* **11**, 153-159.

Stoneham D., (1991). Authenticity testing. In: *Scientific Dating Methods*, eds. H.Y. Göksu, M. Oberhofer and D. Regulla, *Eurocourses Advanced Scientific Techniques* **1**, 175-192, Kluwer Academic Publishers, Dordrecht. XLII
References

Şimşek C., (2004). 2003 Yılı Laodikeia Antik Kenti Kazısı, 26. *Kazı Sonuçları Toplantısı* **1**, 305-320. **ISBN:** 975-17-3149-6 (Tk.No) 975-17-3150-X (1. Cilt)

Taylor R. E. and Aitken M.J., (1997). eds. *Chronometric Dating in Archaeology . Advances in Archaeological and Museum Science*, **vol. 2**. New York: Plenum Press, 1997. xix + 395 pp.

Vandenbergh D., (2003). Ph.D. Thesis: Investigation of the Optically Stimulated Luminescence Dating Method for Application to Young Geological Sediments. *Department of Analytical Chemistry Institute for Nuclear Sciences, Universiteit Gent*.

Vancraeynest L., (1998). Bijdrage tot de studie van de thermoluminescentie-dateringsmethode en toepassing op archeologisch keramiek en eolische sedimenten. Doctoraatsthesis, Universiteit Gent.

Visocekas R., Ceva T., Marti C., Lefauchaux F., and Robert M.C., (1976). Tunneling processes in afterglow of calcite. *Physica Status Solidi A* **35**, 315-327.

Visocekas R. (2000). Monitoring anomalous fading of TL of feldspars by using far-red emission as a gauge. *Radiation Measurements* **32**, 499-504.

Wagner G.A., (1995). Altersbestimmung von jungen Gesteinen und Artefakten: Physikalische und chemische Uhren in Quartärgeologie und Archäologie. Enke-Verlag, Stuttgart, 277p., ISBN: 3-432-26411-9. XLVI References

Wagner G.A., (1998). Age determination of young rocks and artifacts: physical and chemical clocks in *Quaternary geology and archaeology*. Springer-Verlag Berlin Heidelberg, 466p., ISBN: 3-540-63436-3.

Wilkinson A.J. (1997). Theoretical Simulation of Preheat-OSL Cycles. *Radiation Measurements* **27**, 489-497.

Wintle A.G., Aitken M.J. and Huxtable J. (1971). Abnormal thermoluminescence fading characteristics. In: *Proceedings of the third international conference on luminescence dosimetry* (ed.: Mejdahl V.), 14/11/1974, Risø, Denmark. *Risø Report* **249**, 105-131.

Wintle A.G. (1973). Anomalous fading of thermoluminescence in mineral samples. *Nature* **245**, 143-144.

Wintle A.G. (1977). Detailed study of a thermoluminescent mineral exhibiting anomalous fading. *Journal of Luminescence* **15**, 385-393.

Wolfe S.A., Huntley D.J., and Ollerhead J. (1995). Recent and late Holocene sand dune activity in southwestern Saskatchewan. In current research 1995-B; *Geological Survey of Canada*, 131-140.

Yurdatapan E., (1997). M.Sc. Thesis: Optically stimulated luminescence (OSL) and its applications to archaeological materials: a pilot study. *METU Graduate School of Natural and Applied Sciences*.

Zimmerman J., (1971). The radiation-induced increase of thermoluminescence sensitivity of fired quartz. *Journal of Physics C: Solid state physics* **4**, 3277-3291.

VITA

PERSONAL INFORMATION

Surname, Name: Demirtürk, Tayfun
Date and Place of Birth: June 22nd, 1964, Acıpayam-DENİZLİ
e-mail: z7f79@yahoo.com

EDUCATION

<u>Degree</u>	<u>Institution</u>
MS	Texas Tech University, Lubbock, TX, USA (1994-1997)
BS	Ankara University, Ankara (1982-1986)
High School	Şarkışla Lisesi, Sivas (1978-1981)

PUBLICATION LIST

1. M. Özbakan, A. Özer, T. Demirtürk, (2006). Optik Uyarmalı Lüminesans Tekniği ile Laodikeia (Denizli/Türkiye) Yapı Seramiklerinin İncelenmesi. T.C. Kültür ve Turizm Bakanlığı Yayınları: *XXI. Arkeometri Sonuçları Toplantısı*, Yayın No: 3052, 87-96, Ankara. ISBN: 975-17-3191-7
2. T. Demirtürk, M. Özbakan, A. Özer, (3-7 May 2004). Dating of Laodikeia (Denizli) Building Ceramics Using Optically Stimulated Luminescence (OSL) Techniques. *34th International Symposium on Archaeometry*, Zaragoza (Spain).